The late Miocene monsoon evolution and erosion history of the western Himalaya: insight from IODP Site U1457

Mahboob Alam[1,4*], Gurumurthy G.P.[1], Tripti Muguli[2], Mohammad Arif[1], Yoshiki Sohrin[3], ArunDeo Singh[4], Radhakrishna T.[5], Dhananjai Kumar Pandey[6], Komal Verma[4]

[1]Birbal Sahni Institute of Palaeosciences, Lucknow 226007, India
[2]National Centre for Earth Science Studies, Trivandrum 695011, India
[3]Institute for Chemical Research, Kyoto University, Kyoto 6110011, Japan
[4]Department of Geology, Banaras Hindu University, Varanasi 221005, India
[5]Gitam University, Bangalore 561203, Karnataka, India
[6]National Centre for Polar and Ocean Research, Vasco da Gama 403804, Goa, India
*Presenting author: mahboob.alam@bsip.res.in; Tel: +91 9742353385

Introduction

The convergence of Indian plate with Eurasia, the subsequent orogeny and establishment of Asian monsoon system led to formation of Himalayan foreland basins (HFB) and major submarine sedimentary basins in the Indian Ocean, namely the Indus Fan and the Bengal Fan (Molnar et al., 2010). The rapid erosion of Himalayan mountain belt following the late Miocene Himalayan upliftment and plateau extension has supplied terrigenous material to the marine environment leading to alter the biogeochemistry of the Indian Ocean (Molnar, 1984; Molnar and Stock, 2009). The sedimentation pattern, erosional history and sediment provenance (Amano and Taira, 1992, France-Lanord et al., 1993; Clift et al., 2002; Clift, 2006; Clift and Webb, 2019; Lupker et al., 2013) and changes in palaeoceanographic process (Gupta et al., 2015) have been used in the last two decades to explore the link between monsoon evolution and Himalayan erosion. This study investigate the Himalayan erosion and hydro-climatic variation since late Miocene. This study establishes the timing and duration of hydro-climatic change in the western Himalayan region and corresponding Indus fan sedimentation since the late Miocene.

Research Objective

To reconstruct the hydro-climatic condition over Indian subcontinent and subsequent erosion history of the western Himalaya since late Miocene using IODP marine sedimentary core.

Study Area

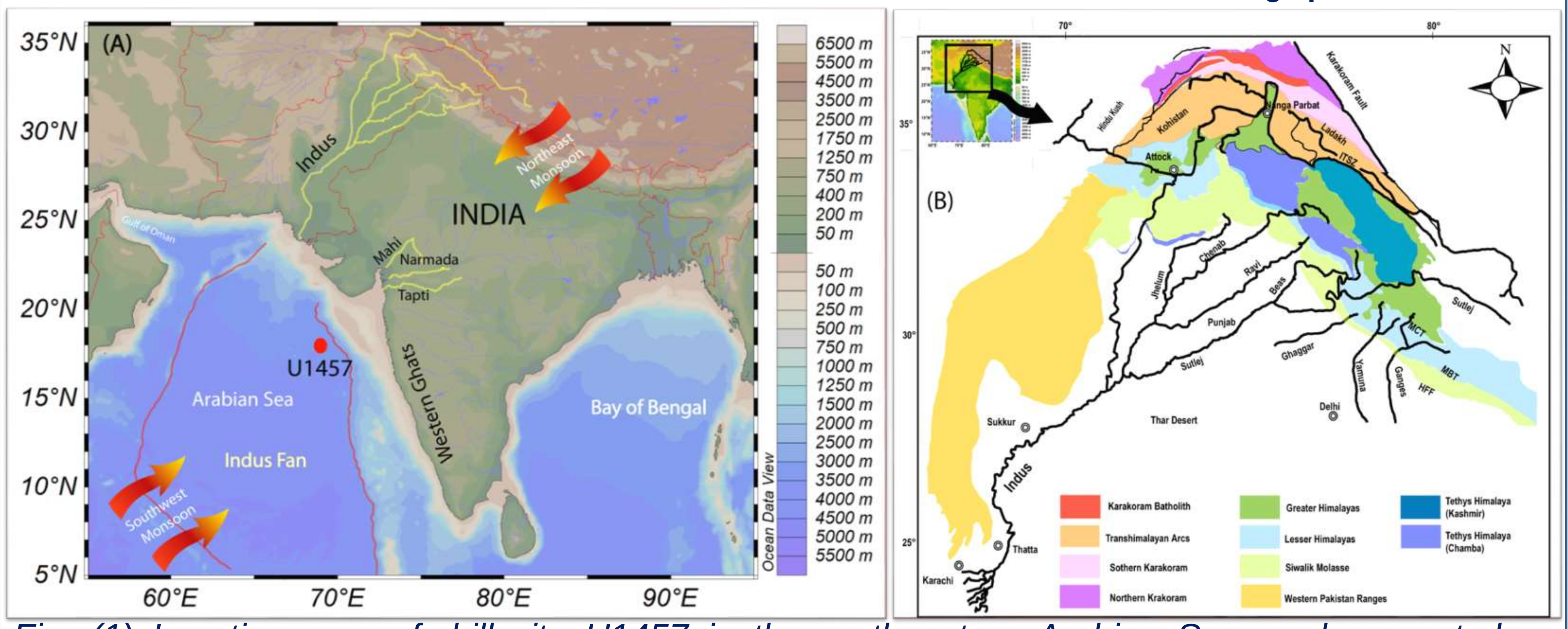

Fig. (1) Location map of drill site U1457 in the northeastern Arabian Sea, and present day drainage map of Indus river basin draining the Western Himalayas. The Indus River is the chief contributor or terrestrial sediments to the Indus Fan in the eastern Arabian Sea through its main distributor channels draining the Himalayan and Tibetan Plateau. Schematic representation of wind direction during southwest monsoon and northeast monsoon seasons is given.

Methodology

- Magnetic χ_{lf}, χ_{ARM}, SIRM, S-ratio, Soft-IRM , Hard-IRM and χ_{ARM}/χ_{lf} measurements were done at palaeomagnetic Lab in BSIP, Lucknow.
- Sedimentary grain size measurements were done at BSIP using Laser Particle Size Analyser.
- Major and Trace element have been measured at Japan using ICP-MS and ICP-AES.

Result and Discussion:

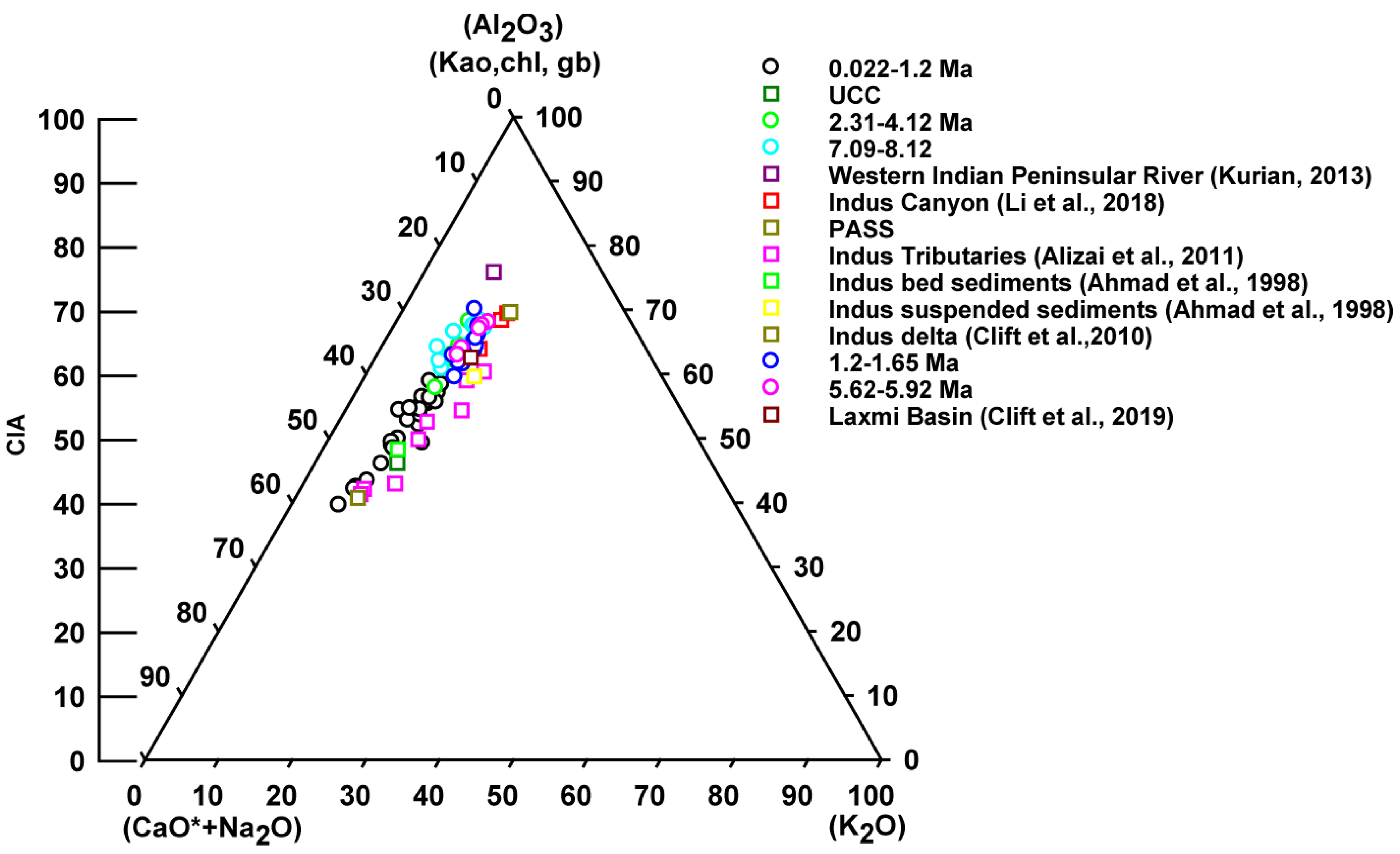

Fig. 2. Comparison of the Site U1457 records from eastern Arabian Sea CN-A-K and Chemical Index of Alteration (CIA).*

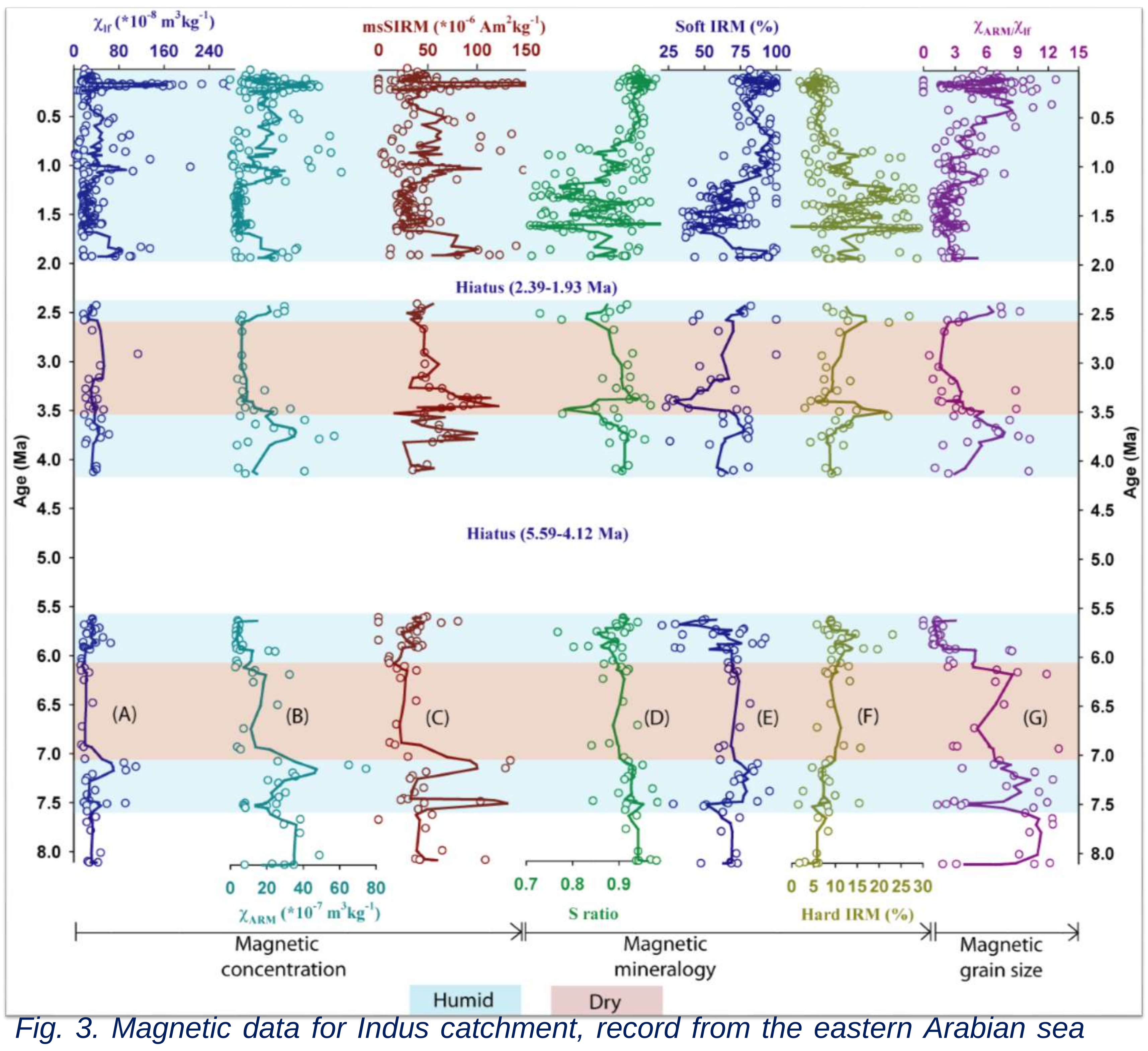

Fig. 3. Magnetic data for Indus catchment, record from the eastern Arabian sea drill site U1457. Solid line represents five-point moving average of data points.

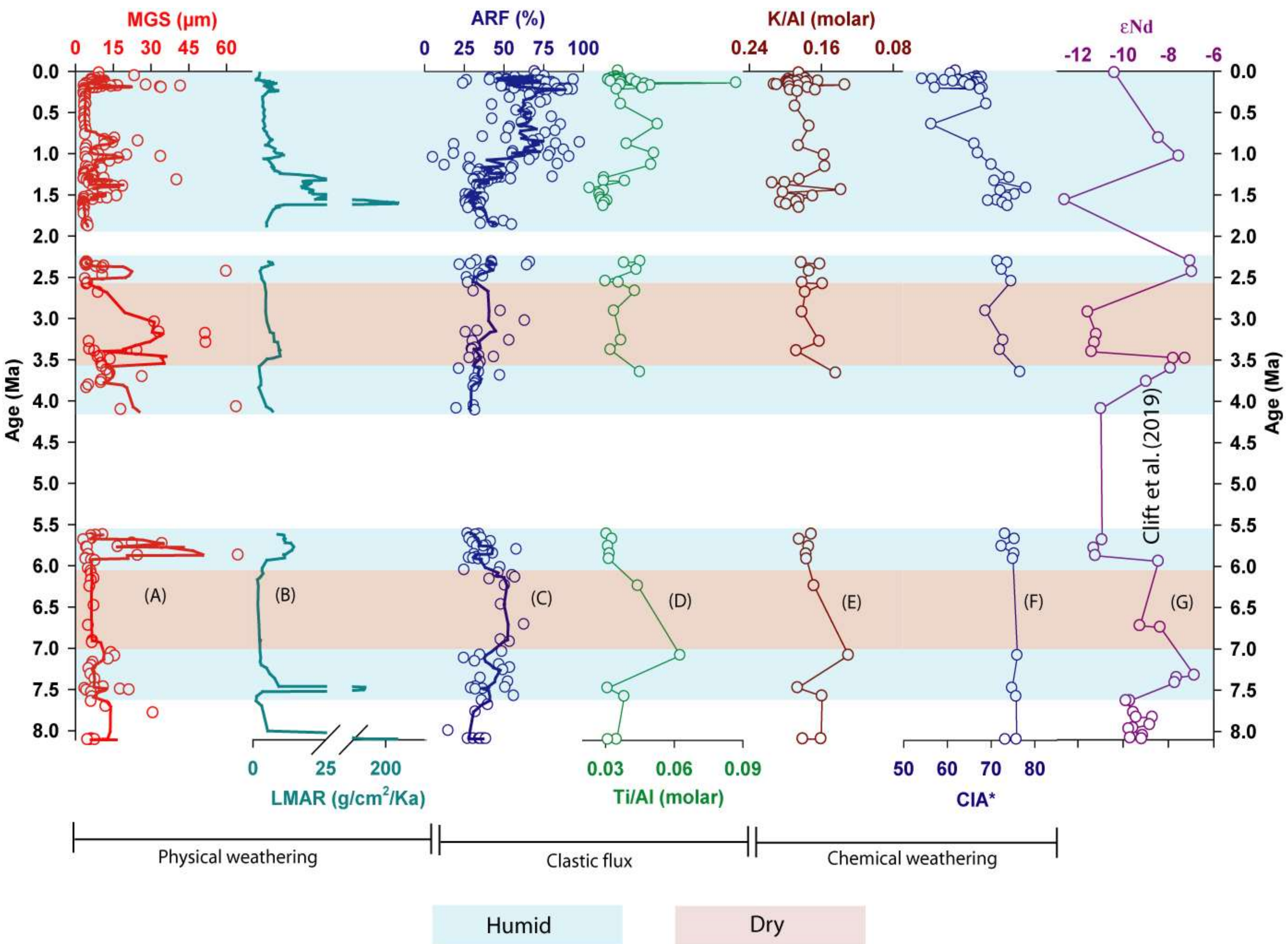

Fig 4. Note: Figure (A, B and C) Individual sample data points are, and a five-point moving average of respective data series is plotted in solid-colour lines.

Conclusion

- The climatic condition in the Western Himalayas during the late Miocene is predominantly arid, except the humid intervals between 6.1- 5.6 Ma and 7.0-7.6 Ma.
- The Pliocene and Pleistocene climate in the Western Himalayas were observed to be humid except for the period from 3.4 Ma to 2.6 Ma.
- The change in the hydroclimatic condition during Pliocene period was due to the palaeoceanographic changes in the world ocean driven by the tectonic rearrangement of seaways.
- The climatic condition during late Pleistocene period (1.7Ma -1.2 Ma) was observed to be intensely humid.
- The environmental magnetism and geochemical proxy records of chemical weathering and clastic sedimentation shows cyclicity during Pliestocene indicating variability in the moisture content during its sedimentation, coinciding with the glacial and interglacial moisture variability.
- The study indicate the dominance source of the sediment during Late Miocene and Pliocene was Indus canyon while during Pleistocene, the Arabian sea receiving the sediment from mixed source through western Indian Peninsular region, Indus canyon and Indus tributaries

Acknowledgment

We thank IODP-India and NCPOR for financial support (Grant No. NCAOR/IODP/20-15/15(V)) to GPG., JOIDES RESOLUTION, International Ocean Discovery Programme (IODP) and all shipboard scientists and crew members of IODP-355 expedition. The Director, BSIP and Dr. Anupam Sharma are thanked for support.

Isotopic characterisation of groundwater of Kerala: Insights into hydrogeological processes

Amit Pandey[1,2]; Virendra Padhya[1]; R.D. Deshapnde[1]

1: Physical Research Laboratory, Navrangpura, Ahmedabad; 38009 India
2: Indian Institute of Technology - Gandhinagar, Palaj, 382355 India

Abstract: Kerala a south western coastal state of India has high level dependency on groundwater which leads to seasonal decline of water table, imbalance in water supply and demand poses a threat of overexploitation and contamination of groundwater. In this situation Understanding the groundwater dynamics and the underlying geohydrological processes is important for effective groundwater management.

In this study stable isotopes of oxygen, hydrogen and their spatio-temporal variation in rain and shallow groundwater for pre and post-monsoon season were used to understanding the rainwater-groundwater relationship, identify effective groundwater recharge sources and their relative contributions, inter-aquifer transfer of water and loss of water through submarine groundwater discharge.

Introduction: Groundwater, the world largest accessible source of freshwater providing 36% of the world's drinking water and nearly 42% of the water for irrigation, for India this fresh water reservoir is even more important as agriculture is largely depend on groundwater which provides job for ~43% of the work force and is a silver lining industry for the Indian economy. Kerala, situated in southwestern coast of India receives a high annual average rainfall (~3000 mm) from southwest as well as northeast monsoonal rain. Despite high rainfall dependency on groundwater is more and ~80% of the rural population and 50% of the agricultural activities in Kerala depends on groundwater. This is primarily due to geohydrological reasons compounded by the high population density, agrarian economy, impacts of climate change, and loss of freshwater as submarine groundwater discharge. In such condition understanding the groundwater dynamics and the underlying geohydrological processes is important for effective groundwater management.

Objectives: The scientific objectives of the present study are: (1) to identify various probable freshwater sources during different seasons (pre-monsoon, southwest monsoon, northeast monsoon) which can feed the groundwater and estimate their seasonally varying relative contribution to groundwater recharge; (2) to delineate the areas recharged by different monsoonal rains; (3) to identify coastal zones where submarine groundwater discharge is expected.

Study area: The study area, lies between the northern latitude of 8º17' 30" N and 12º 47' 40" N and eastern longitude 74º 27' 47" and 77º 37' 12" E cover an area of 38863 km2 (1.2% of country geographical area) and is home for 2.76% of the country's total population (ENVIS). Physiographically the state is divided into four broad physiographic units (Fig:1) (1) the lowland areas which is covered by the coastal alluvial, has the highest open well density in the country (200/km2), and ranges from 0 to 7.5 m (2) Midland area which is covered by laterite and elevation ranges from 7.5 to 75 m. (3) Foothill zone covered by weathered crystalline rocks (4) Highland areas covered by crystalline and weathered crystalline rocks and elevation reaches up to 2600 m.

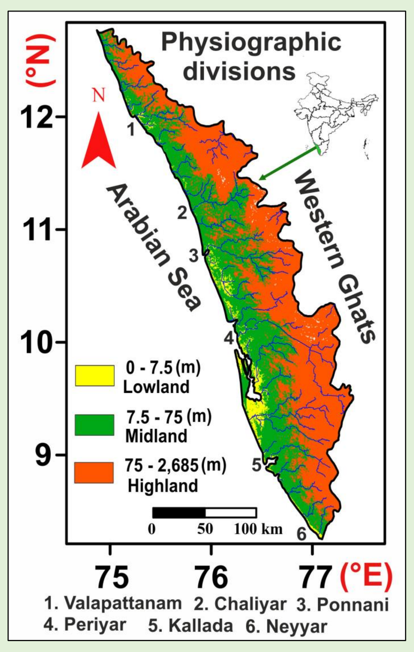

Sample locations & Methodology: The shallow groundwater (maximum water table depth 20m) samples were collected during 2010 for pre-monsoon (April) and post-monsoon (November) seasons from the study area. A total of 235 samples were collected for each season from the same location.
Stable isotopes of O (^{16}O, ^{18}O) and H (^{1}H, ^{2}H) in conjunction with hydrogeological and hydrometeorological parameters were used to understand the groundwater dynamics of the region.

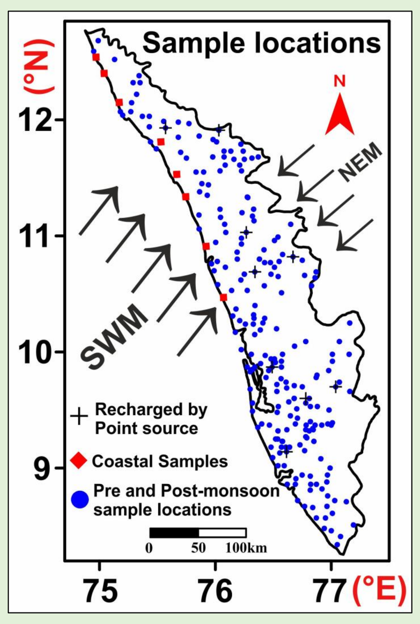

Hydrogeology

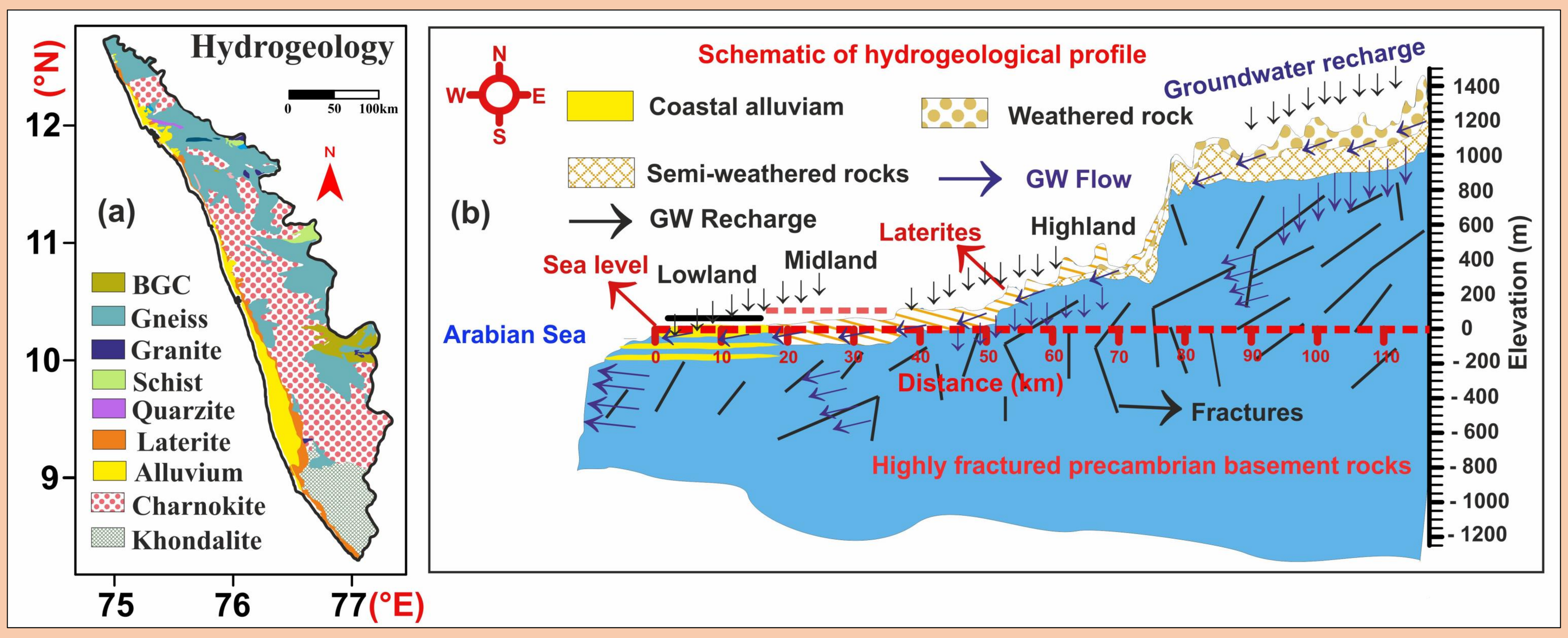

Kerala has four hydro-geologically different aquifers (Figure 2), namely (1) crystalline or hard rock aquifers, (2) Laterite aquifers, (3) Alluvial aquifers, and (4) Tertiary rock aquifers. The alluvial and lateritic aquifers run along the west coast in lowlands. Charnokite constitutes the largest aquifers. Charnokite constitutes the largest aquifers. In some areas, either Khondalite or the Gneissic aquifers stretch from highland to coast.

Results and discussion

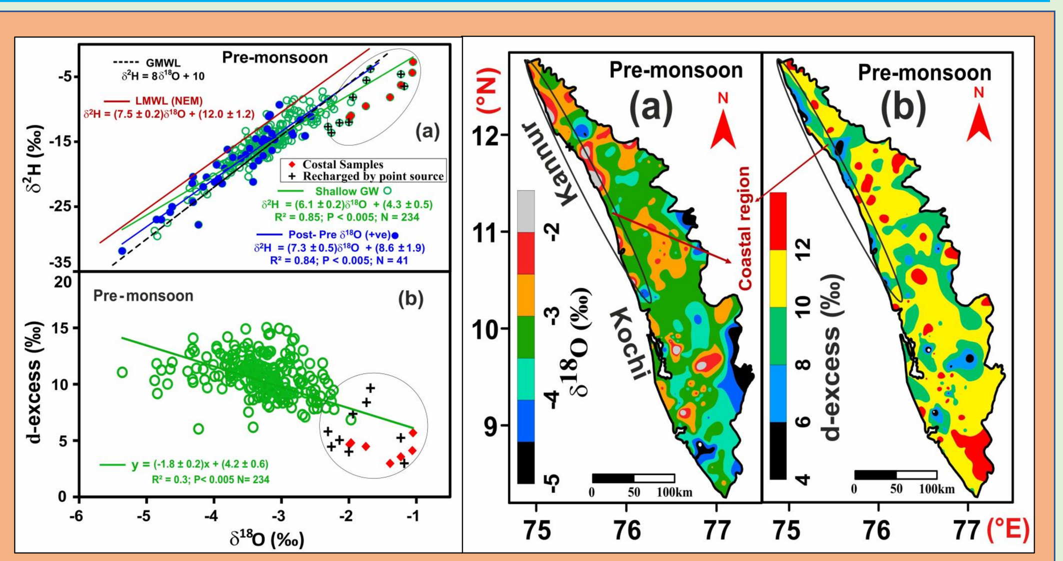

Pre-monsoon: The much lower slope and intercept values of δ^2H - $\delta^{18}O$ regression line for groundwater, compared to that for the Global Meteoric Water Line (Slope 8; Intercept 10) and the local meteoric water line (slope 7.5; intercept 12), indicate that the pre-monsoon groundwater has undergone substantial evaporation through capillary fringe zone. The study area show spatial variation in $\delta^{18}O$ and d-excess in pre-monsoon season. The groundwater with enriched values of $\delta^{18}O$ (-1.5‰ to -2.5‰) and lower value of d-excess (4‰ to 8‰) occurs along the coastal belt of Kerala north of 10º latitude. These enriched $\delta^{18}O$ (~ 0‰) and lower d-excess (~ 4 ‰) values of groundwater in certain coastal patches north of 10º latitude is ascribed to seawater intrusion, because it is not logical to ascribe it to preferential evaporation in these patches alone.

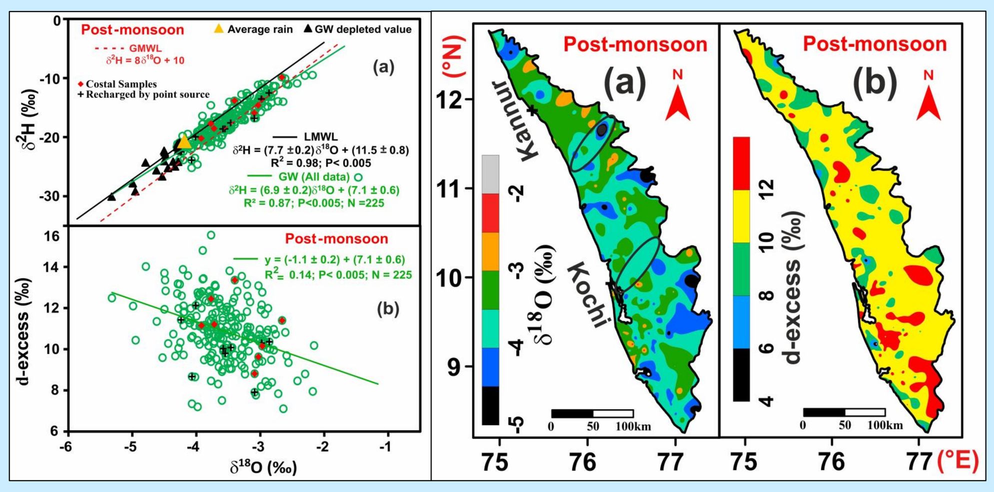

Post-monsoon: The regression line for δ^2H vs $\delta^{18}O$ of post-monsoon groundwater samples has a slope of (6.9 ± 0.2) and the intercept of (7.1 ± 0.6).This slope and intercept is lower than that for the LMWL (7.7 ± 0.2) of the rainfall during May to October, and most of the post-monsoon groundwater samples fall below the LMWL. This indicates post-precipitation evaporative enrichment of infiltrating rainwater, and subsequent mixing with a large reservoir of isotopically enriched pre-monsoon groundwater. The observed spatial variations in the isotopic composition of groundwater are governed by the physiography, isotopic composition of rain, and the aquifer type.

Temporal variation in $\delta^{18}O$: There is a significant difference between the isotopic composition of NEM rainfall (isotopically lighter average) and the rainfall during May to October (isotopically heavier average) which affects the pre-monsoon and post-monsoon groundwater respectively. In view of the above seasonally different isotopic character, the isotopic separation ($\Delta\delta = \delta_{post\text{-}monsoon} - \delta_{pre\text{-}monsoon}$) between post-monsoon and pre-monsoon groundwater can provide geographical information about areas with relatively dominant recharge by NEM rainfall vis-a-vis SWM rainfall. by NEM rainfall and -ve values of $\Delta\delta$ signify the recharge by SWM rainfall. It is seen that groundwater is only about 15% of the geographical area is recharged dominantly by NEM rain fall. Groundwater in the rest 85% of the geographical area seems to be recharged primarily by the SWM rainfall. This information is very useful for the assessment of the geographically different impact of monsoon performance on agriculture and other economic activities.

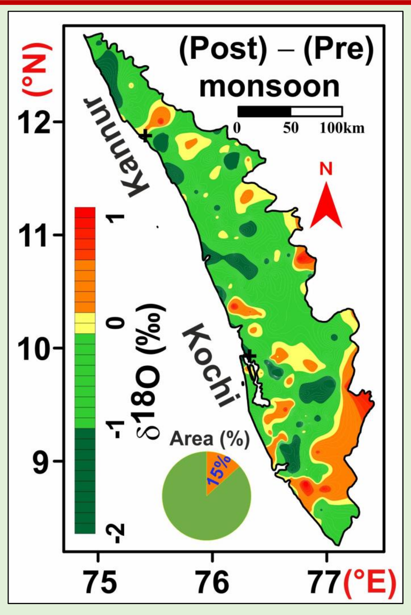

Estimation of groundwater recharge from rain fall: Using two end-member mixing model:

End members	Physiographic Divisions		
	Lowland	Midland	Highland
Pre-monsoon (GW) $\delta_{pre}{}^{18}O$ (‰)	-3.1	-3.2	-3.3
Rain (May-October) $\delta_{rain}{}^{18}O$ (‰)	-4.0	-4.2	-4.5
Post-monsoon (GW) $\delta_{post}{}^{18}O$ (‰)	-3.5	-3.5	-3.6
Contribution of rain in GW recharge (%)	45.0	30.0	25.0
Uncertainty values (%) using formulations of Genereux, (1998)	±13.6	±12.6	±10.6

Summary: The important outcome of the study are-
(1) On an annual basis, a huge 73% (~7.9 BCM) of replenishable groundwater (i.e. 10.8 BCM recharge – 2.9 BCM extraction) is lost into the coastal waters of the Arabian Sea as submarine groundwater discharge (SGD). (2) The 15% of geographical areas additionally recharged by the NE monsoon rainfall (3) The estimated annual groundwater recharge varies physio-graphically with maximum (~2.2 BCM) in the lowland region, minimum (~1.2 BCM) in the highland region, and remaining ~1.5 BCM in the midland region. (4) Groundwater in the coastal area north of 10º N latitude is adversely affected by marine water intrusion during the pre-monsoon season, which is flushed out annually by the high throughflow of freshwater in the post-monsoon season.

References:

- Deshpande, R., Bhattacharya, S., Jani, R., Gupta, S., 2003. Distribution of oxygen and hydrogen isotopes in shallow groundwaters from Southern India: influence of a dual monsoon system. Journal of Hydrology, 271(1-4): 226-239.
- Deshpande, R., Gupta, S., National Programme on Isotope Fingerprinting of Waters of India (IWIN)-a New Initiative.
- Deshpande, R., Gupta, S., 2008. National programme on isotope fingerprinting of waters of India (IWIN). Glimpses of Geosciences Research in India, the Indian Report to IUGS, Indian National Science Academy (eds Singhvi, AK, Bhattacharya, A. and Guha, S.), INSA, New Delhi: 10-16.
- Oza, H., Padhya, V., Ganguly, A., Saikranthi, K., Rao, T., Deshpande, R., 2020. Hydrometeorological processes in semi-arid western India: insights from long term isotope record of daily precipitation. Climate Dynamics, 54(5): 2745-2757.

Ground Water Level Monitoring in the state of Gujarat (1997-2017)

Ishan P. Jariwala & Dr. Hiteshri K. Shastri

M. S. Patel Department of Civil Engineering, CSPIT, CHARUSAT, Anand, Gujarat

INTRODUCTION

- ❖ Ground water is one of the most important source of fresh water in tropical countries.
- ❖ Sustainable ground water management is beneficial for maintaining ground water quality as well as ensuring future water security.
- ❖ Observation of changes in ground water level is helpful to clearly understand usage and replenishment of ground water resources in the region.

OBJECTIVES

- ➢ To analyze the Ground Water level in Gujarat State.
- ➢ To identify high and low ground water regions in Gujarat State.
- ➢ To understand the condition of ground water recharge-discharge in the state of Gujarat.

METHODOLOGY

- ➢ The study provides observation of variation in ground water level in the state of Gujarat during 1997 to 2017.
- ➢ The observations are made for four different seasons namely; summer season, pre- monsoon, post-monsoon and winter season.
- ➢ The collected ground water data is rectified for the consistency and missing observations.
- ➢ The stations providing consistent seasonal ground water level observations are identified and used for this study.
- ➢ The trend in ground water level changes are estimated with the help of standard statistical indices namely Mann Kendall Rank test and Sen Slope estimator.
- ➢ Spatiotemporal analysis of estimated trend and slope is carried out with the help of geospatial technology using software ArcGIS.
- ➢ The observations identifies areas of high ground water depletion and balance of ground water usage in the state of Gujarat.
- ➢ The result of this study are helpful for ground water management and policy making to guide sustainable use of ground water in the state of Gujarat.
- ➢ These results depicts of the change in ground water level which helps to study of water table in different area.

REFERENCES

- http://cgwb.gov.in/gw_profiles/st_Gujarat.htm
- M. Karamouz (July 16, 1954), Ground Water Hydrology(2011).
- Nipun Kithsiri Gunawardena (March 2, 1949), Introduction to Geographic Information Systems (2014).

MATERIALS AND METHODS

- ✓ Materials:
  - i. Central Ground Water Board data distribution portal.
- ✓ Methods:
  - i. Mann Kendall Rank Test
  - ii. Sen Slope Estimator

CONCLUSION

- ▪ The regions Kutch, Saurashtra, Ahmedabad, and Anand shows a remarkable depletion of ground water level.
- ▪ Good recharge for ground water has been found increasing over these years. While, the some Northeastern part shows sign of bad recharge.
- ▪ To overcome the problem of bad recharge area, artificial recharge should be constructed to store rain water and improve porosity of soil. Thus, results in development of better recharge systems.

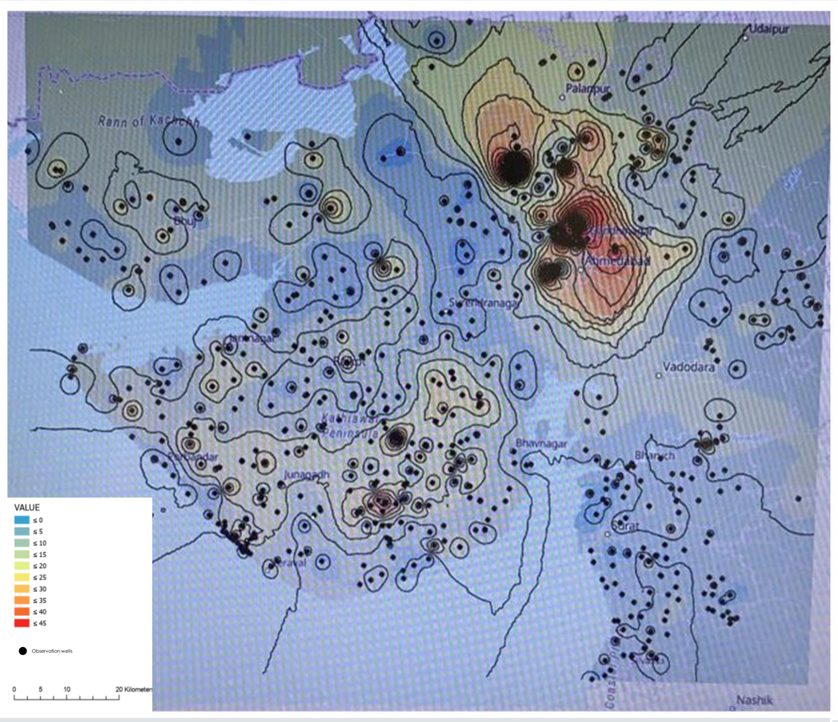

Contour of Ground Water Table for year 1996 post-monsoon season.(Red color indicates ground water depletion, Blue indicates ground water recharge)

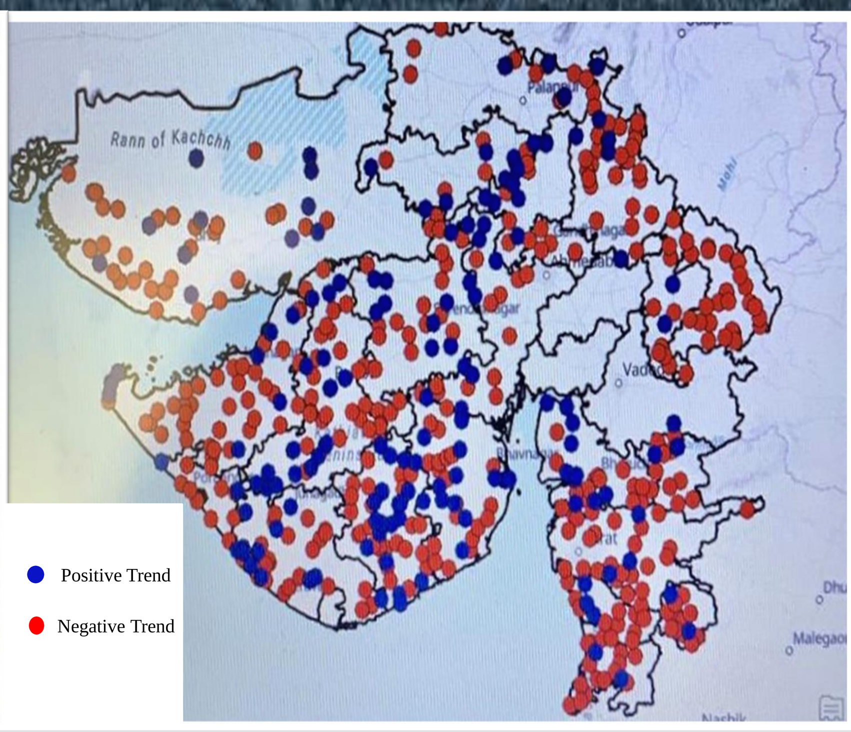

Trend of Ground water level change in different observation wells

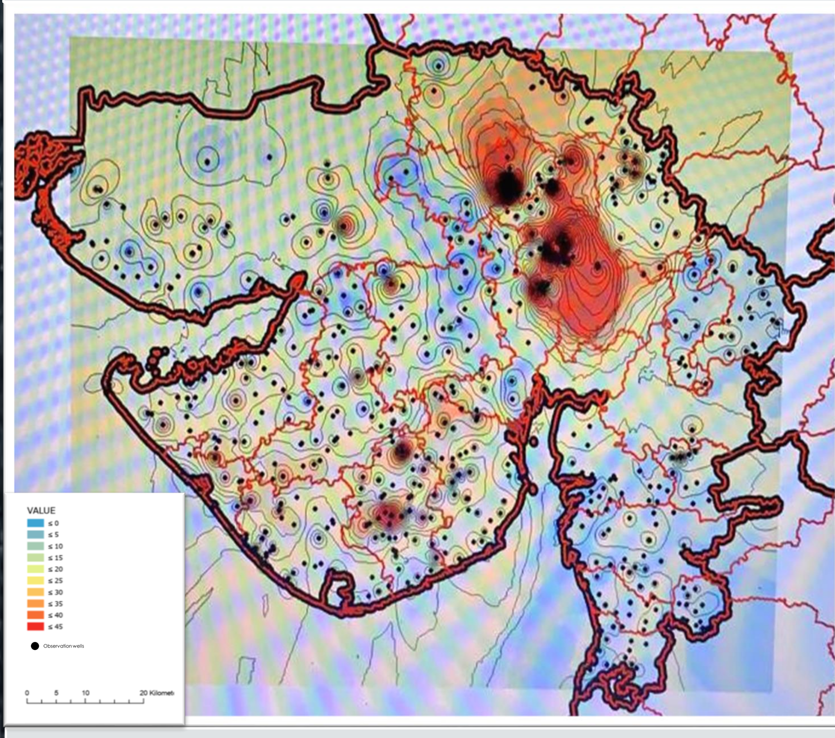

(January- June) Mean Ground water depth (1997-2017)

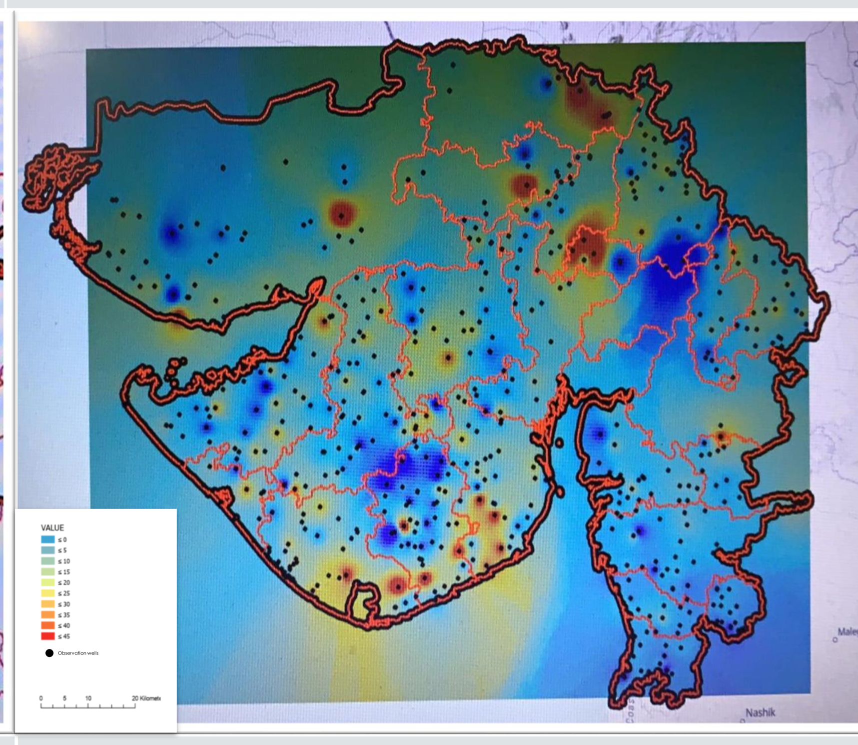

(July- December) Mean Ground water depth (1997-2017)

Mean monsoon climate shift at the edge of Roman Warm Period

Phanindra Reddy A[1,2], Naveen Gandhi[1]

[1]Indian Institute of Tropical Meteorology, Pune, India

[2]Savitribai Phule Pune University, Pune, India

E-mail ids: annapureddy.jrf@tropmet.res.in; naveen@tropmet.res.in

Abstract

Background: Since the early Holocene, monsoon strength appears to follow the precision-based solar insolation. This close relation seems to be weakened in the last two millennia. Abrupt climate transitions were recorded in the past within a decade and further unusual monsoon climate transitions were often coinciding with the global climatic shifts. However, shift in monsoon's mean state in the last three millennia has not been reported.

Objectives: To analyse the monsoon mean climate shifts during the late Holocene and their forcing mechanisms.

Methods: Near annually resolved stalagmites (NAKA-A1, NK-1305) from Kadapa cave, Peninsular Indian region were used to deduce the Indian summer monsoon rainfall (ISMR) variability for the last 3.2 kyr. Age chronology was obtained from U/Th dating by analysing a set of 11 subsamples that were extracted from different layers along the growth axis of each stalagmite. Several carbonate samples were drilled along the growth axis with 100 micron distance and each sample was reacted with 100% pure Ortho-Phosphoric acid to evolve carbon dioxide gas. These gaseous samples were analysed for $\delta^{18}O$ values on stable Isotope Ratio Mass Spectrometer, at Physical Research Laboratory. U/Th dates and $\delta^{18}O$ values were employed on COPRA age model to obtain $\delta^{18}O$ time series, and variations in $\delta^{18}O$ values are interpreted as ISMR variations.

Results: Our ISMR record shows the mean state of monsoon climate shifted around the edge of Roman Warm Period (RWP), i.e., ~1.7-1.8kyr B.P. (Before Present; relative to 1950 CE). Signature of such climate shift is evidently available in the different proxy records from the subcontinent; yet this monsoon climate shift remains overlooked. Further it is noted that, this monsoon climate shift had occurred within few decades to a century.

Discussion: Though the Solar forcing remains the primary driver of long-term ISMR variations, on shorter time scales and during weaken Solar Insolation, internal forcings (such as ENSO) intensification may dominate and dictate the ISMR variability. On this line, a dramatic increase in El Niño/Southern Oscillation (ENSO) variability and intensification of El Niño and La Niña events around 1.75-2 kyr B.P. (Thompson et al. 2017) would have forced the mean monsoon climate to departure from the solar insolation driven drying trend which was continuing since the mid- to late Holocene.

Introduction

The mean state of monsoon transitions and its strength were not uncommon in the past (Deplazes et al., 2014; Higginson et al., 2004). These unusual monsoon climate transitions were often coinciding with the global climatic shifts (Deplazes et al., 2014; Higginson et al., 2004). Basic mechanisms for abrupt monsoon transitions were proposed and modelled by several investigators; however, yet the origin of monsoon climate shifts remains unclear and debatable.

Very scarce studies documented/addressed the mean monsoon state shift in the recent past, at least for the last ~3.2 kyr. Here we present near annually resolved ~3.2 kyr long ISMR variations from the composite speleothem $\delta^{18}O$ data from the peninsular India. This composite ISMR variations show last ~3.2 kyr have recorded a shift in mean monsoon climate, i.e., a sudden drop of ~2‰ in $\delta^{18}O$ values at the edge of the Roman Warm Period (RWP). Further, there is a contrast in stalagmite isotopic signatures, for the last 0-1.7 kyr B.P. to 1.7-3.2 kyr B.P. We aim to study the observed sudden shifts in monsoon climate and their association with the latitudinal movement of ITCZ owing to the response of Earth's internal climate forcing or natural forcing.

Methodology

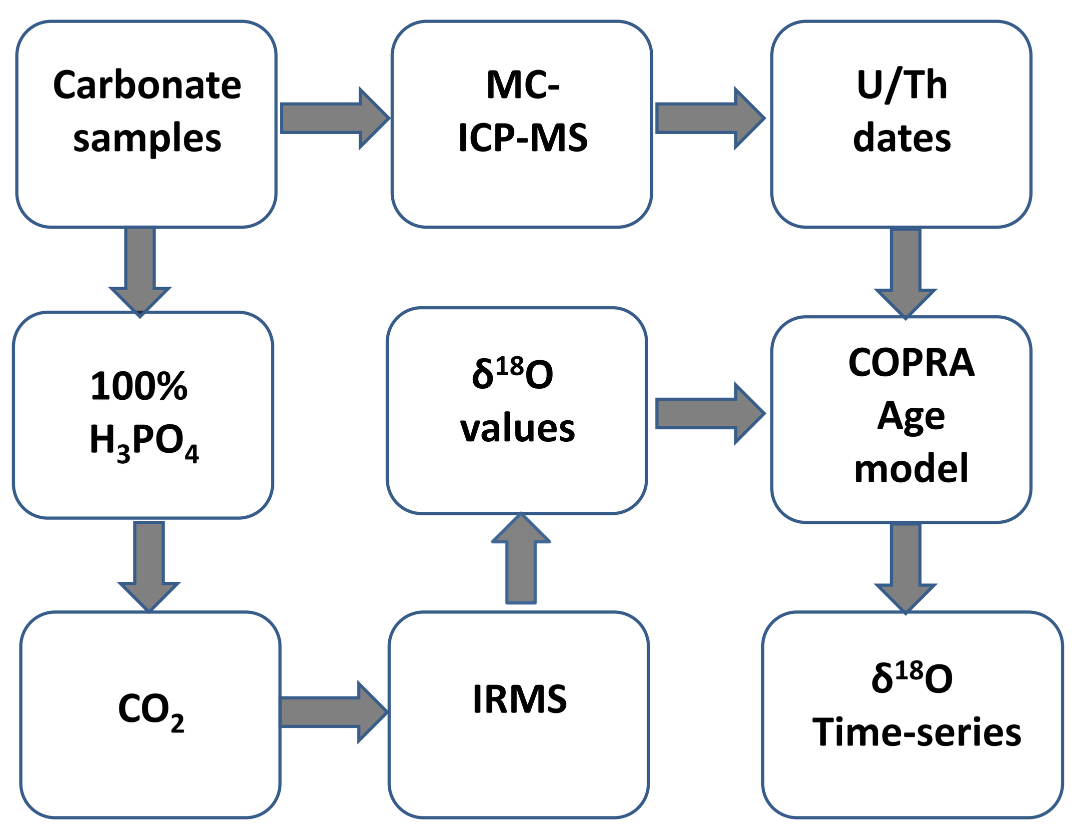

Discussion

- Our monsoon record shows the mean state of monsoon climate shifted around the edge of RWP.
- Signature of such climate shift is evidently available in the different proxy records from the subcontinent (Figure 1) ; yet this monsoon climate shift remains overlooked.
- A dramatic increase in ENSO variability and intensification of El Niño and La Niña events around 1.75-2 kyr BP (Thompson et al. 2017) would have forced the monsoon climate's mean state to departure from the solar insolation driven drying trend which was continuing since the mid- to late Holocene (Figure 2).

Results

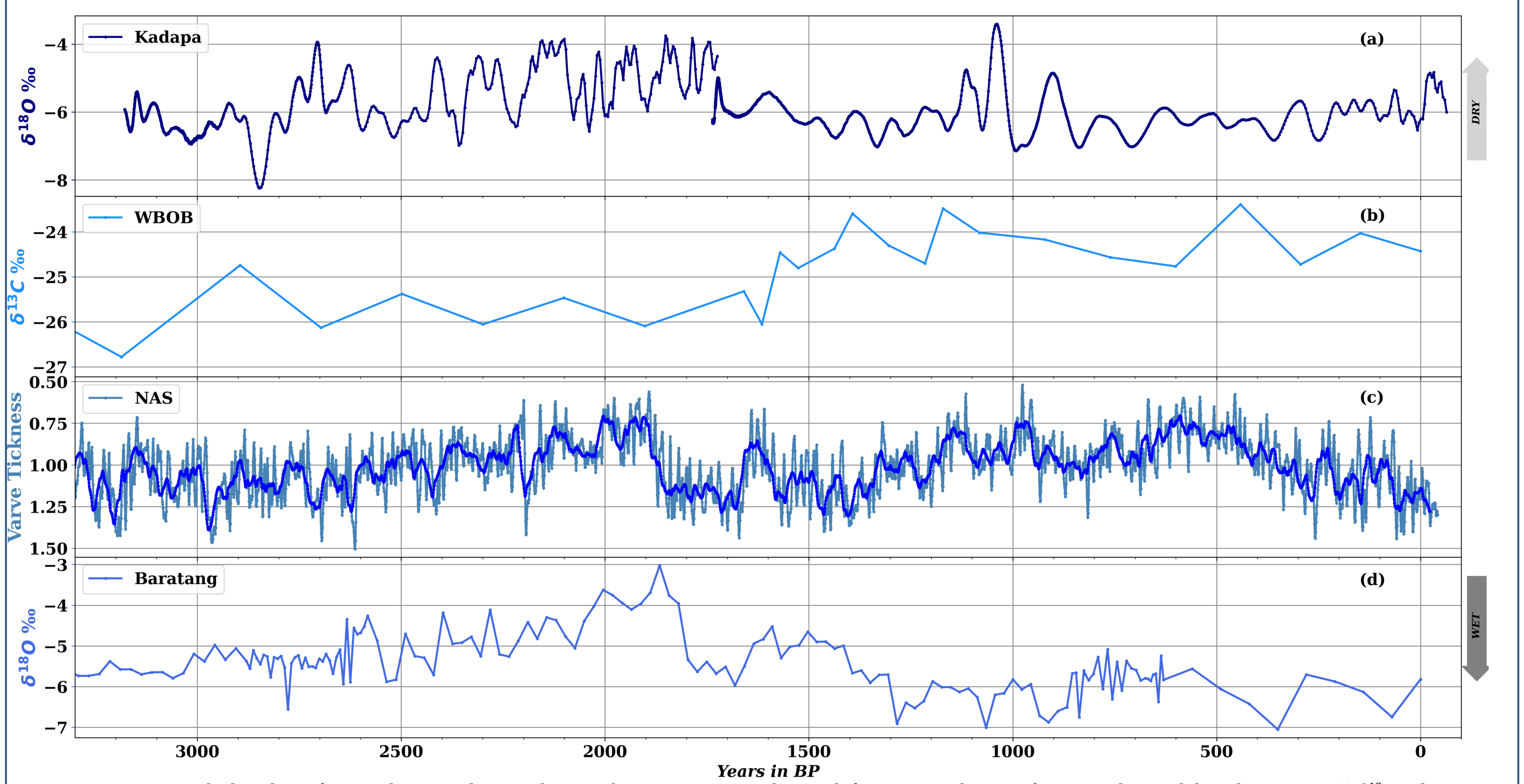

▲Figure 1: Marked evidence from Multi-proxy datasets showing the mean monsoon climate shift at ~1.7-1.8 kyr B.P. from in and around the subcontinent. (a) $\delta^{18}O$ values of Kadapa stalagmites composite, (b) $\delta^{13}C$ values of plant wax from western Bay of Bengal sediment core, (c) Varve thickness from Indus river delta, northern Arabian sea sediment, (d) $\delta^{18}O$ values of Baratang cave, Andaman island stalagmite. Proxy values are interpreted as strength of monsoon, red up and blue down arrows represents weak and strong monsoon.

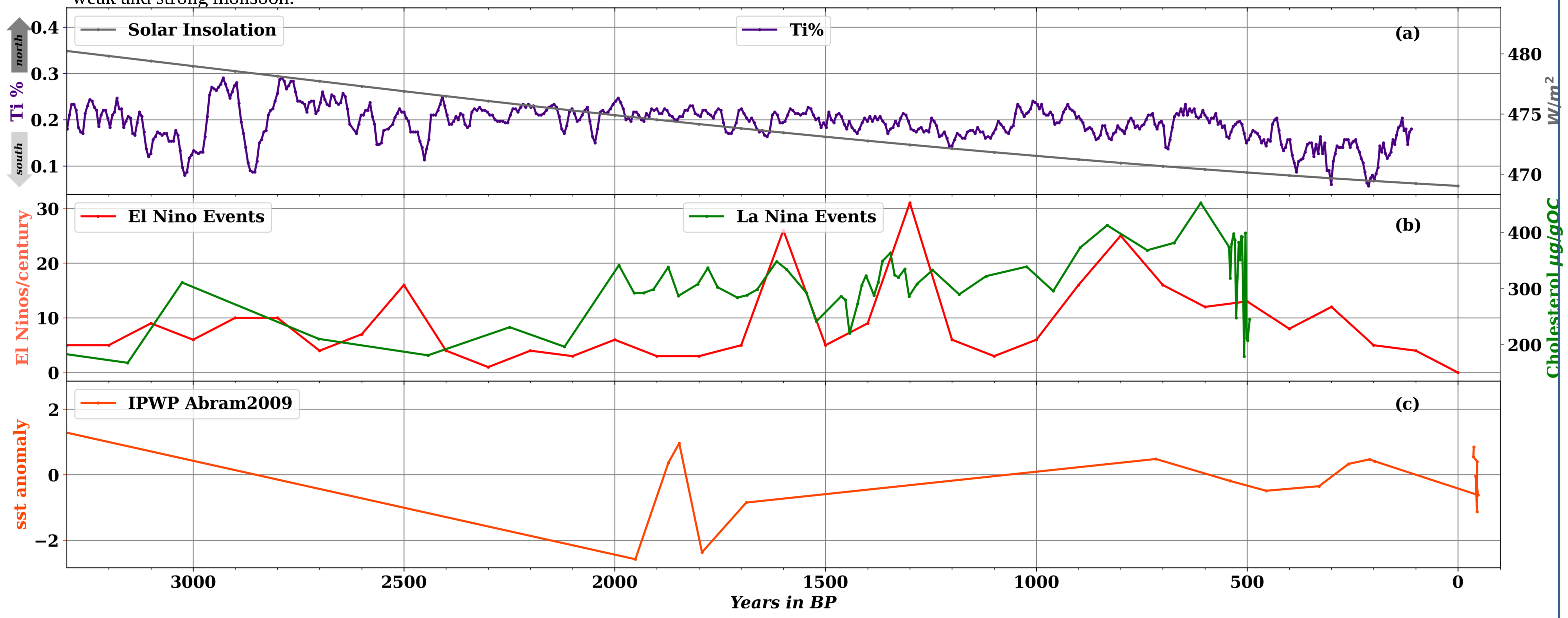

▲Figure 2: Temporal evolution of climate phenomena during late Holocene, i.e., for the last ~3 kyr. (a) Mean latitudinal position of ITCZ (violet), interpreted from Ti % variations and solar insolation (in grey). (b) El Nino and La Nina events interpreted from redcolor intensity and cholesterol values of sediment deposits, respectively. (c) mean Indo-Pacific Warm Pool sea surface temperatures anomalies. All the proxy datasets used in this study are freely available NOAA paleoclimatology data website.

Conclusions

- Mean monsoon climate shifted around the edge of Roman Warm Period.
- ITCZ and Natural forcing appears does not play any role in this abrupt climate shift.
- Tropical equatorial Pacific forced mean monsoon climate to shift during end of Roman Warm Period.

References

- Deplazes, G., Lückge, A., Stuut, J.B.W., Pätzold, J., Kuhlmann, H., Husson, D., Fant, M., Haug, G.H., 2014. Weakening and strengthening of the Indian monsoon during Heinrich events and Dansgaard-Oeschger oscillations. Paleoceanography 29, 99–114. https://doi.org/10.1002/2013PA002509
- Higginson, M.J., Altabet, M.A., Wincze, L., Herbert, T.D., Murray, D.W., 2004. A solar (irradiance) trigger for millennial-scale abrupt changes in the southwest monsoon? Paleoceanography 19. https://doi.org/10.1029/2004PA001031
- Thompson, D.M., Conroy, J.L., Collins, A., Hlohowskyj, S.R., Overpeck, J.T., Riedinger-Whitmore, M., Cole, J.E., Bush, M.B., Whitney, H., Corley, T.L., Kannan, M.S., 2017. Tropical Pacific climate variability over the last 6000 years as recorded in Bainbridge Crater Lake, Galápagos. Paleoceanography 32, 903–922. https://doi.org/10.1002/2017PA003089

Acknowledgements

We thank M.G. Yadava, Physical Research Laboratory, Ahmedabad for providing facilities for stable isotope analyses. Authors acknowledge NOAA/ National Climatic Data Center (NCDC) paleoclimatology program for providing proxy data. The work is supported by PACMEDY Project under the Ministry of Earth Sciences, India and Belmont Forum, Paris, France.

Reconstructing the variability of deep water circulation in the Indian sector of the Southern Ocean during the last glacial cycle

Pranav S Prem (pranav@ncpor.res.in), Waliur Rahaman, Lathika N, Priyesh Prabhat, M. Thamban
National Centre for Polar and Ocean Research, Goa

Introduction

Deep Water Circulation (DWC) in the Southern Ocean is a crucial component of thermohaline circulation that modulates the transport of heat, carbon, and other nutrients around the globe and plays a significant tole in global climate. The relative changes in the formation and export of deep watermasses (North Atlantic Deep Water(NADW) and Antarctic Bottom Water(AABW)) to the Southern Ocean in the past affected the basin's carbon sink capacity and resulted in glacial-interglacial variability. In order to constrain the variability of DWC and its relation to sea ice extent and global climate, we have reconstructed the DWC in the Indian sector of Southern Ocean using authigenic Neodymium isotopes for the last 156kyr and compared it with published records of Winter Sea ice concentration (WSIC) and Sea Surface Temperatures (SST) from the same core site.

Study Area

Gravity core SK200/33 was collected from the Southwest Indian Sector of the Southern Ocean from a water depth of 4204m. At Present, AABW bathes the core site.

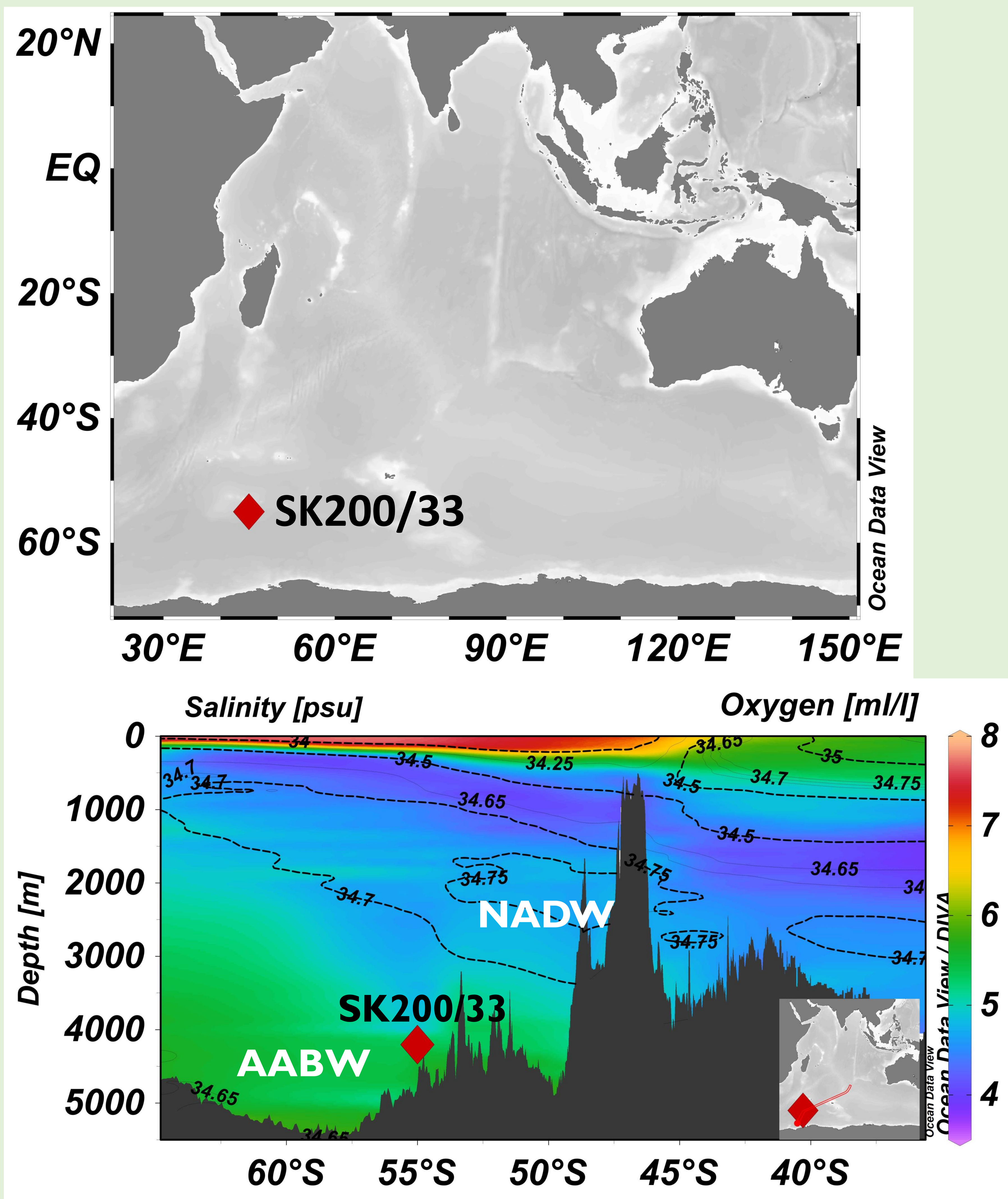

Fig. 1 Location map and hydrography

Neodymium isotopes as a paleo circulation proxy

- Residence time < Ocean Mixing time
- Water masses have distinct eNd values derived from the source region(e.g.: Pacific Deep Water has positive(radiogenic) values between 0 to -4 and NADW has lower(Less radiogenic) values between -10 to 13.5.
- Not affected by physical and biological Processes
- Variability in ε_{Nd} indicates mixing of water masses

Results and Discussions

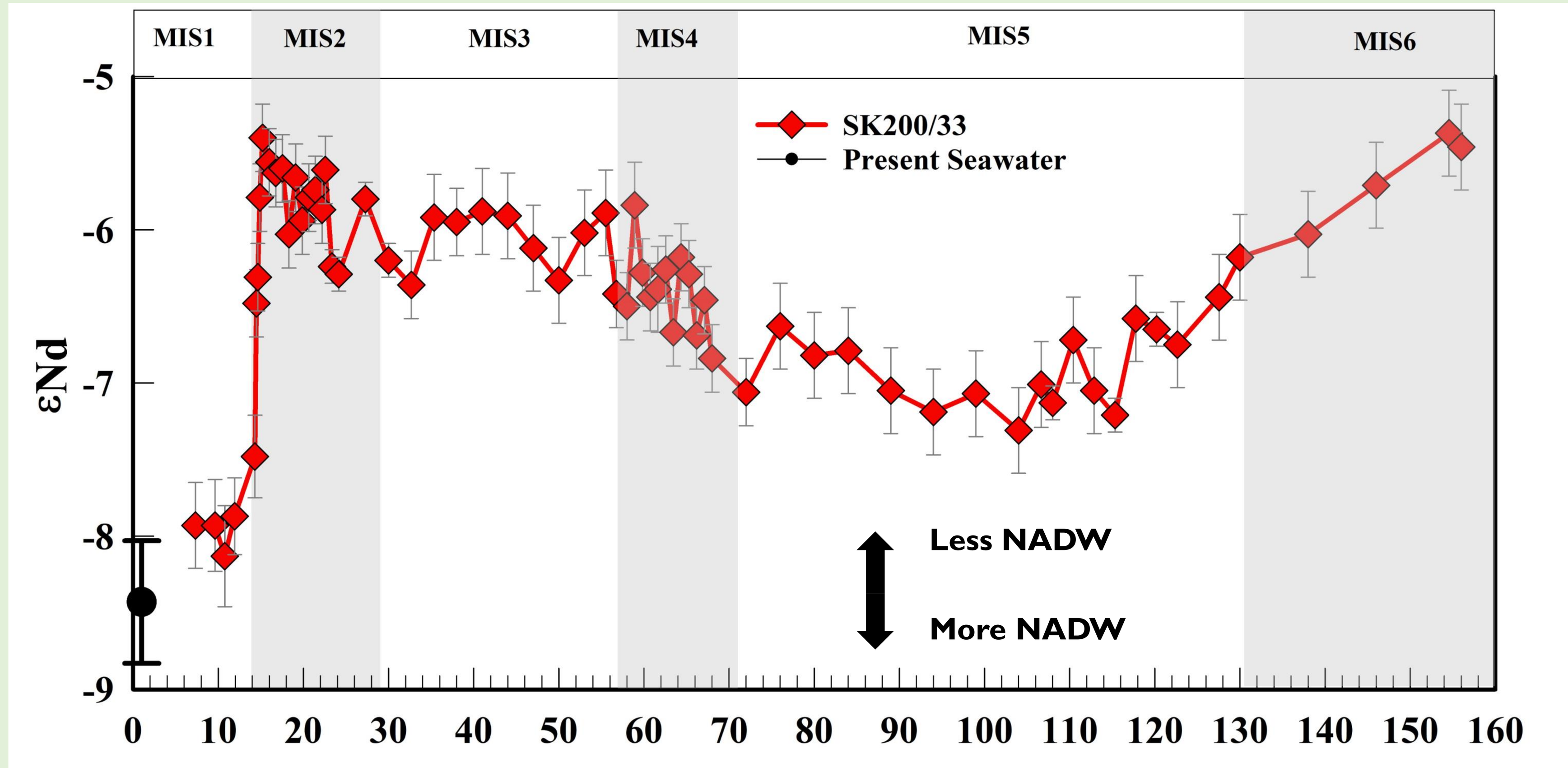

Fig. 2 ε_{Nd} record of SK200/33

- ε_{Nd} values varies between -5.3 to -8.1; Showing radiogenic values during glacial stages and less radiogenic values during interglacials.
- Radiogenic values indicate a dominant Pacific source for AABW and a different circulation structure.
- Modern values are obtained by early Holocene (~12kyr)

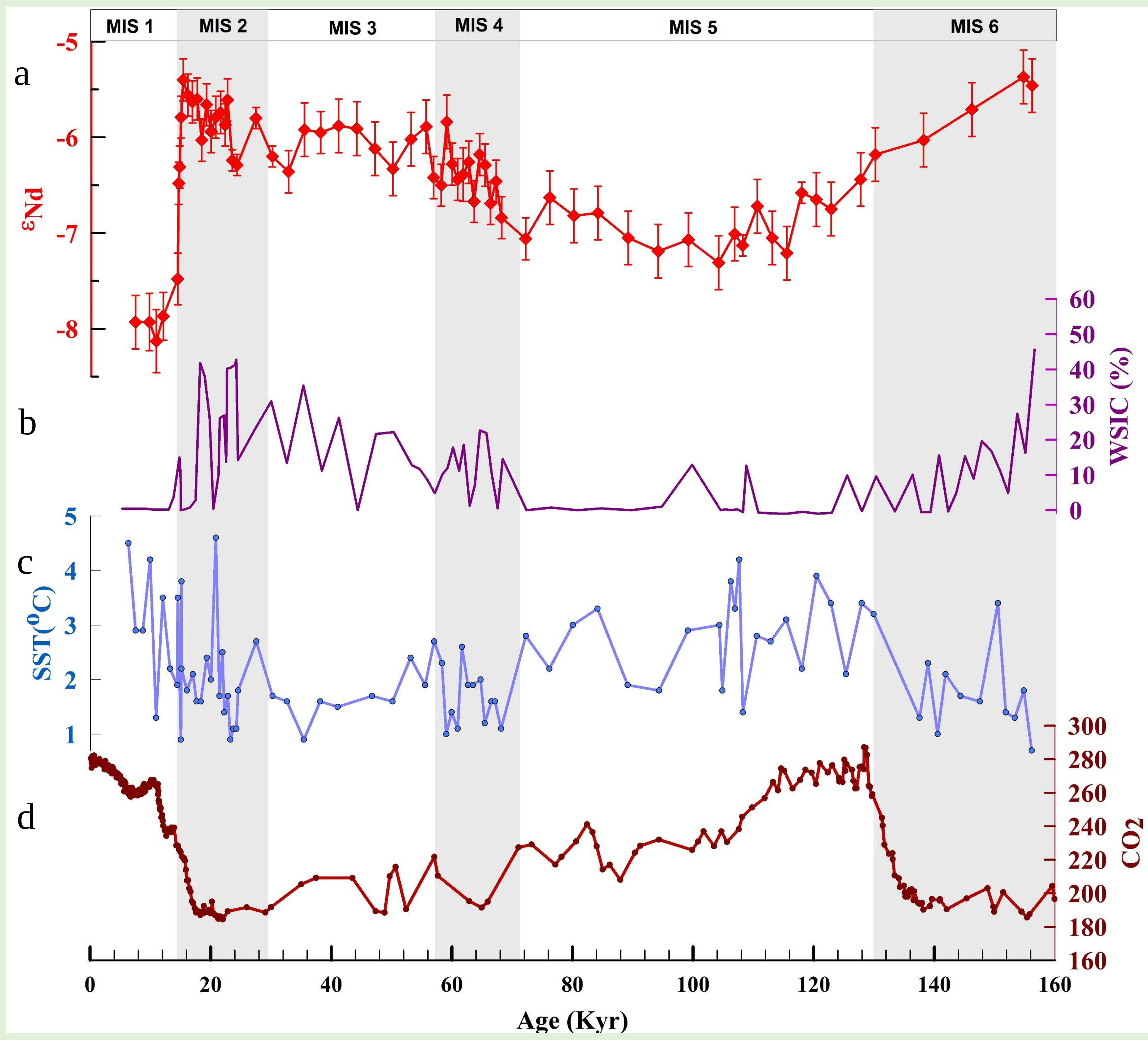

Fig. 3 (a-c) ε_{Nd} record of SK200/33 with WSIC and SST from same core site, (d) Atmospheric CO_2 record from Antarctic cores

- There appears to be a good correspondence between ε_{Nd} and Sea ice concentration and SST (Expanded Sea ice can produce more AABW which is more denser and more cold. This 'modified AABW' on reaching Pacific Ocean can increase the density of Pacific Deep Water and this high density Pacific Deep Water could have replaced Northern Component Water as the lower cell, causing more positive ε_{Nd} values)
- Second declining of CO_2 occurs along with significant changes in ε_{Nd}

Conclusion

- ➢ In the last glacial cycle, significant deep water changes in the Indian sector of Southern Ocean occurred at the MIS5/4 boundary
- ➢ Increased sea ice extent and lower SST could have produced denser AABW which caused the reorganization of Southern Ocean Water Masses.
- ➢ Initial decline of the Atmospheric CO_2 was not associated to the deep ocean circulation

References

1. Frank, M. (2002). Radiogenic isotopes: Tracers of past ocean circulation and erosional input. Reviews of Geophysics, 40(1), 1001. Doi: 10.1029/2000RG000094

2. Pooja Ghadi, Abhilash Nair, Xavier Crosta, Rahul Mohan, M.C. Manoj, Thamban Meloth, Antarctic sea-ice and palaeoproductivity variation over the last 156,000 years in the Indian sector of Southern Ocean, Marine Micropaleontology, , Doi: 10.1016/j.marmicro.2020.101894

Continuous Measurements of Atmospheric Water Vapour Isotopic Composition from Western India

Pratheeksha Nayak[1], P. Kiran Kumar[2], M. G. Yadava[1]

[1] Physical Research Laboratory, Ahmedabad

[2] Central Ground Water Board, Nagpur

Abstract

Isotopic composition of atmospheric water vapour is a natural tracer of the hydrological cycle and provides valuable information regarding moisture sources, atmospheric transport patterns and mixing. We present the water vapour isotopic composition measurements conducted from July 2017 to December 2019 at Physical Research Laboratory, Ahmedabad. Continuous high resolution monitoring of the stable isotopic composition of ambient air is performed using laser absorption spectroscopic techniques. The high resolution data is averaged at ~ 8 minutes based on the results of Allan deviation to minimize the noise in the setup and calibrated as per standard protocols.

Further analysis was performed on post-monsoon data from September 2018 to November 2018. The decreasing trend in the mixing ratio indicates the withdrawal of monsoon and the onset of dry conditions. The d-excess is observed to increase and has large variability which is attributed to the dominance of the locally recycled evaporated components over weak contribution from oceanic sources. The kinetic process of evaporation has strong dependence on atmospheric parameters whose diurnal variation is reflected in an intense 24 hour component in the wavelet analysis of d-excess.

Introduction

- The stable isotopic composition of atmospheric water vapour is a valuable resource that helps us understand the processes occurring in the hydrological cycle.
- They can provide a direct observation on limiting values of mixing ratio, $\delta^{18}O$ and δD which can be used in simulation studies of isotope based climate models.
- They can be used to further improve our understanding of atmospheric transport patterns and variability in sources of moisture.
- Such studies can also provide an improved framework to understand the paleoclimatic processes governing the isotopic composition of precipitation in proxies.
- The advent of cavity-enhanced laser spectroscopic techniques has provided increased capability for long-term studies of water vapour isotopic composition of ambient air.

About the Data

- Observation period : July 2017 to December 2019.
- Location : Physical Research Laboratory, Ahmedabad.
- Instrument : LGR make triple isotope water analyzer.

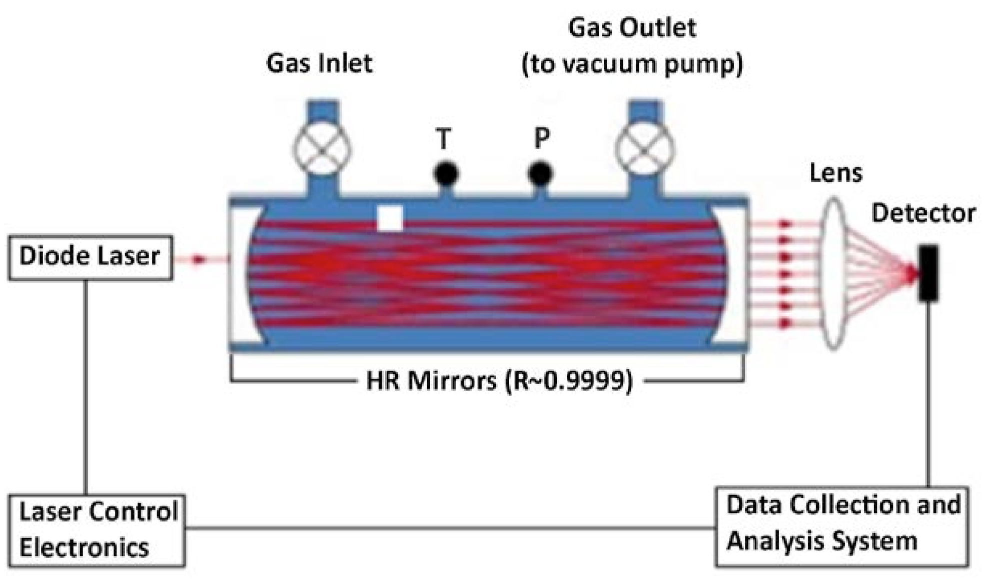

Fig. 1 : Schematic of an Off-Axis ICOS Analyzer.

- Noise characterization : Based on minimum value of Allan deviation (Figure 2), the high resolution data is averaged at ~8 minutes.
- Data is calibrated as per standard protocols. Figure 3 shows the calibration curves used for humidity-isotope response calibration.

Stable Isotopic Composition of Ambient Water Vapour

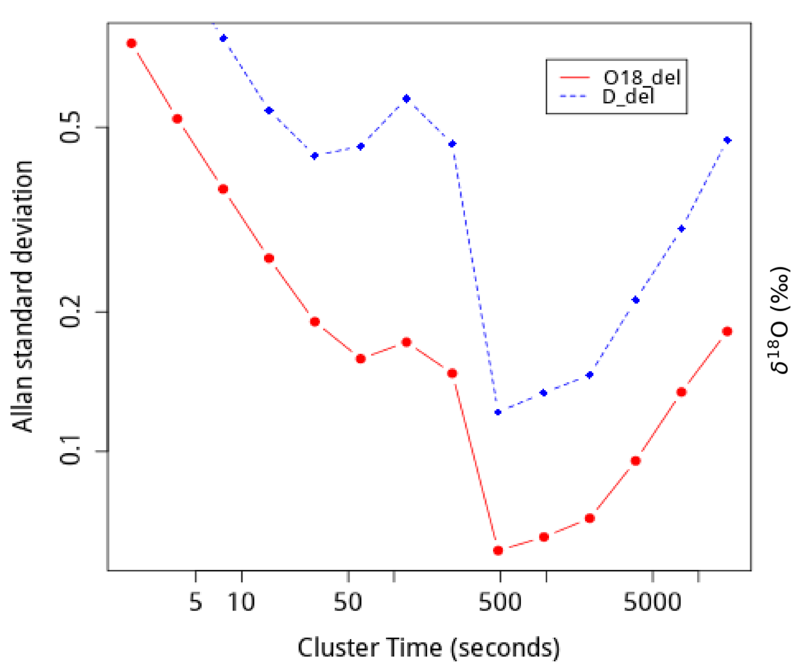

Fig. 2: Min. Allan deviation at 482 s.

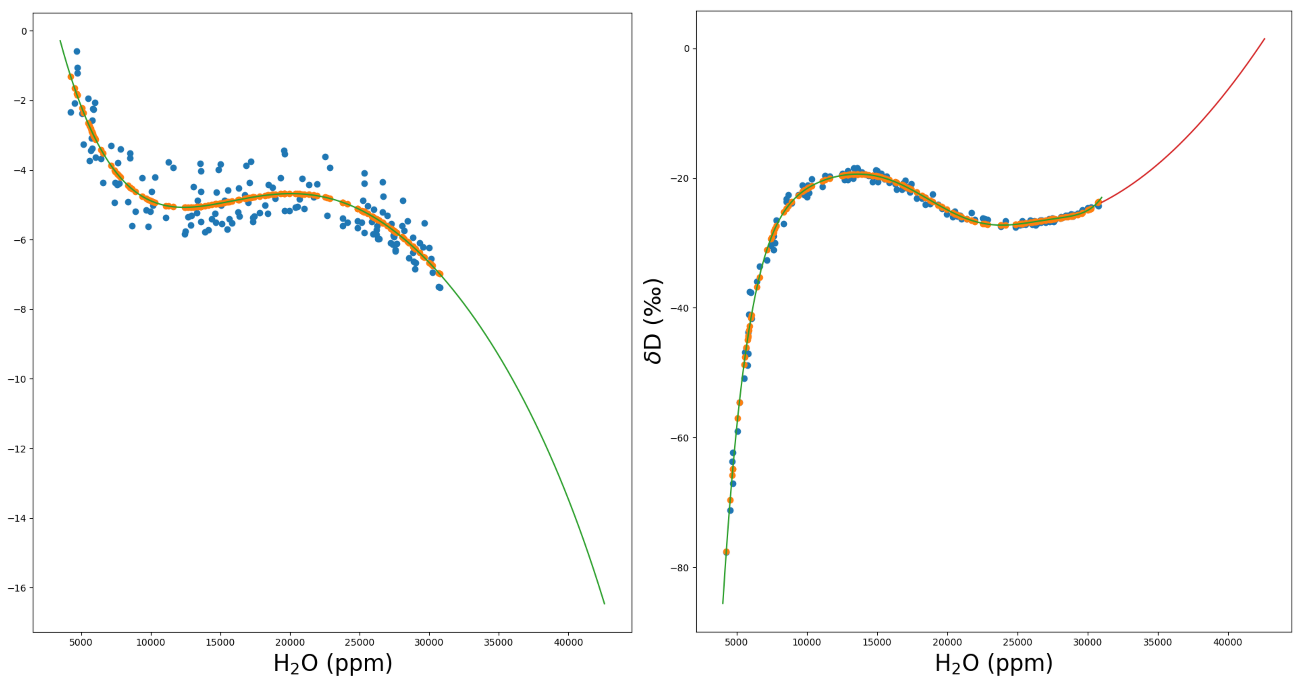

Fig. 3: Humidity-isotope response calibration of $\delta^{18}O$ and δD.

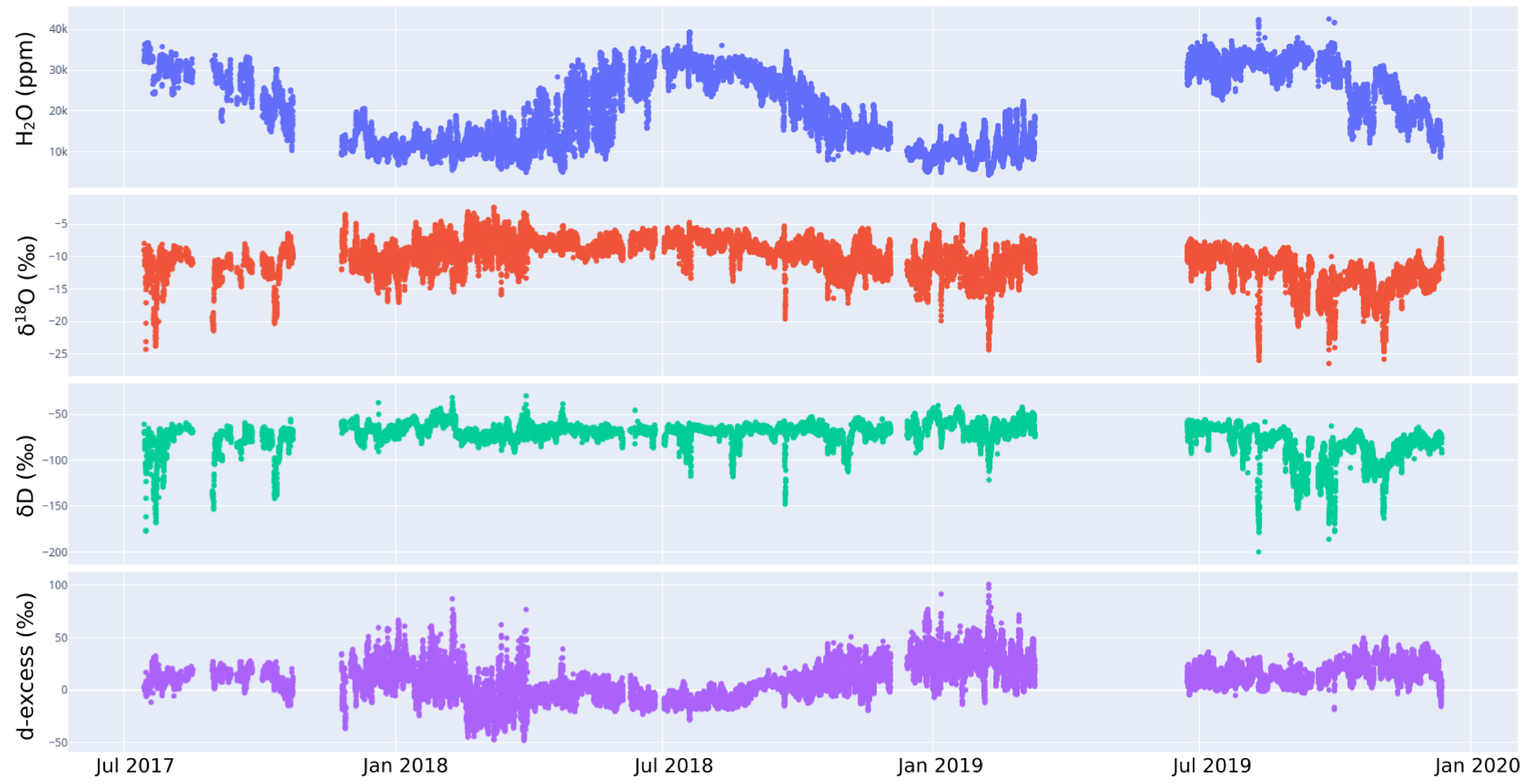

Fig. 4 : Water vapour isotopic composition data for the period of July 2017 to December 2019.

Analysis of a Post-Monsoon Period

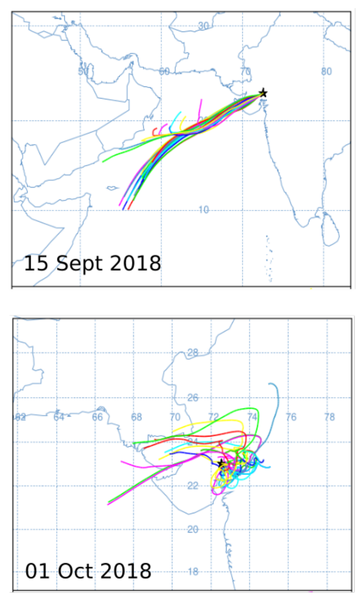

- The depletion observed on 22 Sep 2018 corresponds to a rain event following which the declining trend in mixing ratio indicates withdrawal of monsoon.
- The onset of dry conditions is characterized by an increase in d-excess values along with higher variability. This is attributed to the shift of the source of moisture from oceanic sources to locally recycled evaporated components, as seen from the HYSPLIT trajectories.
- Wavelet analysis of d-excess indicates a strong 24 hour component after the withdrawal of monsoon, which is due to the dominance of locally recycled evaporated components. Evaporation being a kinetic process, has a strong dependence on atmospheric parameters, which have a diurnal variation.

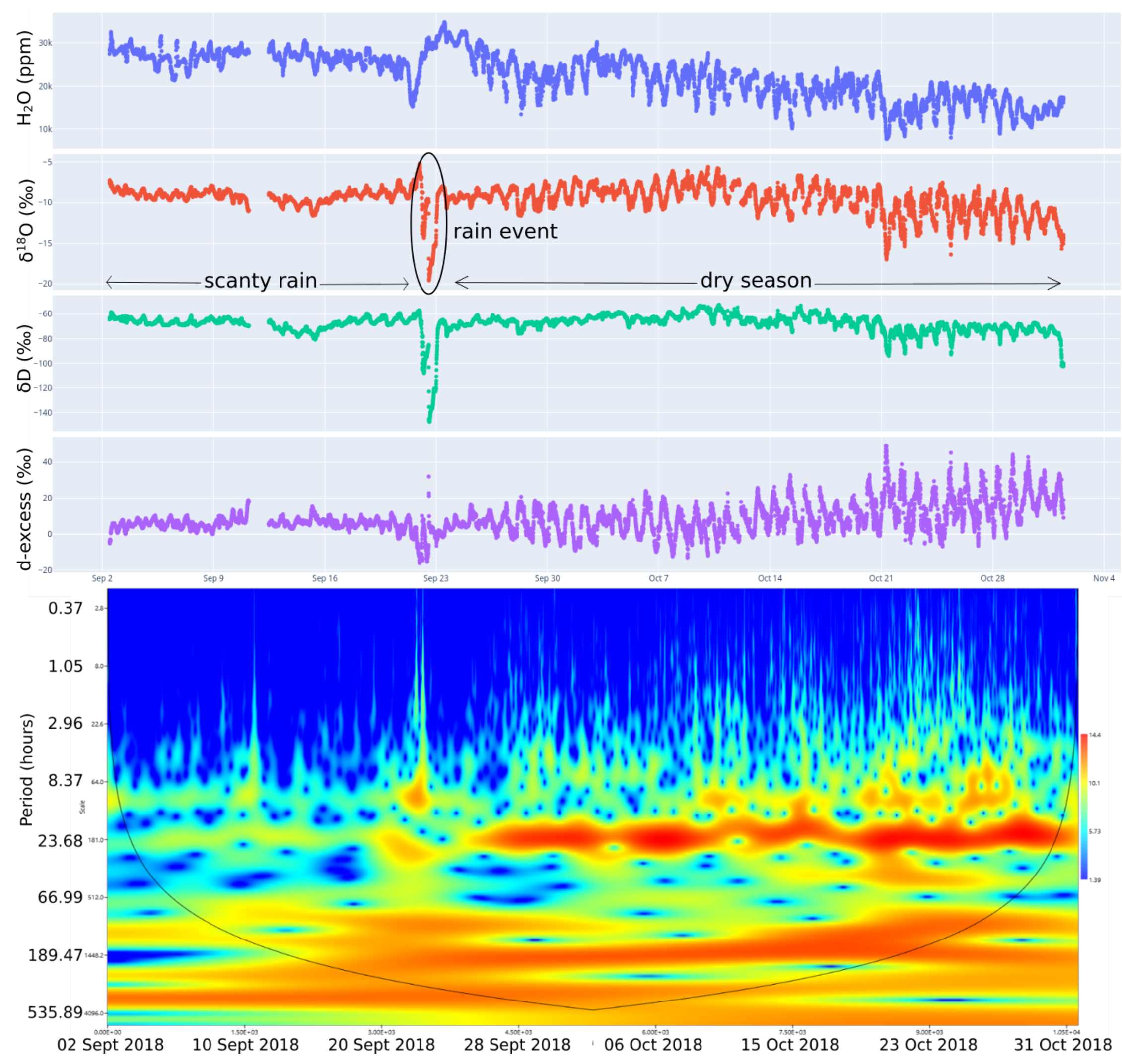

Fig. 5 : Post monsoon period from Sep 2018 to Nov 2018.

Future Directions

- Investigate meteorological events occuring at smaller timescales and the factors contributing to them.
- Understand the correlation of stable isotopic composition of ambient water vapour with various atmospheric parameters.
- Identify and quantify the variability in sources of moisture in different seasons.

Contact

1. pratheeksha@prl.res.in
2. pkirankumar-cgwb@gov.in
3. myadava@prl.res.in

References

1. Galewsky, J., Steen-Larsen, H. C., Field, R. D., Worden, J., Risi, C., & Schneider, M. (2016). Stable isotopes in atmospheric water vapor and applications to the hydrologic cycle. Reviews of Geophysics, 54(4), 809–865.
2. Clark, I. D., and P. Fritz. (1997). Environmental Isotopes in Hydrogeology, 328 pp., CRC Press, Boca Raton, Fla.
3. Steen-Larsen, H., Johnsen, S., Masson-Delmotte, V., Stenni, B., Risi, C., Sodemann, H., Balslev-Clausen, D., Blunier, T., Dahl-Jensen, D., Ellehøj, M., Falourd, S., Gkinis, V., Grindsted, A., Jouzel, J., Popp, T., Sheldon, S., Simonsen, S., Sjolte, J., Steffensen, J., & White, J. (2013). Continuous monitoring of summer surface water vapour isotopic composition above the Greenland Ice Sheet. Atmospheric Chemistry and Physics Discussions, 13.

Silicicclastic paleosols revealed paleoclimatic and provenance geochemistry during Gondwana sedimentation; featuring permo- Triassic sequences of Satpura Basin, Madhya Pradesh, India.

Y. Priyananda Singh[a]*, Oinam Kingson[b], K. Milankumar Sharma[a], Jitendra Kumar Pattanaik[a], Ningthoujam Premjit Singh[c] and N. Amardas Singh[a].

[a]Department of Geology, Central University of Punjab, VDO Guddah, Bathinda-151401, India.
[b]Department of Geology, Institute of Science, Banaras Hindu University, Vanarasi-221005, India.
[c]Wadia Institute of Himalayan Geology, Dheradun-248001, India.
*Corresponding author: priyananda1234@gmail.com (Y. Priyananda Singh)

Introduction: Our study integrate the existing geochemical data for different formations of the Satpura basin and compares them with that of Denwa sediments to better understand the shift in the provenances, tectonic setting, paleoweathering and paleoclimates during deposition. We estimated relative contribution of the source rocks involved for sedimentation during deposition of different formations and generated a conceptual model for the evolution of the basin sedimentation.

Geological setting:

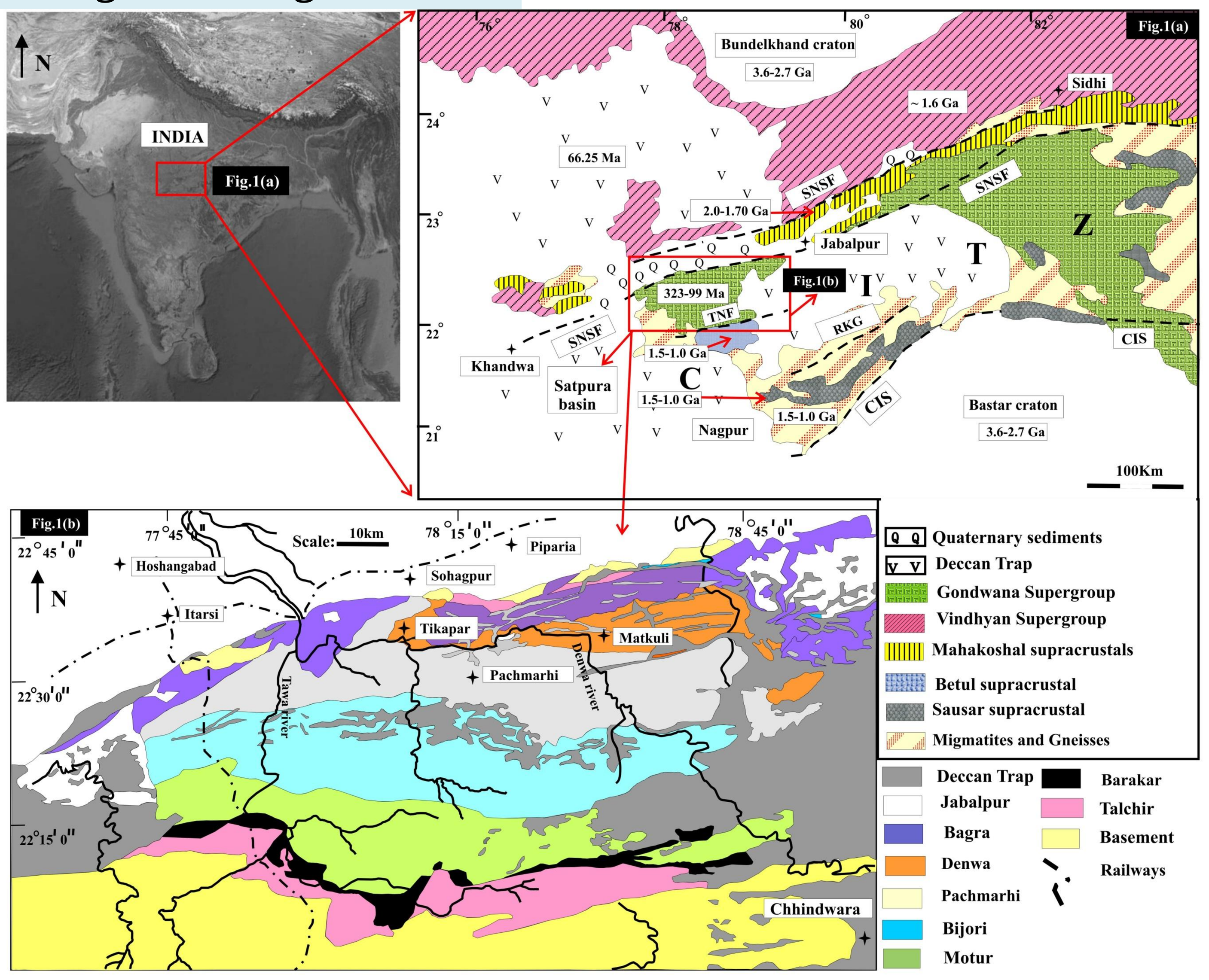

Fig. 1. (a) Geological map of the central sector of the CITZ (Modified after, Roy et al., 2001). Abbreviations: CIS-Central Indian Shear Zone, SNNF-Son-Narmada North Fault, SNSF-Son-Narmada South Fault and TNF- Tapti North Fault. (b) Geological map of the Satpura Gondwana Succession, Central India (Maulik et al., 2000; Chakraborty and Ghosh, 2008).

Methodology: A total of 30 samples were subjected to the analysis of major, trace and rare earth elemental concentration using X-Ray Fluorescence Spectrometer and Inductively Coupled Plasma Mass Spectrometry.

Results: Major element concentrations show SiO_2 (55.4 to 81.12 wt.%); moderate Al_2O_3 (8.81-19.46 wt.%), low TiO_2 (0.11 to 1.11 wt.%), Fe_2O_3 (8.64 to 0.23 wt. %), MnO (0.01 to 0.16 wt.%), MgO (0.52 to 3.14 wt.%), CaO (0.19 to 1.64 wt.%), Na_2O (0.08 to 2.92 wt.%,) and K_2O (0.14 to 4.54 wt.%) concentration .

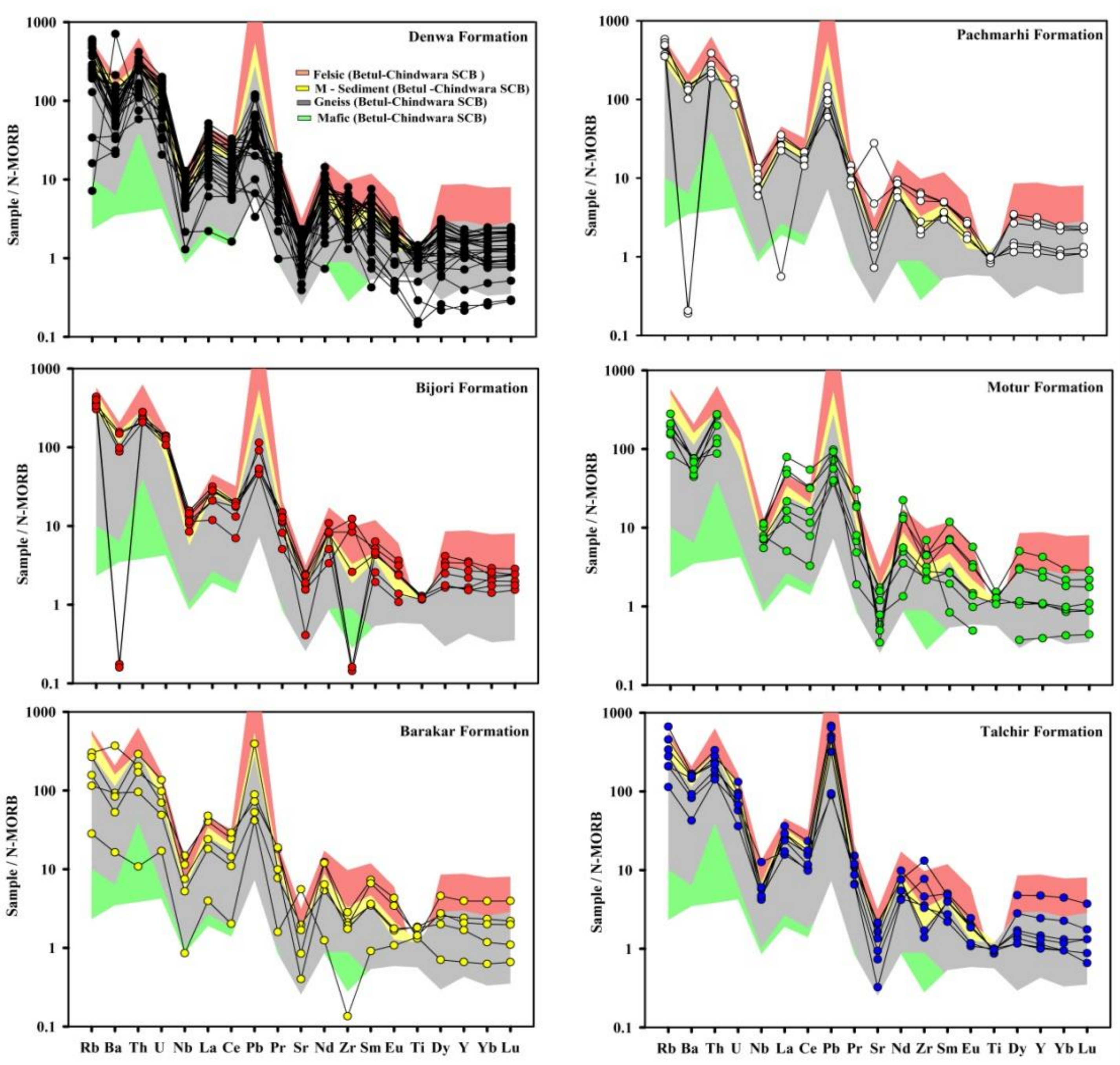

Fig. 2. N-MORB normalized multi element plots for the samples of the Satpura basin and the basement with normalizing values (Sun and McDounough, 1989). The multi elements pattern of different formations of the Satpura basin except the Denwa Formation and basements rocks- are using the published data of Gosh and Sarkar (2010). The published data of felsic volcanic (Yousuf et al., 2019) and mafic volcanic (Alam et al., 2009) were also used for the basements.

Discussion:

a) Paleoweathering and paleoclimate:

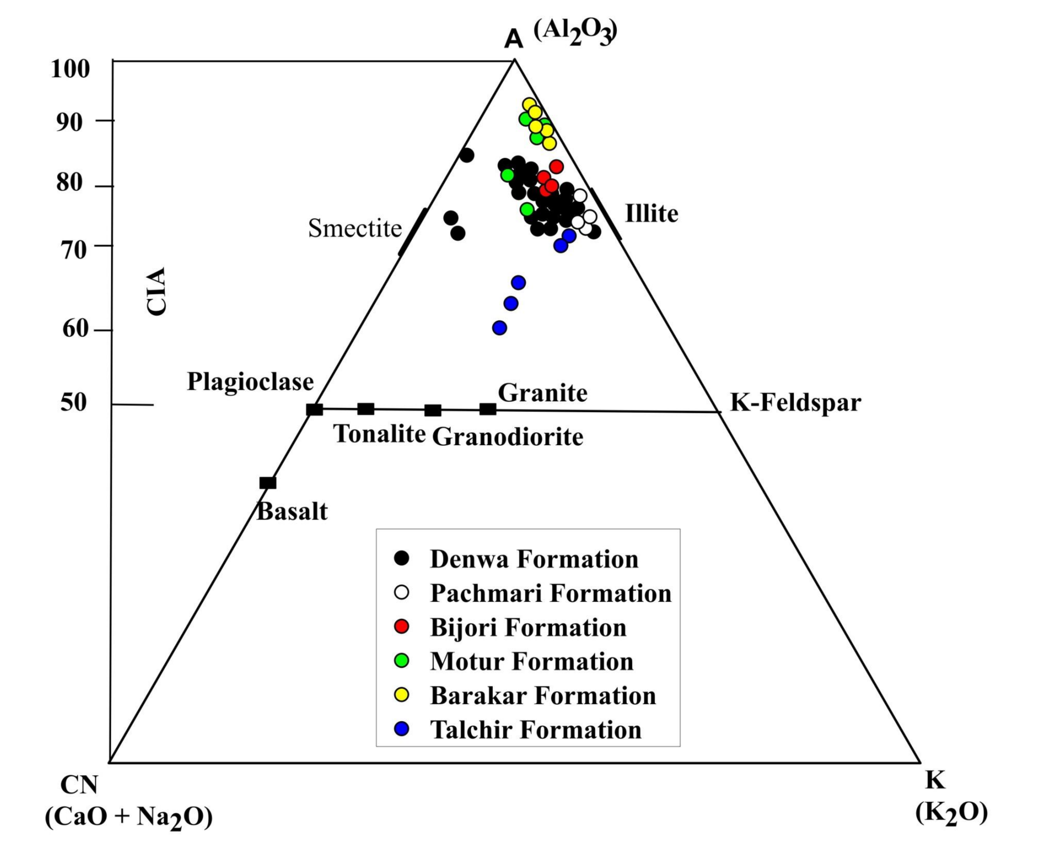

Fig. 3. Plots in the A-CN-K diagram (Nesbitt, 2003) for mudstones of the Talchir, Barakar, Motur, Bijori, Pachmarhi and Denwa formations. Data for the formations except Denwa Formationare used from the Published data (Ghosh and Sarkar, 2010).

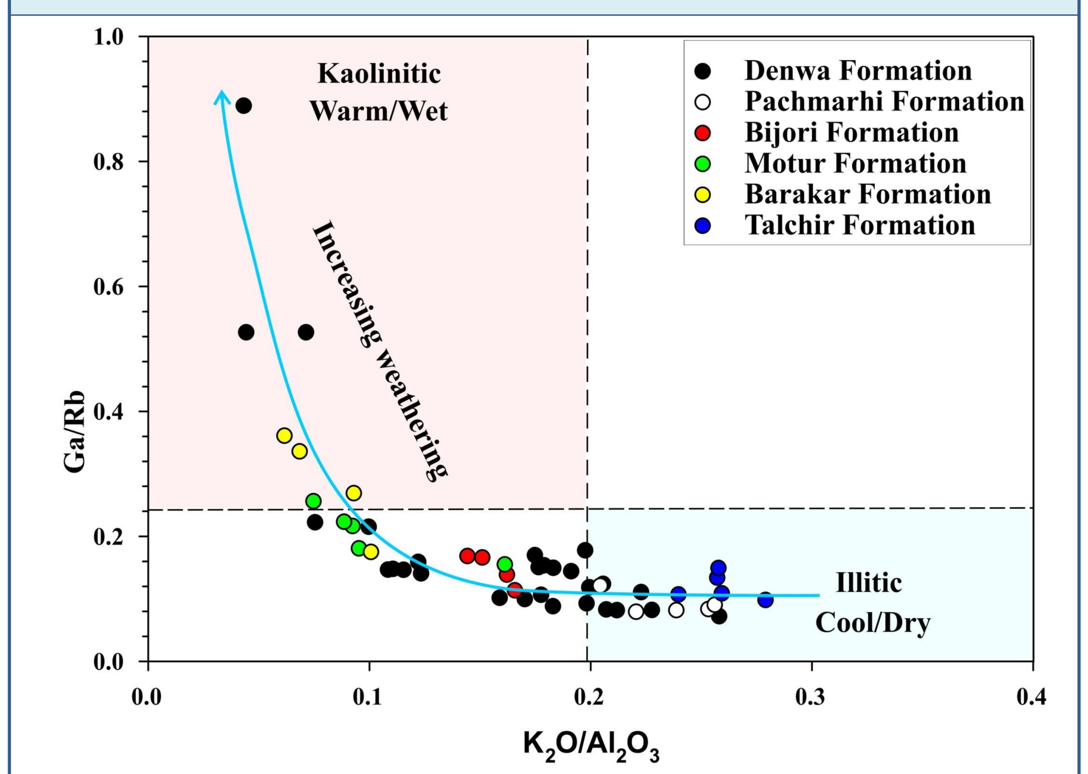

Fig. 4. K2O/Al2O3 vs Ga/Rb diagram (Roy 2013).The plots of other formations of Satpura basin except Denwa Formation have used the published data (Ghosh and Sarkar, 2010).

b) Provenance and basin evolution:

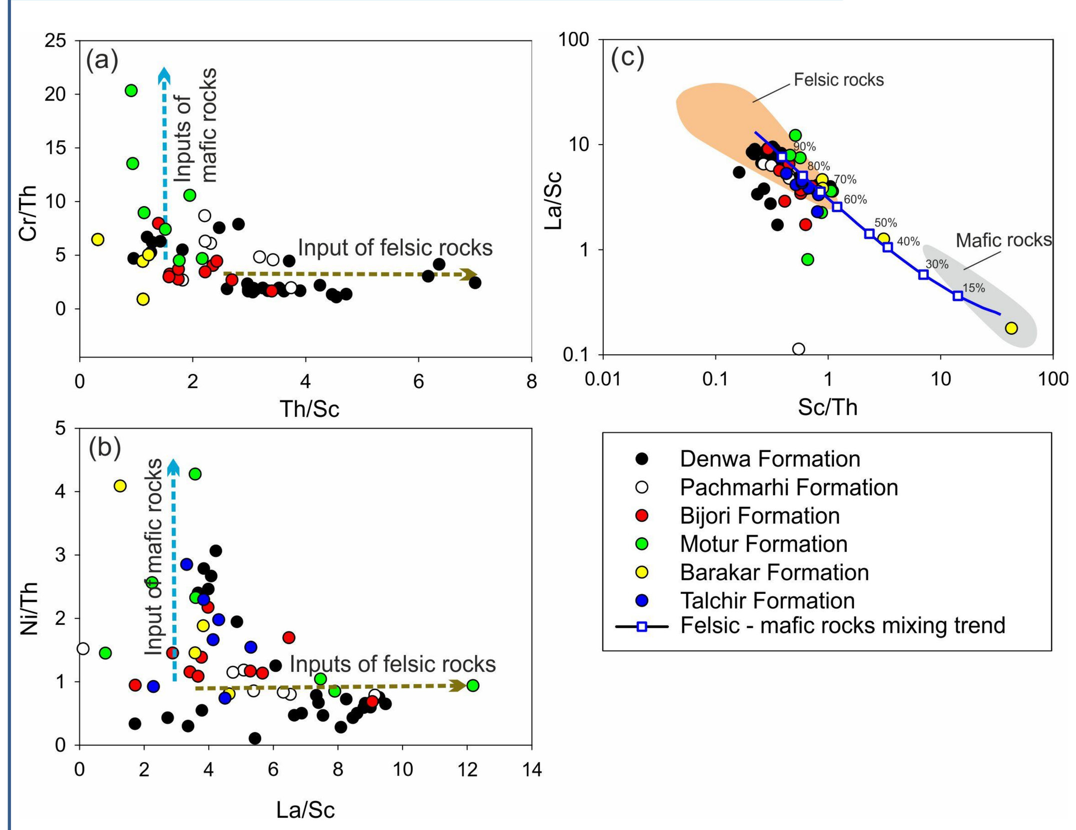

Fig. 5. (a) Th/Sc vs Cr/Th plots (after Condie and Wronkiewicz, 1990) of the Satpura basin, India. (b) La/Sc vs Ni/Th plots of the Satpura basin, India. Except the Denwa Formation, all the plots of the formations of Satpura basinsand the basement rocks are taken from the published data (Ghosh and Sarkar, 2010). Data of the felsic volcanic rocks after Yousuf et al, (2019) and data of the mafic volcanic rocks after Alam et al., (2009) were utilized.

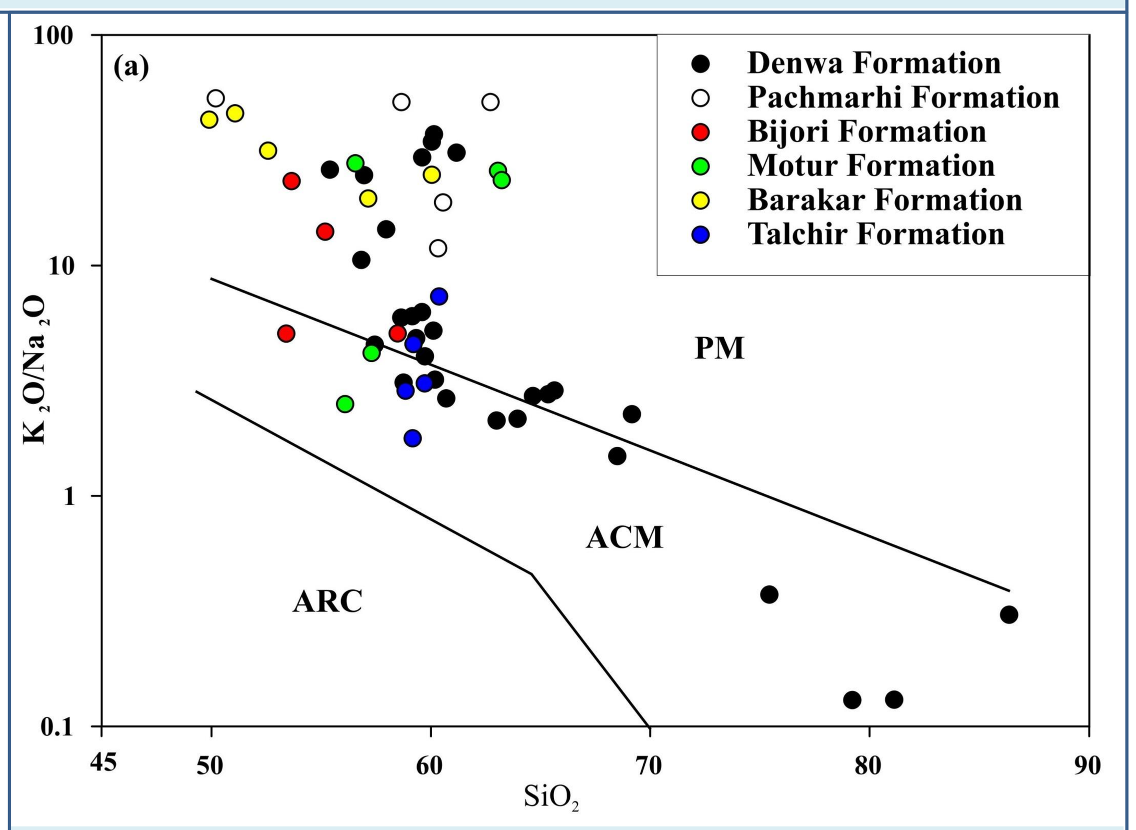

Fig. 6. The SiO2 vs K2O/Na2O tectonic setting diagram (after, Roser and Korsch, 1986) of the samples from the Satpura basin. The geochemical data of all the formations except Denwa Formation were taken from Ghosh and Sarkar, (2010).

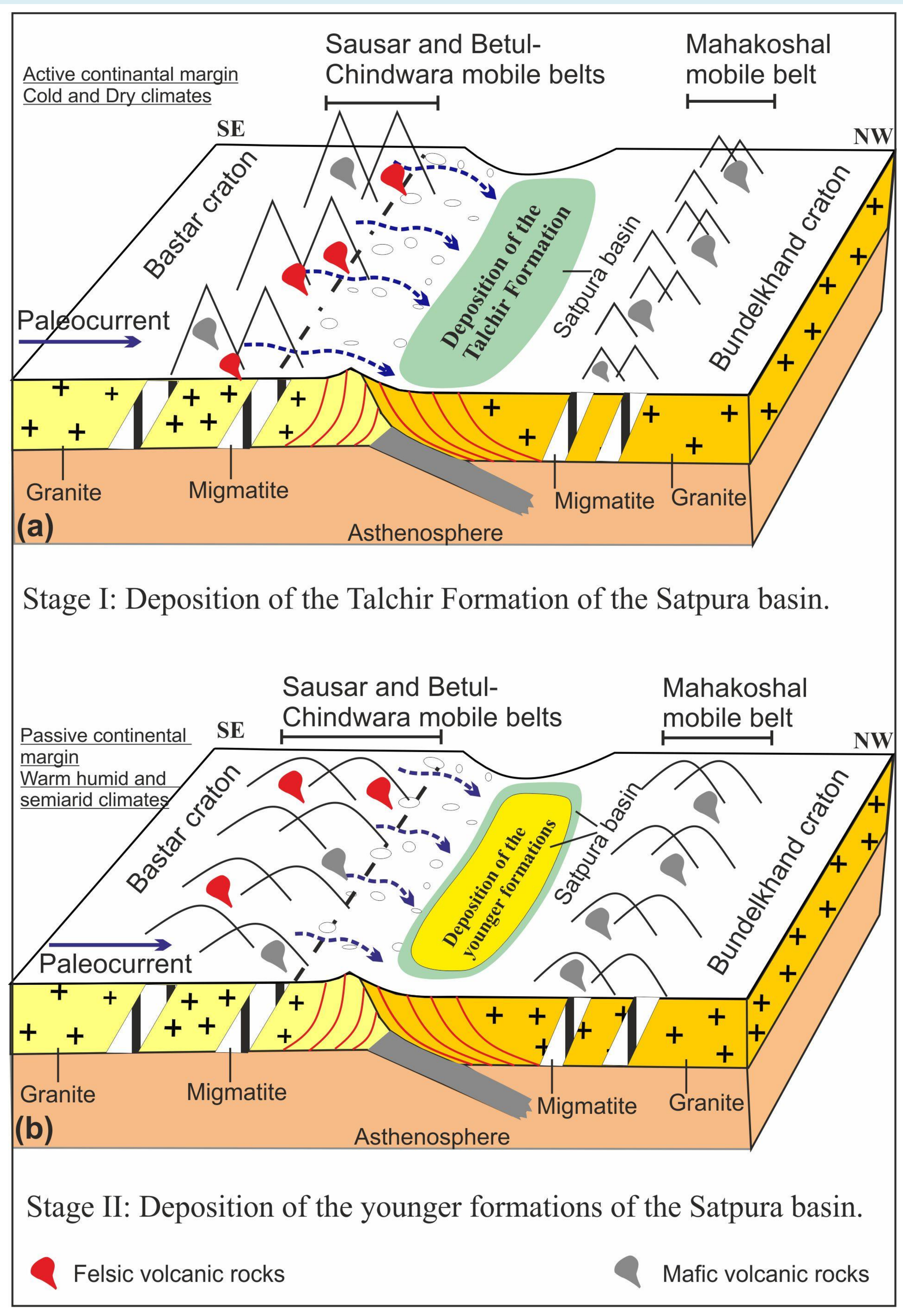

Fig. 7. Cartoon diagram depicting the evolution of the Satpura basin.

Conclusion:

1. the Denwa, Pachmarhi and Bijori formations have experienced warm and semi-arid climate, Motur and Barakar formations have recorded hot and humid climate and the Talchir Formation has experienced cold and arid climatic conditions.
2. The sediments of Pachmarhi, Bijori and Denwa formations were derived mainly from felsic sources but mafic rock-derived sediments are relatively higher in the Talchir, Barakar and Motur formations.
3. The sources which have supplied the sediments to the Satpura basin have experienced mixed tectonic settings i.e., active and passive continental margins.

Acknowlegdge: K M Sharma is thankful to SERB-DST for Early Career Research(ECR/2016/001100) and YPS is thankful to SERB for providing JRF.

Reference: Roser and Korsch, 1986; Sun and McDounough, 1989; Condie and Wronkiewicz, 1990; Maulik et al., 2000; Nesbitt, 2003; Chakraborty and Ghosh, 2008; Gosh and Sarkar, 2010; Alam et al., 2009; Yousuf et al, 2019.

Timing and mechanism for the onset of modern like deep water circulation in the Indian Ocean

*Priyesh Prabhat, Waliur Rahaman, Lathika N., Mohd Tarique, Ravi Mishra

Affiliation: National Centre For Polar And Ocean Research, Goa

*Email: priyeshprabhat@hotmail.com

Introduction

Tectonically driven re-organisation of seaways had influenced the late Neogene climate globally and regionally. Such re-organisations and associated changes in global climate had a direct impact on the global overturning circulation, influencing the formation of deep-water masses at high latitudes such as North Atlantic Deep Water (NADW) and Antarctic Bottom Water (AABW), and their export to the global ocean.

Due to the absence of any major deep water formations, Indian Ocean only acts as a host for abyssal water and hence provides an ideal location to test prevailing hypothesis related to the timings and mechanisms for the onset of modern like deep water circulation system.

In the present study, we extracted authigenic Nd of sediments from the deeper depths of the Arabian Sea core site U1457. We used Nd isotopic composition (ε_{Nd}) to reconstruct the deep water circulation in the Indian Ocean during the late Miocene to early Pleistocene (11.3 to 1.98 Ma).

$$\varepsilon_{Nd} = [(^{143}Nd/^{144}Nd)_{sample}/(^{143}Nd/^{144}Nd)_{CHUR} - 1] \times 10^4$$, where CHUR (Chondritic Uniform Reservoir) has $^{43}Nd/^{144}Nd$ ratio 0.512638

The quasi-conservative property and the short residence time (~300-1000 years) of the Nd in the water column makes it a reliable tracer for water mass mixing.

Study Area

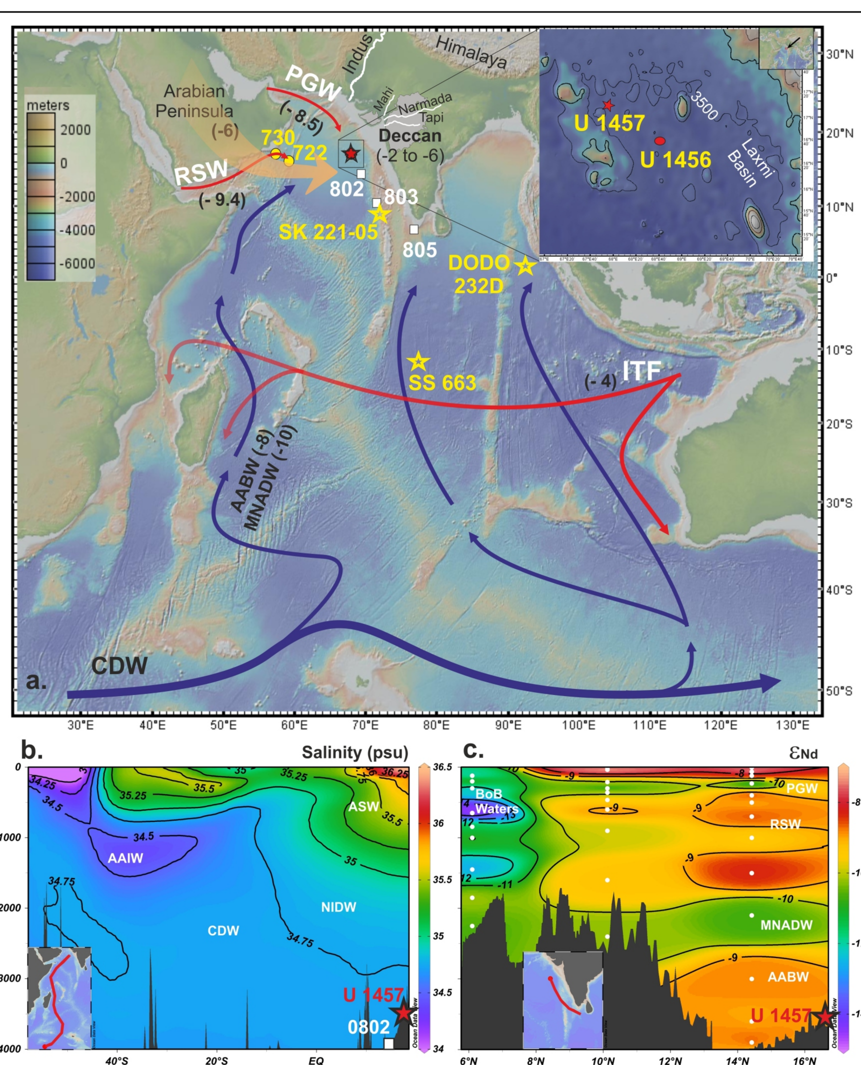

- Core : IODP expedition 355, Site U1457
- Location : 17°9.95' N, 67°55.81' E
- Water Depth: 3522 m
- Modern day study site is bathed by the mixture of modified NADW and AABW
- ε_{Nd} value of modern day water column at 3500 m water depth from nearby water station (802) is -9 ± 0.4
- Unlike Bay of Bengal, Arabian Sea is not affected by the release of particulate Nd supplied by the Himalayan river system.

Materials and methods

Archives Used

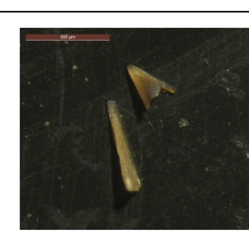

Authigenic Fraction of Sediments	Fish teeth/debris
Powdering of Sediment Sample & addition of Hydroxylamine Hydrochloride (HH) Leach	Picking of fish teeth (>150μ) and cleaning it with methanol followed by MilliQ
↓	↓
Ultrasonication of the sample, followed by centrifugation	Ultrasonication of the sample, followed by centrifugation
↓	↓
Collection of supernatant, with authigenic component in it, followed by drying	Treated the sample with 1:1 solution of H_2O_2 and MilliQ and dissolved in $HCl:HNO_3$(1:1)
↓	↓
Two stage chromatographic separation and the purification of Nd	Two stage chromatographic separation and the purification of Nd
↓	↓
Measurement of Nd using MC-ICP-MS	Measurement of Nd using MC-ICP-MS

Results and discussion

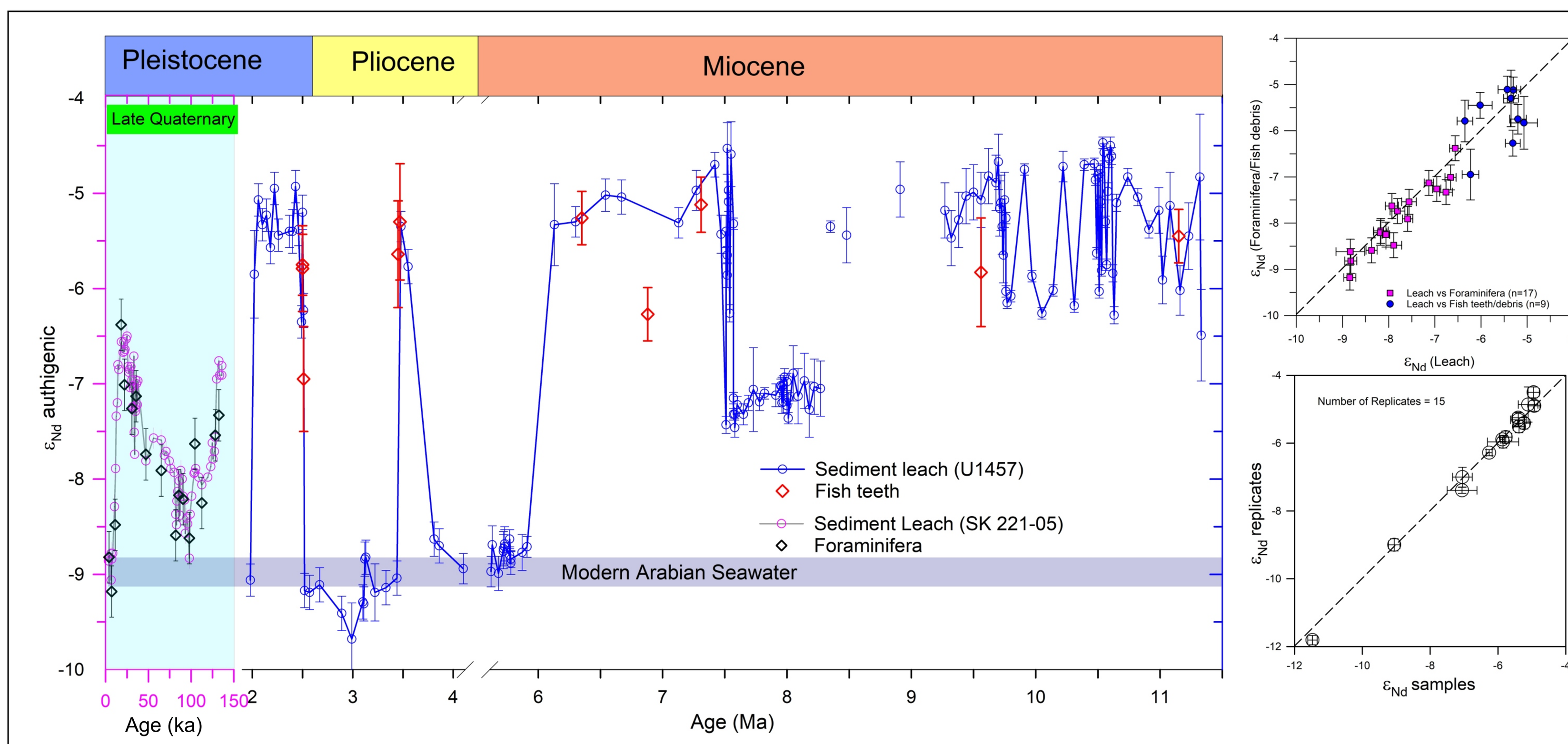

- The overall ε_{Nd} variability recorded at study site is between -9 to -4.5.
- This variability is higher than the earlier report from the Arabian Sea and equatorial Indian ocean record (-9 to -6.5) during the late Quaternary glacial-interglacial periods.
- The ε_{Nd} record shows an average of -5.5 ± 1 from 11.2 Ma to 9.3 Ma.
- Afterwards, ε_{Nd} pofile shows over all declining trend with three distinct positive excursions of similar magnitude (-5.5 ± 0.5) during the past intervals of 7.4 to 6 Ma, ~3.5 Ma and 2.5 to 2 Ma.

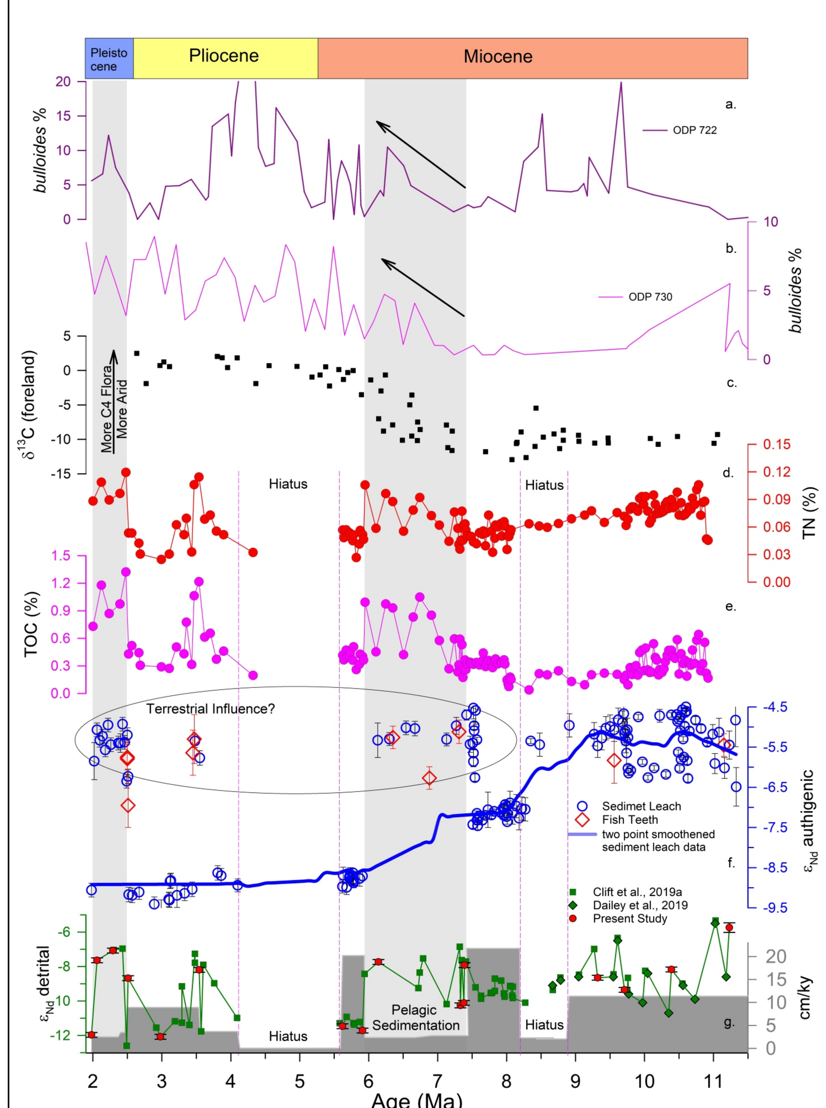

- The periods of the positive excursions in the authigenic ε_{Nd} profile coincides with, slow sedimentation rate, increasing detrital ε_{Nd} value, arid condition and the higher percentage of total nitrogen (TN%) and total organic carbon percentage (TOC%) indicating higher productivity.
- These period can be considered to be influenced by the terrestrial input possibly due to enhanced supply and dissolution of the dust from Arabian peninsula.
- The smoothed authigenic ε_{Nd} curve (bule line) based on two points running average, excluding the extremely radiogenic values highlighted in circle (Figure f) shows a long-term discernible declining trend from -5.5 ± 1 at ~9 Ma and to -9 ± 0.5 at ~6 Ma which is similar to that of the late Holocene and modern values in the Arabian Sea.

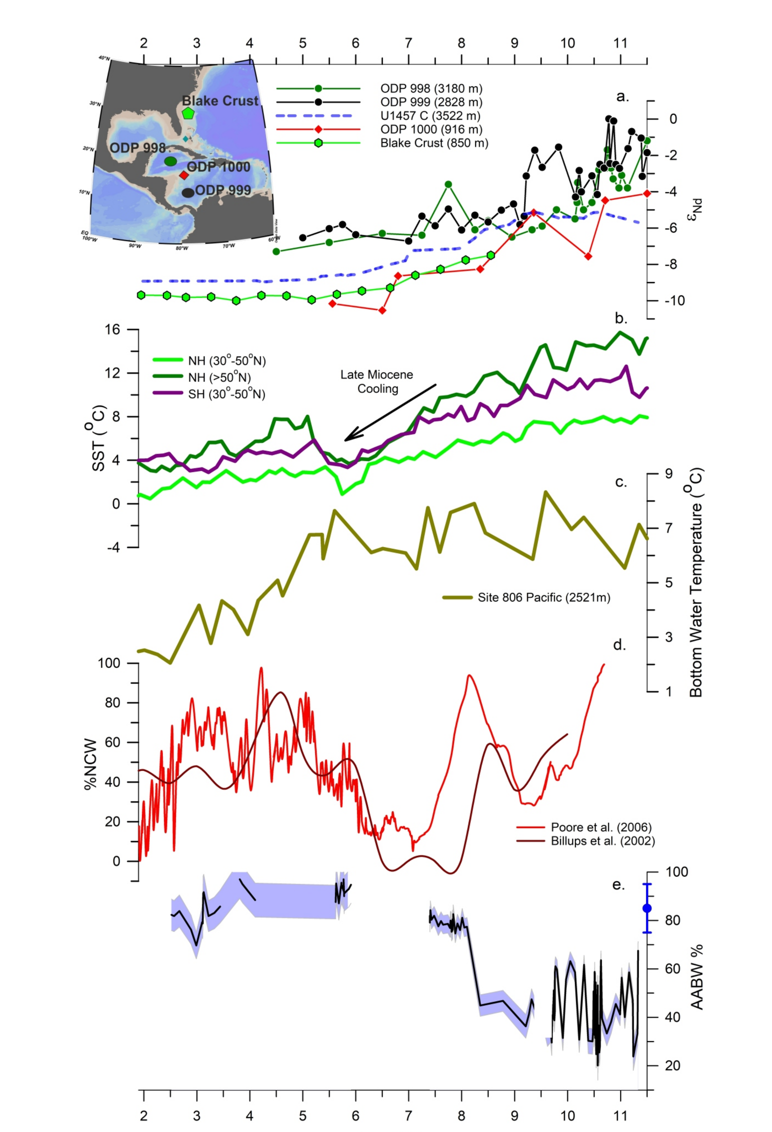

- Influx of PW into the Atlantic Ocean gradually reduced after 9.5 Ma as reflected in the ε_{Nd} records from the Caribbean Sea due to the constriction of the Central American Seaway (CAS) and the NCW (proto NADW) was established in its full strength at ~6Ma.
- Evidence suggests that during early late Miocene, the AABW exported to the Arabian Sea had higher percentage of rPDW charcterised by more radiogenic ε_{Nd} and less influx of NCW.
- ε_{Nd} values at study site became less radiogenic (-9) at ~6Ma like Holocene and modern values with the increased southward influx of the NCW.
- The increased production of NCW was also aided by the late Miocene cooling events.

Conclusions

- Strong, warm and fresh Pacific water (PW) influx to the Atlantic Ocean resulted in weaker AMOC and weaker NCW export to southern ocean for the past 11.2 to 1.9 Ma. In addition, the rPDW and the AABW formed the major component of CDW.
- Constriction and shoaling of the CAS resulted in reduced influx of PW to the Atlantic Ocean, strengthening of the AMOC and enhanced export of NCW to southern ocean during the interval of 9 to 6 Ma. This also resulted increase in NADW and decrease rPDW contribution to the CDW.
- Constriction of CAS to its final stage and its shoaling to critical height resulted in near complete cessation of PW influx into Atlantic. Further, aided by northern hemisphere cooling (between 8-6 Ma) AMOC strengthened and resulted in increased NCW formation with physical properties similar to that of modern day. This strengthened NCW mixed with AABW to form CDW with properties similar to modern day.

References

Clift, P. D., Zhou, P., Stockli, D. F., and Blusztajn, J., 2019, Regional Pliocene exhumation of the Lesser Himalaya in the Indus drainage: Solid Earth, v. 10, no. 3, p. 647-661.

Goswami, V., Singh, S. K., and Bhushan, R., 2014, Impact of water mass mixing and dust deposition on Nd concentration and ε Nd of the Arabian Sea water column: Geochimica et Cosmochimica Acta, v. 145, p. 30-49.

Khim, B.-K., Lee, J., Ha, S., Park, J., Pandey, D. K., Clift, P. D., Kulhanek, D. K., Steinke, S., Griffith, E. M., Suzuki, K., and Xu, Z., 2019, Variations in δ13C values of sedimentary organic matter since late Miocene time in the Indus Fan (IODP Site 1457) of the eastern Arabian Sea: Geological Magazine, p. 1-10.

Lathika, N., Rahaman, W., Tarique, M., Gandhi, N., Kumar, A., and Thamban, M., 2021, Deep water circulation in the Arabian Sea during the last glacial cycle: Implications for paleo-redox condition, carbon sink and atmospheric CO2 variability: Quaternary Science Reviews, v. 257, p. 106853.

Revised calibration for otolith clumped isotope thermometry: An extended application to determine growth temperature of travertine

SANCHITA BANERJEE[1], PROSENJIT GHOSH[*,1,2], LUIS F. AUQUÉ SANZ[3], CINTA OSÁCAR[3], MARÍA J. GIMENO[3], STEVEN E CAMPANA[4], JOHN EILER[5]

[1]Centre for Earth Sciences, Indian Institute of Science, Bangalore- 560 012, India; [2]Divecha Centre for Climate Change, Indian Institute of Science, Bangalore, India; [3]Department of Earth Sciences, University of Zaragoza, C/Pedro Cerbuna 12, 50009, Zaragoza, Spain; [4] Life and Environmental Science, University of Iceland, Reykjavik, Iceland; [5] Division of Geological and Planetary Sciences, California Institute of Technology, Pasadena, CA, 91125, USA.

Abstract

The empirical relationships of clumped isotope thermometry[1] useful in paleotemperature determination from natural carbonates can be categorized into biogenic and abiogenic types. The mechanism of precipitation for these sets of carbonates differs, depending on presence or absence of enzymatic reactions which govern the reaction kinetics. In this study, we have revisited the clumped isotope analysis using Break seal method[2] on six aragonitic otolith specimens with known growth temperature (2-25°C), which were analyzed earlier for the calibration[3] purposes. Previous calibration results are re-evaluated from raw data incorporating updated scaling factors and compared with the present study. The revised calibration for aragonitic otoliths proposed here is given by the equation with temperature (T) expressed in degree Kelvin:

$$\Delta_{47} = 0.0594 \pm 0.0049 * \frac{10^6}{T^2} + 0.0541 \pm 0.0576$$

The revised calibration is extended to include abiogenic travertines[4] (containing aragonite and calcite) from Fitero thermal spring, Spain, grown at a temperature range between 33-40°C. We have also compared the offset of estimated clumped temperature from actual or observed growth temperatures for travertines adapting different empirical relationship proposed for calcite and aragonite minerals. Our observations showed the role of acid digestion protocol and reaction temperature during experimentation in controlling the extent of deviation of clumped temperature from the actual depositional temperature. A systematic offset in clumped isotope values for different acid digestion reactions protocols is established here and can serve as a tool to compare and correct results from using different acid digestion protocol and temperature.

CONTACT

Prof. Prosenjit Ghosh
Centre for Earth Sciences
Indian Institute of Science
Bangalore
Email: pghosh@iisc.ac.in
Phone: +918022932599
Website:http://ceas.iisc.ernet.in/~pghosh/pghosh/oasis.html

Introduction

Fish otoliths are small white aragonitic structures found in the heads of fish that grow continuously. An otolith can contain a complete record of both the temperature and composition of the water in which the host fish lived, and these variables can be reconstructed using spatially resolved isotopic analyses.

Ghosh et al., 2007 reported the relationship between the abundance of $^{13}C^{18}O^{16}O$, as measured by the Δ_{47} value, in CO_2 produced by phosphoric acid digestion of fish otoliths and the environmental temperatures of the fishes in which those otoliths grew.

[Arctic Exploration 2002, Ian MacDonald, Texas A&M University, NOAA/OER]

Travertine is a form of limestone composed of the minerals calcite and aragonite, ($CaCO_3$) that precipitates at high-temperature hot springs when hot water is expelled from the subsurface. The decrease in pressure and temperature at the surface causes degassing of carbon dioxide dissolved in the water which in turn causes calcium carbonate to precipitate.

Aragonite having two different origin - otolith (biogenic) and travertines (abiogenic) were re-analysed for clumped isotopic studies.

Materials and Methods

Aragonitic travertines

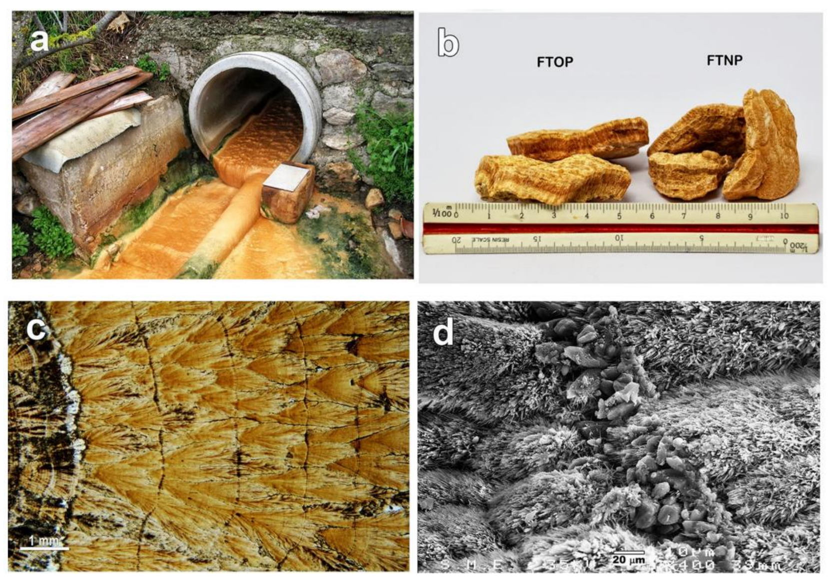

a. New pipe at its discharge point on the Cidacos river, where travertine FTNP is precipitating. b. FTOP and FTNP travertines with alternate yellowish and reddish. c. Fibrous-radial texture with fan-shaped aggregates (FTOP). d. FESEM image of the FTOP travertine showing the aragonitic bands(on the right and left of the image) and a calcite interlayer in between. (Blasco et al., 2020)

Break seal method of clumped isotope analysis

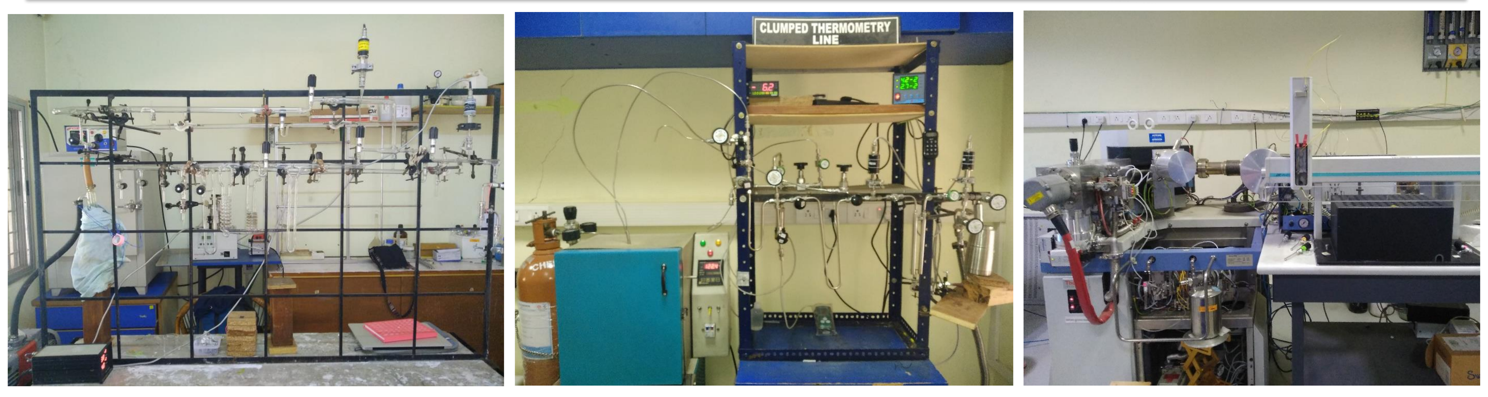

Acid digestion of carbonate using break seal method was found to be efficient for the clumped isotope analysis of carbonates that require longer reaction time at 25°C. Otoliths, travertines and other carbonate reference materials widely used in the clumped isotope community were acid-digested and analysed for their $\delta^{13}C$, $\delta^{18}O$ and Δ_{47} values with a dual inlet MAT 253 isotope ratio mass spectrometer following standard gas chromatography purification and data evaluation protocols.

Results

Revised calibration based on otoliths

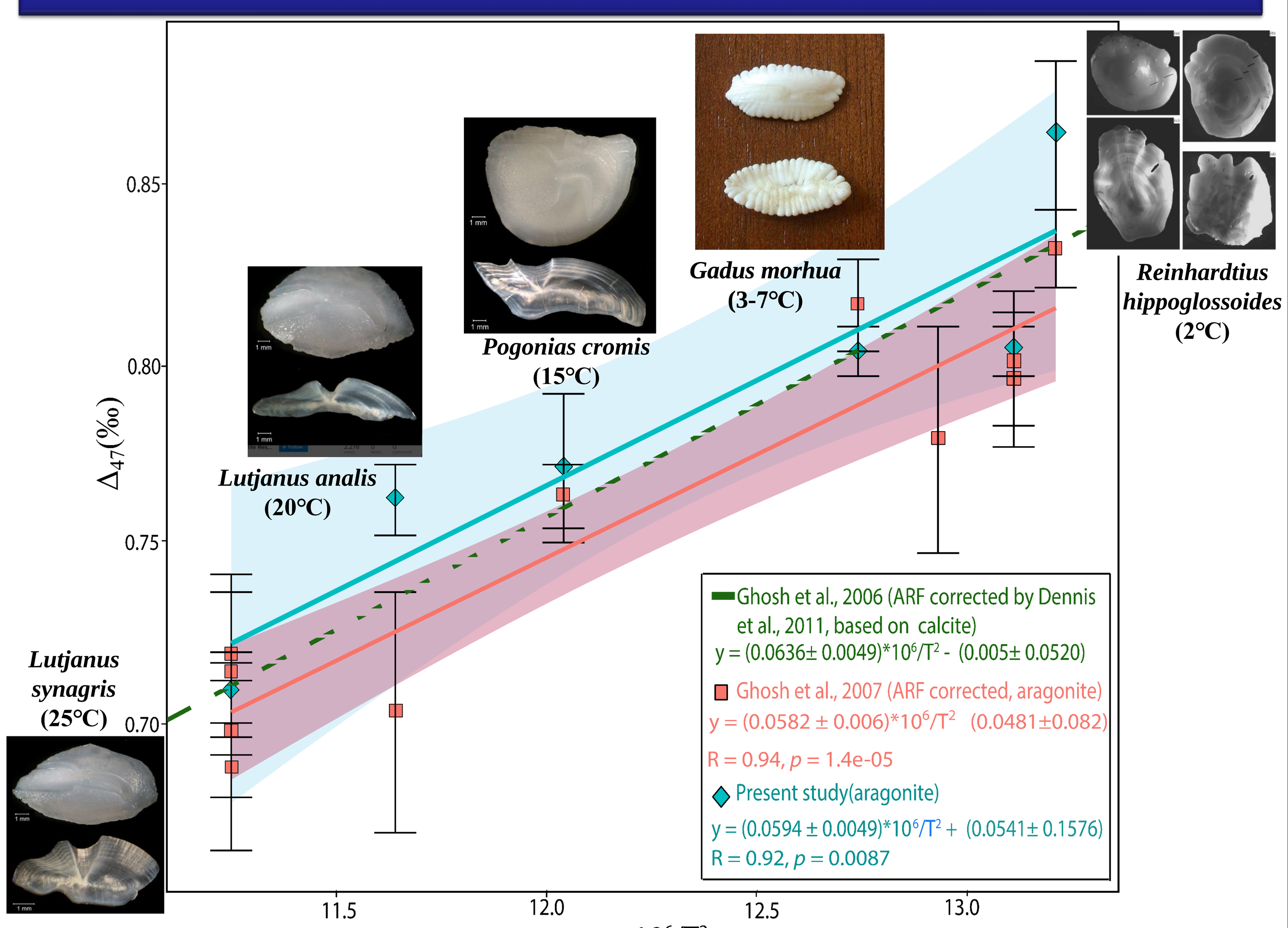

Display of analytical results comparing ARF corrected Δ_{47} values of extracted CO_2 from acid digestion using two different methods and mineralogy; break seal (present study for aragonite) and McCrea type (Ghosh et al., 2006 for calcite and Ghosh et al., 2007 for aragonite) within temperature range of 2-25°C. Note both these methods are indistinguishable.

Application of revised calibration for travertines

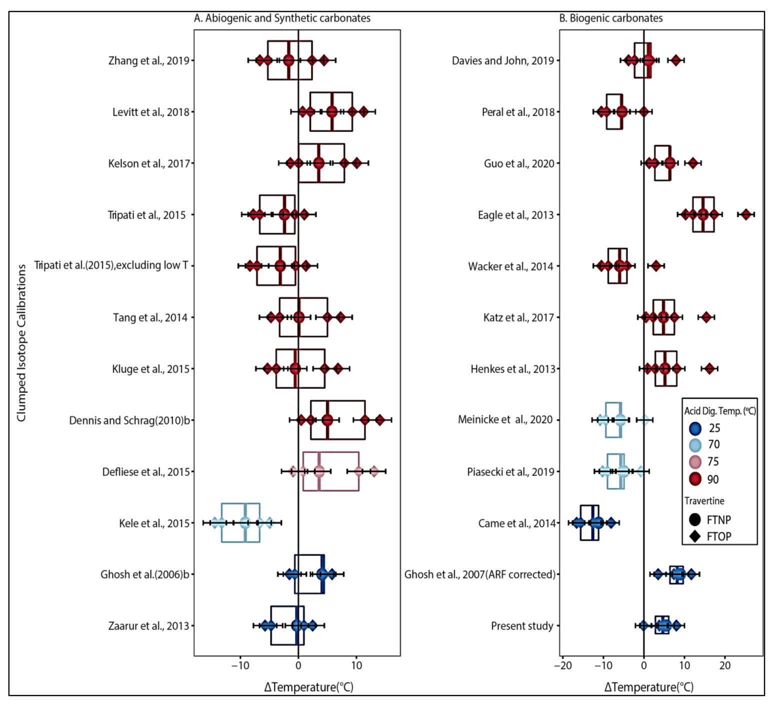

Deviation of clumped isotope temperature estimates using the extension of aragonite otolith thermometry from the true growth temperatures observed for two travertine specimens. Here we plotted the performance of existing clumped isotope thermometry equations after taking into account fractionation due to acid digestion temperatures for A. Synthetic and abiogenic. B. Biogenic calcium carbonates. Note that that the thermometry using, inorganic calcite provides the best estimates and therefore more appropriate for travertine precipitation without any biological interplay.

Oxygen isotope composition of water

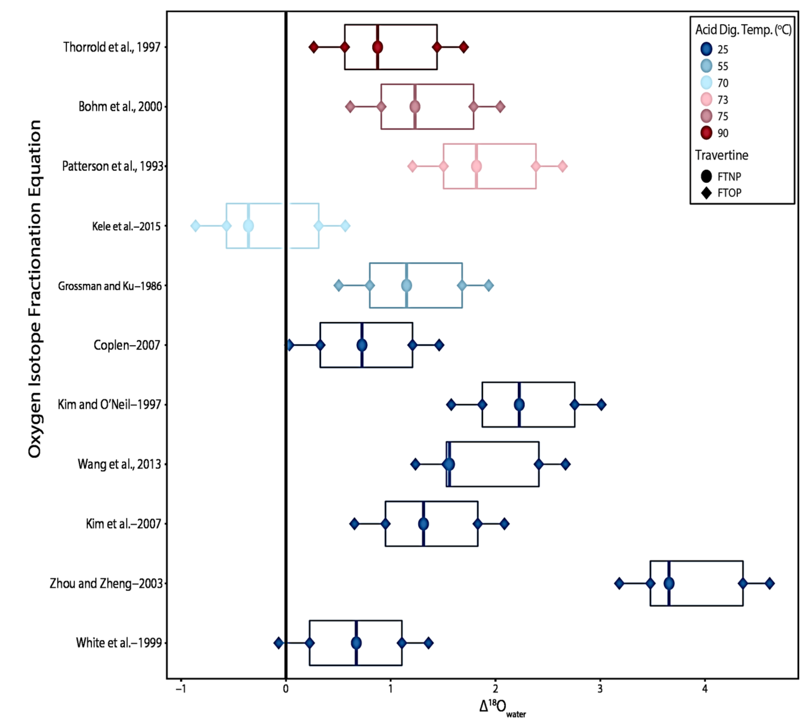

Deviation of oxygen isotopic composition of aragonite($\Delta^{18}O_{water}$) estimated using different empirical relationship available for calcite and aragonite from the observed values recorded during precipitation of carbonates in case of travertines. Performance of different oxygen isotope fractionation equations are evaluated, where Kele et al. (2015) provided best estimates compared to the other equations.

Correction factor for temperature sensitivity and intercept associated with Common Acid Bath and Acid Drip Method

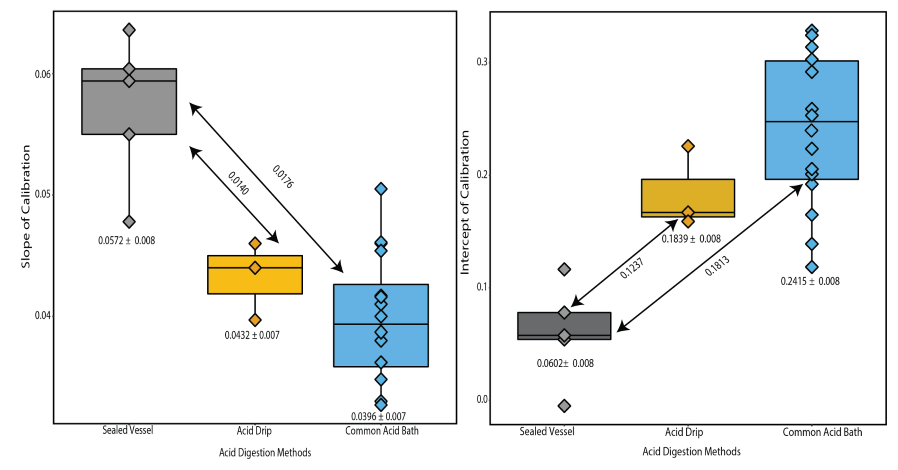

Slopes and intercepts of linear clumped isotope thermometry equations proposed in ARF scale at variable acid digestion temperatures and methods for CO_2 preparation from inorganic synthetic or abiogenic and biogenic calcium carbonates with known growth temperatures.

Experimental observations are categorized into A. McCrea type/ sealed reaction vessel method with 25°C acid digestion temperature, B. Acid drip method with 70°C acid digestion temperature and C. Common Acid Bath method 90°C acid digestion temperature.

Conclusion

The linear relationship defining the Δ_{47} values with carbonate growth temperature is expressed with a temperature sensitivity value of 0.0594. This calibration yields nearly the same temperature sensitivity as the ARF corrected values of the dataset downloading the raw values from Ghosh et al. (2007).

The present study has identified the uncertainty associated with these calibrations represented at 25°C in ARF scale and observed the systematic calibration offset depending on the method adopted for CO_2 preparation.

References

[1] Ghosh et al., 2005 RCM 19; [2] Fosu et al., 2019, RCM 33; [3] Ghosh et al., 2006 GCA 70; [4] Ghosh et al., 2007 GCA 71; [5] Blasco et al 2020, IJES 109; [6] Kele et al., 2015 GCA 168.

Acknowledgements

Council of Scientific and Industrial Research-University Grants Commission, India Ministry of Earth Science (MoES), India and Department of Science and Technology (DST), India

Stable isotopes and nitrogen functionalities in coals and their crafty responses to coal metamorphism

Santanu Ghosh[a,b], Tushar Adsul[a], Anwita Ojha[a], Dinesh Kumar[a,c], Atul Kumar Varma[a]

[a] Coal Geology and Organic Petrology Laboratory, Department of Applied Geology, Indian Institute of Technology (Indian School of Mines) Dhanbad-826004, Jharkhand, India (Corresponding and presenting author's email id: gsantanu09@gmail.com)

[b] Department of Earth Sciences, Indian Institute of Technology Bombay, Powai, Mumbai, Maharashtra, 400076, India

[c] Petroleum Engineering Branch, University Departments, Rajasthan Technical University, Kota 324010, Rajasthan, India

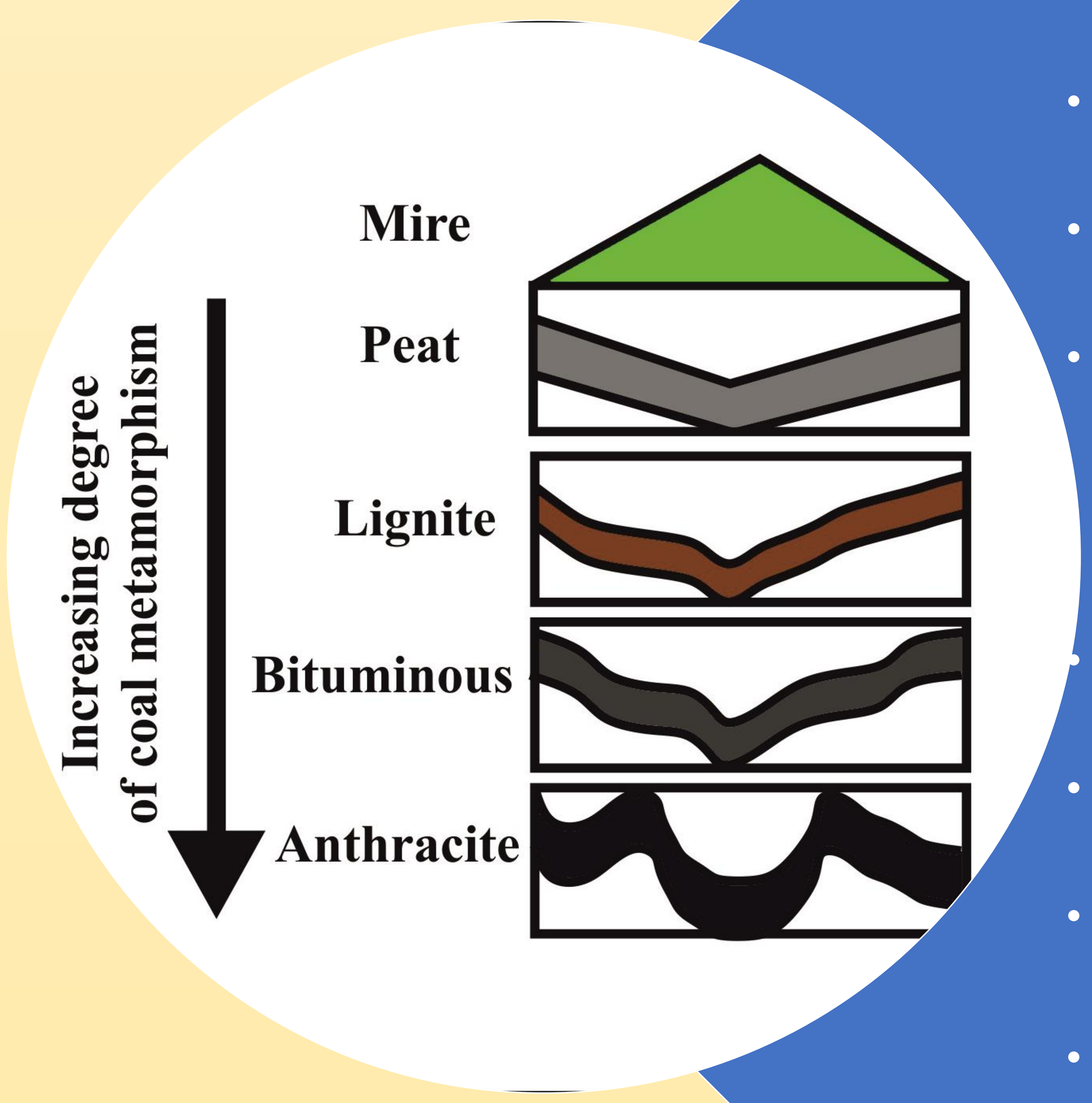

Scientific content:

- The $\delta^{13}C$ values in the Paleogene lignite samples indicate angiospermic sources of organic matter, while the Gondwana bituminous and the anthracite samples depict the $\delta^{13}C$ signature of the gymnosperms. The non-linear trend of the $\delta^{13}C$ values with increasing coal rank implies that the coalification did not alter the source signature of the organic carbon.
- Further, the non-linear trend of the $\delta^{15}N$ parameter from bituminous to anthracite may suggest that the organic nitrogen was not totally depleted with the coalification.
- Meanwhile, the C_{org}/N_{org} increases from the Paleogene lignites to the Paleogene bituminous coals implying the plausible influences of the coalification.
- The Gondwana bituminous coals exhibit a lower C_{org}/N_{org} ratio than the Paleogene bituminous coals. Besides, the anthracite samples show an almost similar range of the C_{org}/N_{org} ratio to that of the bituminous rank.
- At the lignite rank, the dominance of pyridines occurs due to transformations of amine and amide and oxygen removal from pyridones.
- At the bituminous rank, the pyridinic nitrogen again dominates over the other moieties due to cyclization of pyrroles, loss of oxygen and deprotonation of cyclazines.
- At the anthracite stage, the pyrrolic nitrogen alleviates, but the pyridines and cyclazine nitrogen intensify.
- During the anchizonal metamorphism at the anthracite rank, the pyrrolic structure thermochemically converted to cyclazine.
- Protonation of pyridines formed the cyclazines and cyclization of pyrroles again formed the pyridines.
- The cyclazine and pyridinic moieties were not further altered due to inert microstructure. So, instead of leaving the coal microstructure, the organic nitrogen was encapsulated within the stable functionalities,.
- This preserved organic nitrogen represents the bulk $\delta^{15}N$ values in the anthracite, which may explain the non-linear trend of this isotopic parameter with increasing coal rank.

Portrait of the responses from the stable isotopes and functionalities with coalification:

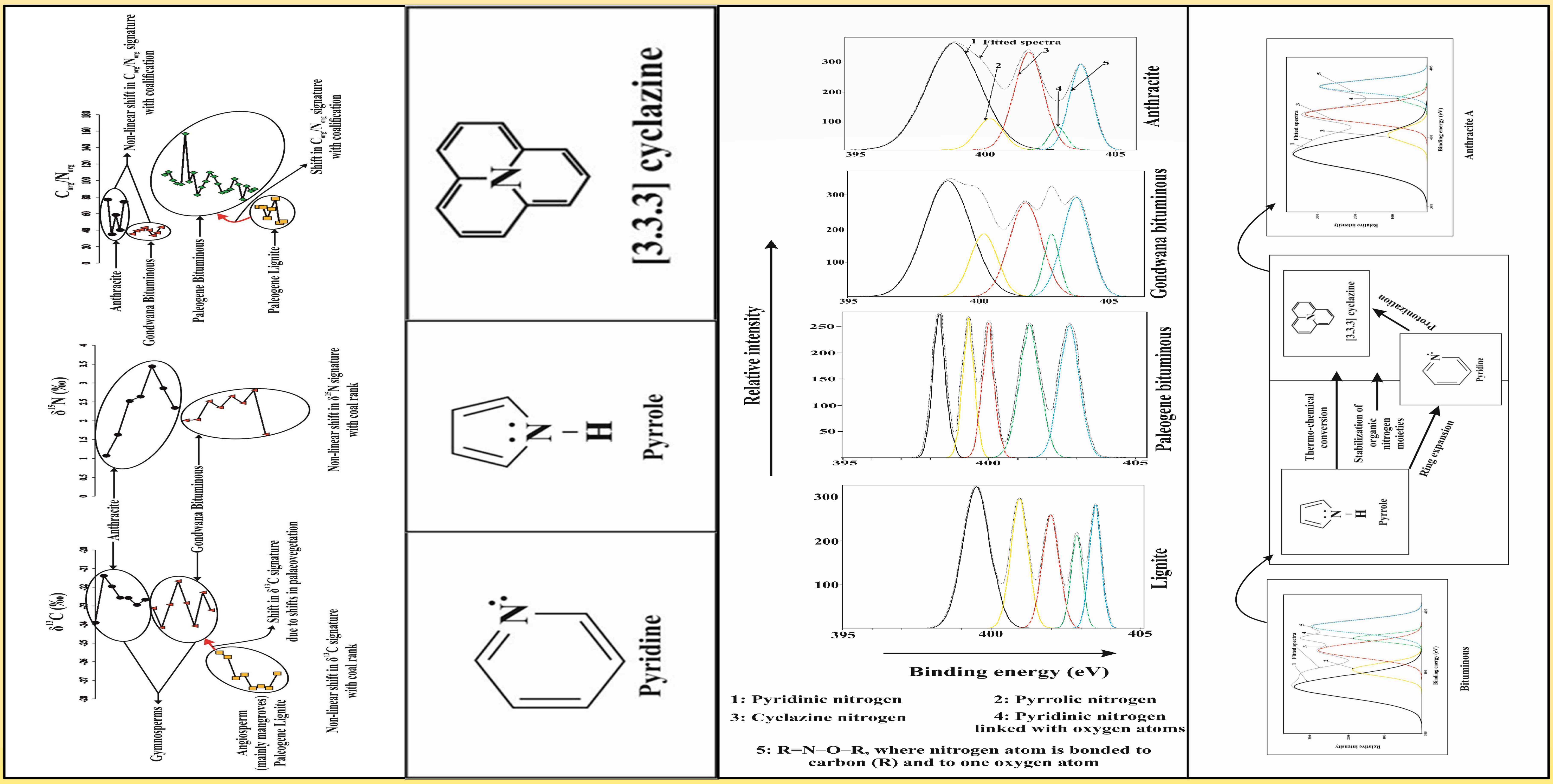

References:

- Anwita, Ghosh S., Varma, A.K., Das, S.K., Pal, D., Solanki, G., 2020. Metamorphic transformations of nitrogen functionalities: stabilization of organic nitrogen in anthracite and its effect on δ15N parameter. Mar. Pet. Geol. 112, 104090.
- Kumar, D., Ghosh, S., Tiwari, B., Varma, A.K., Mathews, R.P., Chetia, R., 2021. Palaeocene-Eocene organic sedimentary archives of Bikaner-Nagaur Basin, Rajasthan, India: An integrated revelation from biogeochemical and elemental proxies. Int. J. Coal Geol. 247, 103848.
- Mitra-Kirtley, S., Mullins, O.C., Branthaver, J.F., Cramer, S.P., 1993. Nitrogen chemistry of kerogens and bitumens from X-ray absorption near-edge structure spectroscopy. Energy Fuels, 7, 1128–1134.
- Valentim, B., Guedes, A., Boavida, D., 2011. Nitrogen functionality in ''oil window'' rank range vitrinite rich coals and chars. Org. Geochem. 42, 502–509.

Acknowledgement:

The authors are indebted to the Peer Committee of the Frontiers in Geosciences Research Conference, PRL, Ahmedabad, India, for accepting the abstract and providing a valuable opportunity to present their research works.

Tracing the impact of basin topography on the hydrological processes in a Himalayan River: A stable isotopic (δD and δ^{18}O) approach

Satyabrata Das, Santosh K. Rai
Wadia Institute of Himalayan Geology, 33 GMS road, Dehradun, India, 248001
*E-mail: satyabratadasgeo@gmail.com, rksant@gmail.com

INTRODUCTION

Stable isotopic compositions (δ^{18}O and δD) and their spatiotemporal variations in stream water provide a useful tool in delineating its differential source contributions and understanding the hydrological processes (snowmelt contribution, evaporation, evapotranspiration and moisture recycling) operating on basin wide scale (Rozanski et al., 1993; Liu et al., 2015; Licht et al., 2017). All these processes can cause a deviation in the simple Rayleigh distillation model of isotopic depletion and biasness during paleoaltimetry estimation of the respective basin (Bershaw et al., 2012). Therefore, to circumvent the uncertainty in paleoaltitude estimation, it is required to demarcate the role of various hydrological process in bringing the variation in stable isotopic composition of river water. However, most of the δ^{18}O and δD compositional studies of the Himalayan rivers have focused on the source of moistures to the precipitation. Therefore, in the present study, we have analysed the δ^{18}O and δD of one of the major Himalayan rivers, the Teesta River and its tributaries, during pre-monsoon period of 2018, when melting of the Himalayan glaciers is common and the precipitation amount is minimum.

OBJECTIVES

- To delineate the roles of individual hydrological processes (snowmelt contribution, evaporation, moisture recycling) in bringing isotopic alteration of the river water.
- To demarcate the possible impact of precipitation front and artificially constructed check-dams on the stable isotopic composition of river water.
- Approximation of rainout percentage in the basin and controlling factors.

GEOLOGICAL MAP & SAMPLING LOCATION

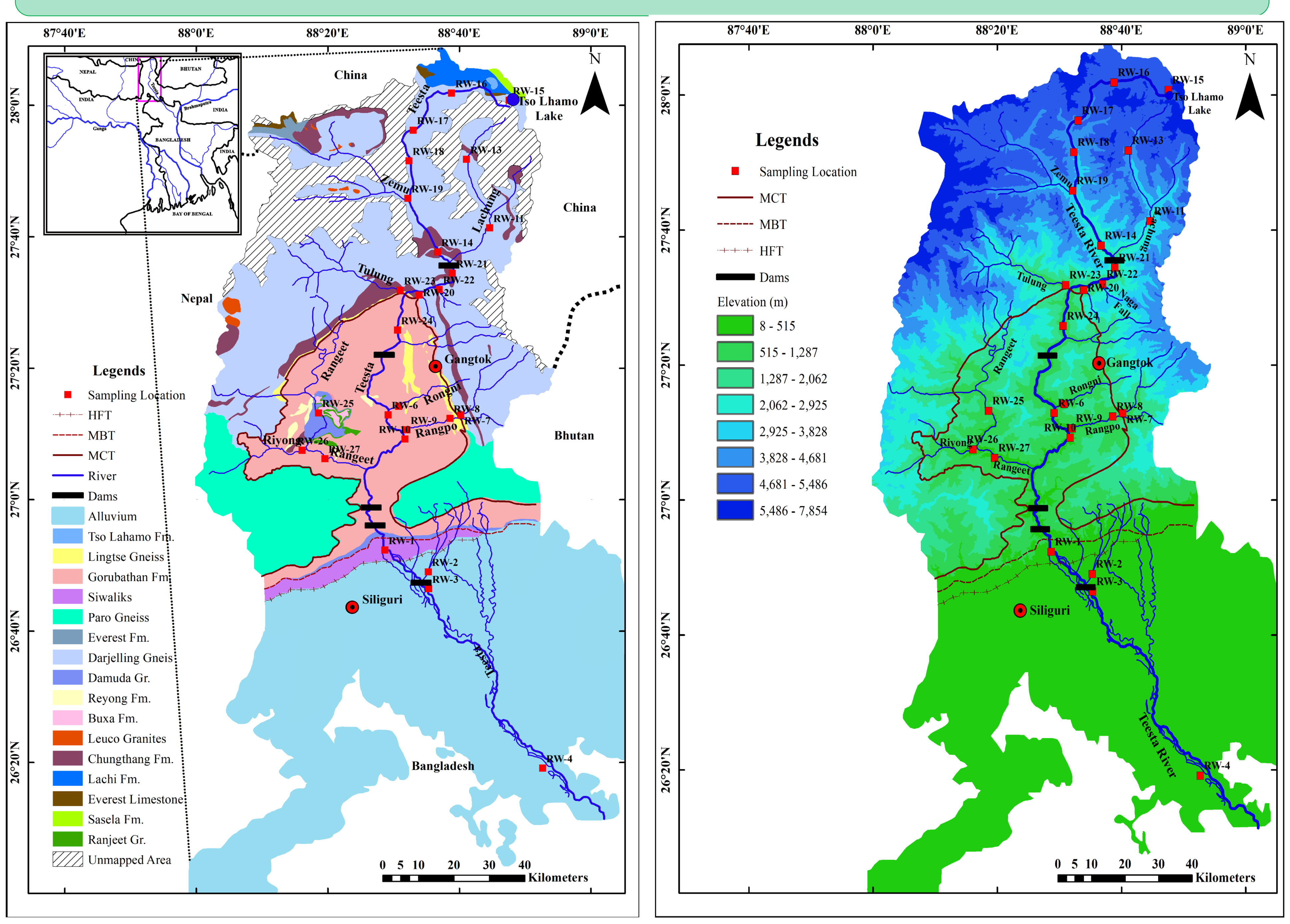

Fig.1 (a) Geological map of the study area with sampling locations and dams present in the basin (Map modified from Das et al., 2021). (b) Elevation map of the study area (Elevation data from SRTM)

RESULTS

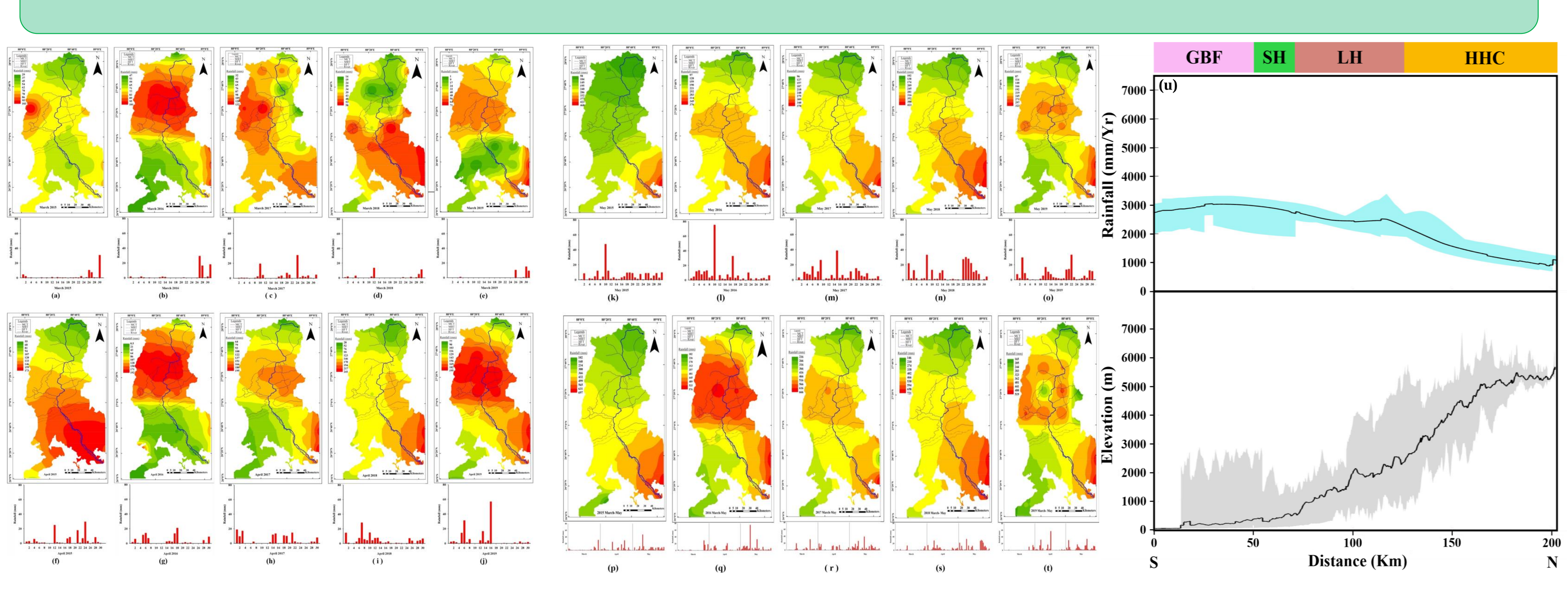

Fig.2 (a-t) Precipitation pattern and amount in the study area during the pre-monsoon season from 2015-2019 (u) Elevation and precipitation swath profile of the basin

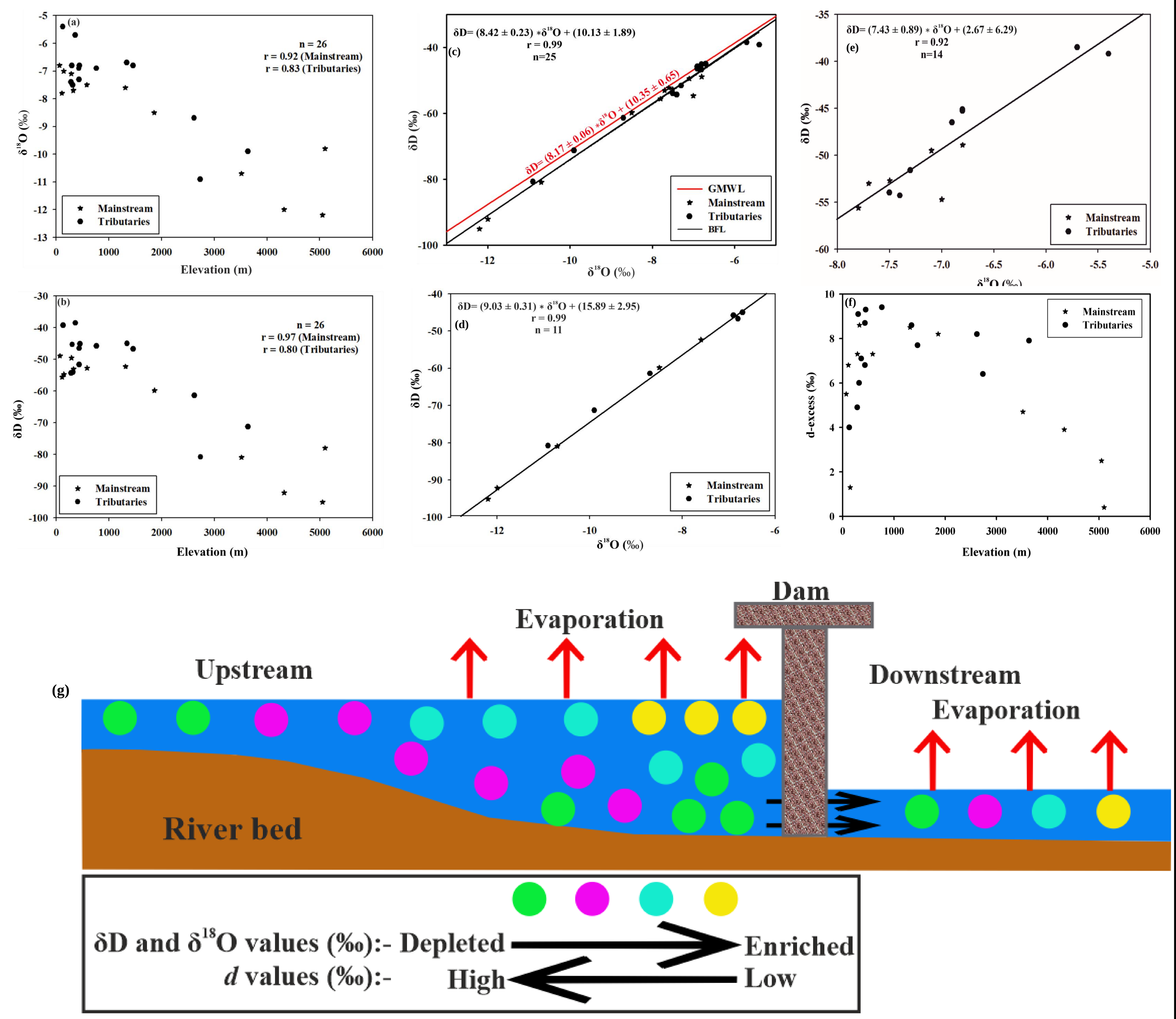

Fig.3 (a) Variation of (a) δ^{18}O and (b) δD values of river water with elevation in the study area. The figure clearly depicts that both δ^{18}O and δD get enriched from the source up to MCT.(c) Relation between δ18O and δD of the water samples collected from the river Teesta and associated tributaries with GMWL and LMWL. (d) δ^{18}O and δD relationship of the Teesta River samples and its tributaries in Higher Himalayan reaches of the basin. (e) δ^{18}O and δD relationship of the Teesta River samples and its tributaries in Lesser Himalaya and plain regions of the basin. (f) Variation of d values with elevation in the study area. The figure clearly depicts an increase in the d values with increasing elevation before achieving a negative correlation at MCT. (g) Stable isotopic variation and stratification process in reservoir water (Figure modified after Wang et al., 2019).

CONCLUSIONS

- There occurs early melting of the snow in the study area.
- The contrasting pattern of the *d* values and elevation infers about variational degree of recycled moisture contribution and river water evaporation.
- The northern side of MCT witnesses evaporation due to arid climate under low humidity condition, whereas temperature controlled water evaporation occurs on the southern side.
- Differential magnitudes of the hydrological processes in a comparatively smaller basin area seem to be chiefly controlled by the elevation rather than other physical parameters.
- This rapidly increasing altitude also resulted in a relatively larger amount of rainout percentage in the basin (35 ± 4) %.

ACKNOWLEDGEMENT

We are thankful to the Director, WIHG, Dehradun for providing the analytical and financial support to carry out the work. We also thank the organising committee FGRC-2021, Physical Research Laboratory (PRL) for giving an opportunity to present the current work.

REFERENCES

1. *Bershaw et al., (2012). Journal of Geophysical Research: Atmospheres, 117(D2). https://doi.org/10.1029/2011JD016132.*
2. *Das et al., (2021) Geochemistry, Geophysics, Geosystems, e2020GC009324. https://doi.org/10.1029/2020GC009324.*
3. *Licht et al., (2017). Am. J. Sci.317, 1–33. https://doi .org /10 .2475 /01.2017.01.*
4. *Liu et al., (2015), Atmospheric Research, 153, https://doi.org/10.1016/j.atmosres.2014.07.029.*
5. *Rozanski et al.,(1993). GMS, 78, 1-36. https://doi.org/10.1029/GM078p0001.*
6. *Wang et al., (2019) JoH, 568, 604-610. https://doi.org/10.1016/j.jhydrol.2018.11.016.*

STRUCTURAL CONTROL ON GROUNDWATER FLOW IN TRANS YAMUNA REGION PRAYAGRAJ AS INFERRED USING REMOTE SENSING AND GIS

Swarnim, Irjesh Sonker, Jayant N. Tripathi

Department of Earth and Planetary Sciences, University of Allahabad, Prayagraj - 211002

Abstract

Trans Yamuna, Prayagraj region has very severe problem related to water scarcity. In this area, the drinking water problem is very drastic since Groundwater level is poor and water quality is contaminated. Major rivers in this area are Yamuna, Tons and Belan. The lithology of this area is covered by the Younger Alluvium, Older Alluvium and Vindhyan Sandstone. Vindhyan sandstone covers less part than Older Alluvium but it shows fractures in the area. This area consists of four Tehsils namely, Karchhana, Bara, Meja and Koraon. Landsat 8 OLI bands are used to digitized lineament map in Arc GIS 10.4 software and rose diagram of lineament has been prepared using Rockworks software. Results show that the lineaments orientation is correlated to the Groundwater flow, in this area, which is also supported by the rose diagram trend. Trans Yamuna region consists of fractured hard rock on the surface and as well as below the surface. Thus, fracture is one of the factors which controls the Groundwater flow and also shows the potential zone of Groundwater.

Objective:

To find the ground water flow direction in the Trans Yamuna region in Prayagraj District using integrated geographic Information system (GIS) and Remote sensing technique.

To evaluate the ability currently used GIS and Remote Sensing techniques to produce the thematic map of the Lineaments using satellite image.

Study area

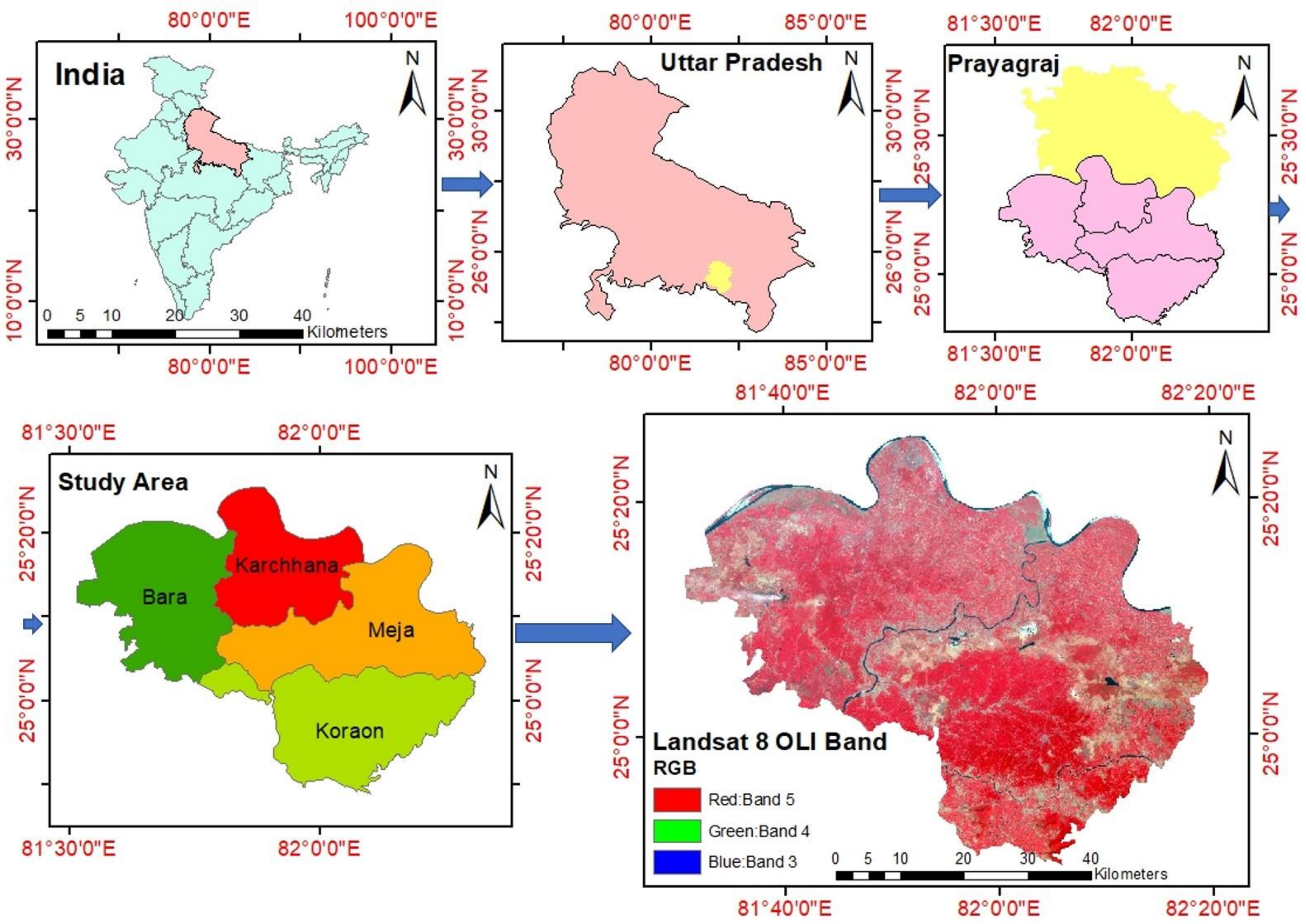

Materials and methods:

1-Preparing lineaments map using Landsat 8 OLI band, different bands combination ,filters and Arc GIS 10.4 software

2-Rose diagram of lineaments using RockWorks17 Software.

3-For Validation the result, the Hydrogeological map of district Prayagraj digitized from CGWB 2018-2019 report.

4-Preparation of thematic layers and generation of groundwater potential mapping

Eight different thematic layers such as lithology, geomorphology, lineament density, slope, rainfall, drainage density, NDVI and LULC were generated using remote sensing and conventional/existing data with the help of ArcGIS software.

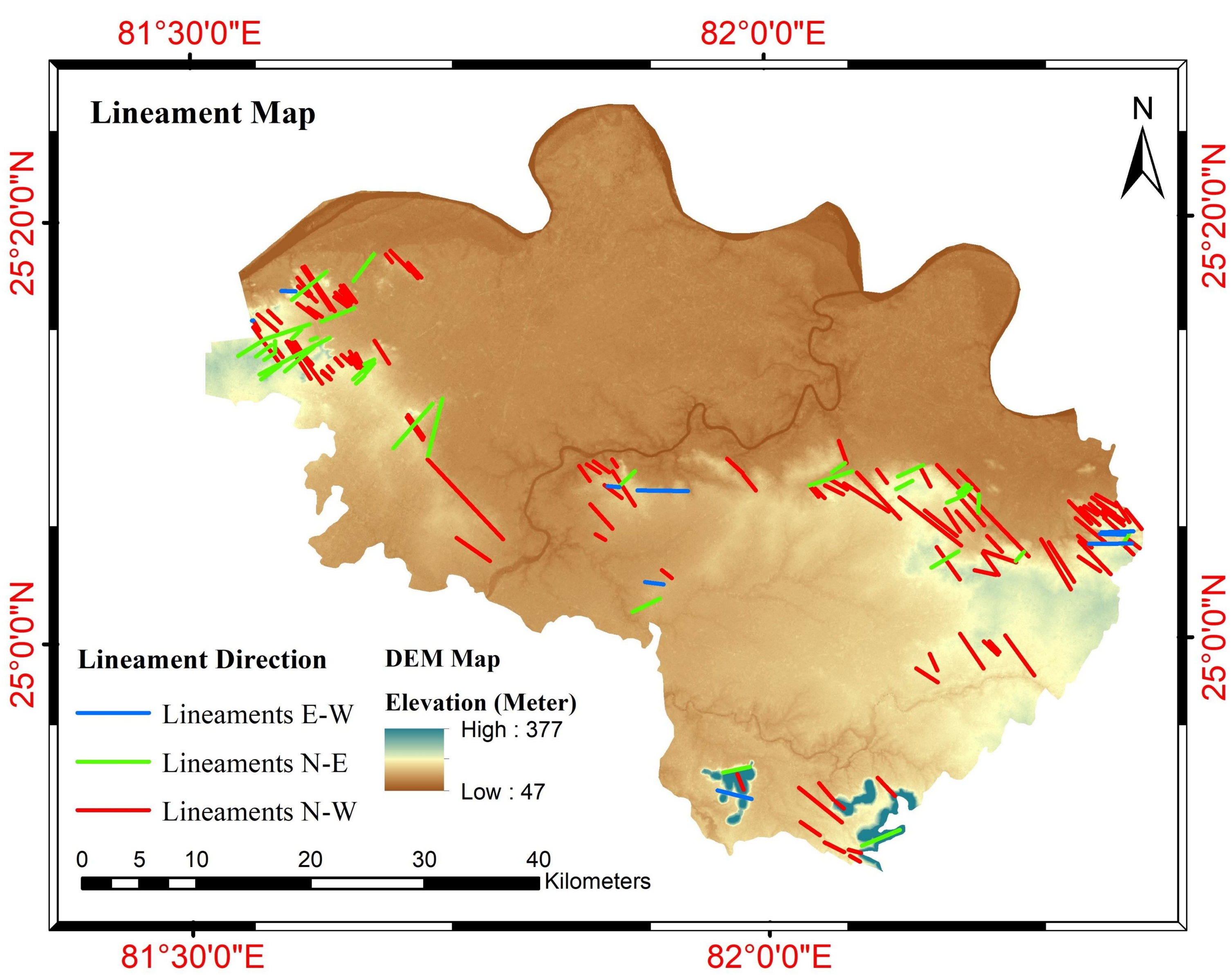

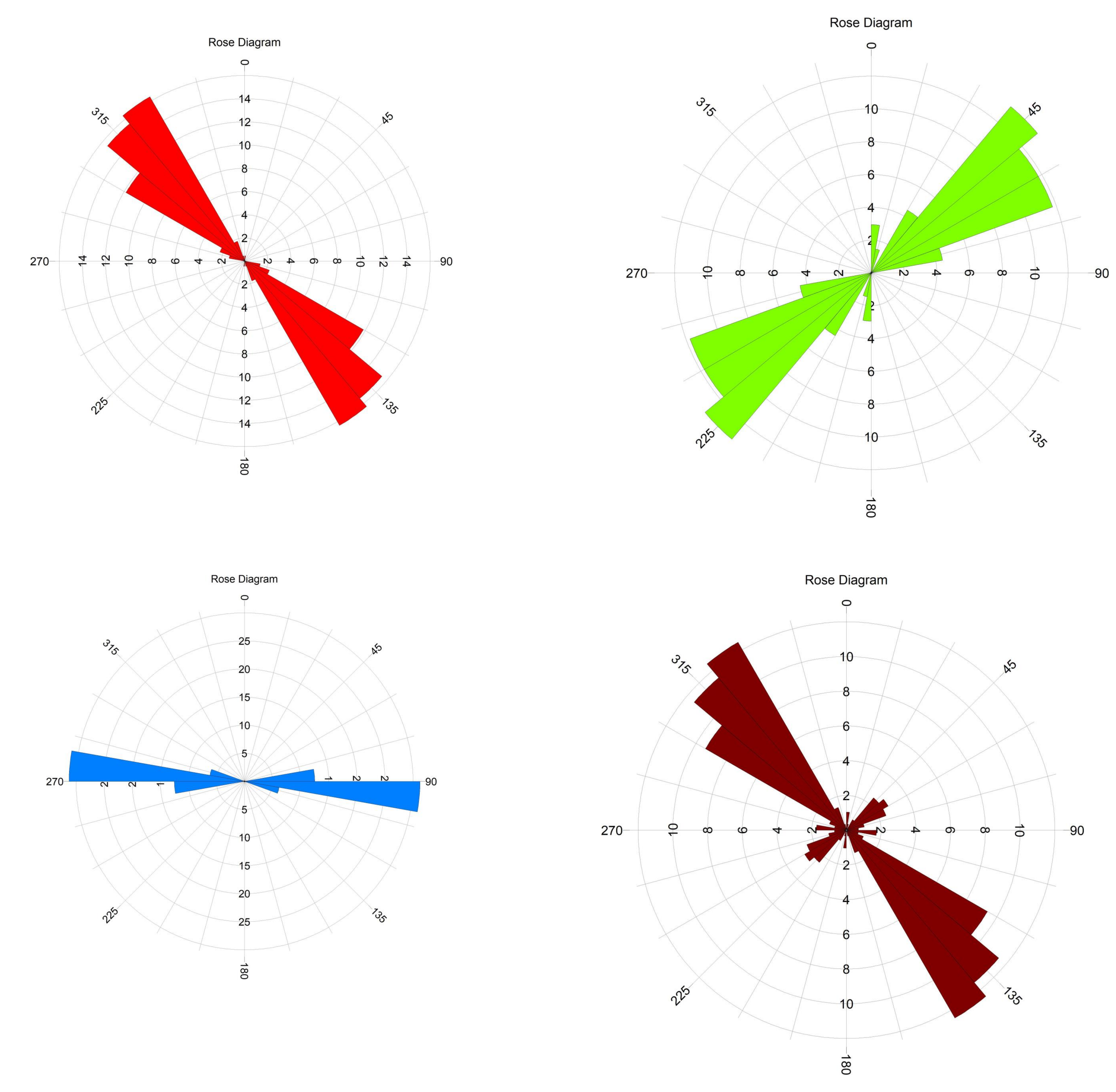

Lineament direction	Number of Lineaments	Total length of Lineaments (km)	Percentage
NE-SW	110.00	81.71	72.37
NW-SE	34.00	244.34	22.37
E-W	8.00	20.26	5.26
Total	152.00	346.31	100.00

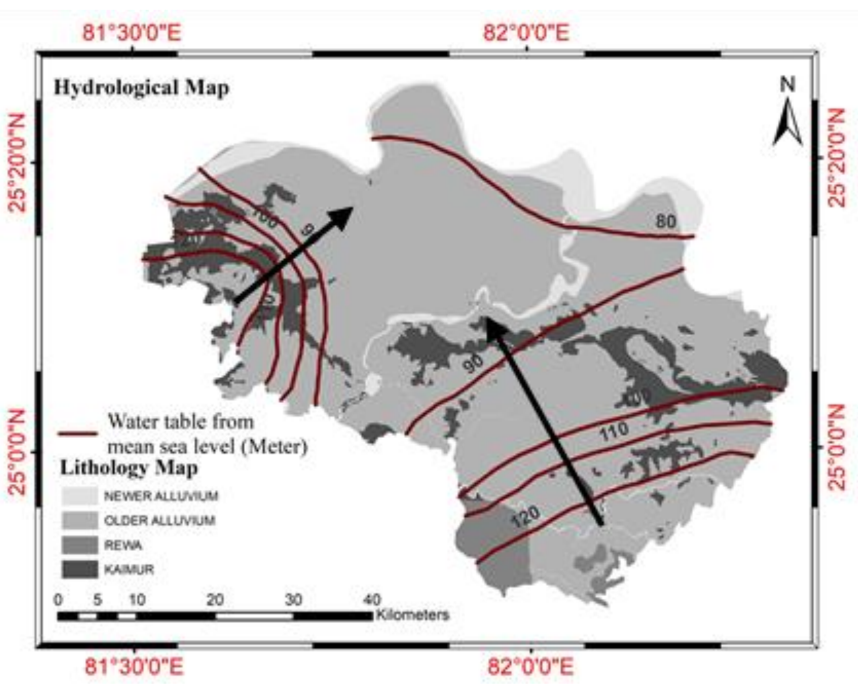

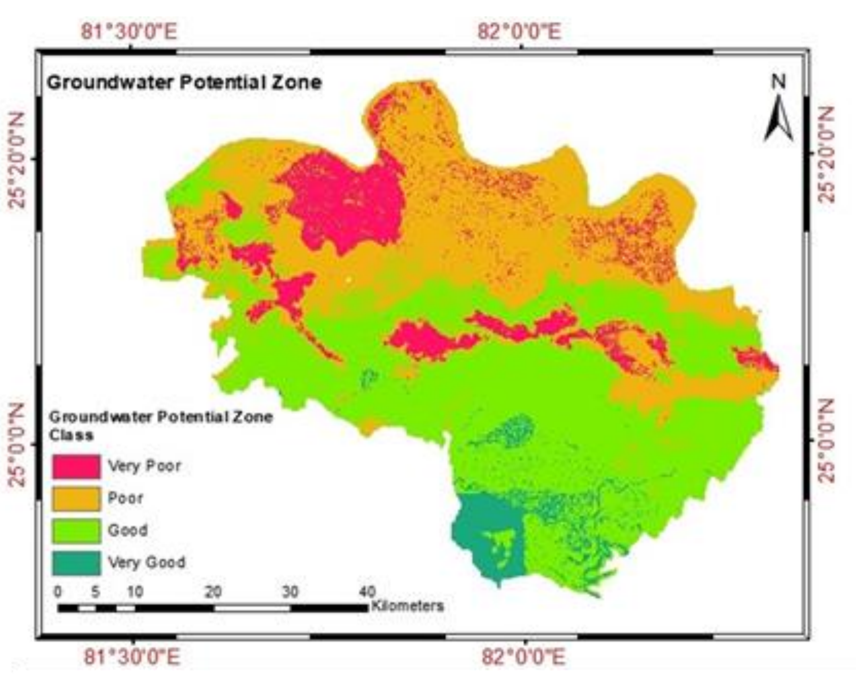

Conclusion:

It is concluded that the integrated GIS and Remote Sensing techniques are very effective and useful, time and cost effective tool for the identification of groundwater flow direction. Groundwater flow direction mostly occur in NE-SW and NW-SE direction of lineaments but this direction shows the poor groundwater condition according to the groundwater potential map.

References:

Dasgupta, S., & Mukherjee, S. (2019). Remote Sensing in Lineament Identification: Examples from Western India. In *Problems and Solutions in Structural Geology and Tectonics* (1st ed., Vol. 5). Elsevier Inc. https://doi.org/10.1016/b978-0-12-814048-2.00016-8

Odeh, T., Salameh, E., Schirmer, M., & Strauch, G. (2009). Structural control of groundwater flow regimes and groundwater chemistry along the lower reaches of the Zerka River, West Jordan, using remote sensing, GIS, and field methods. *Environmental Geology*, *58*(8), 1797–1810. https://doi.org/10.1007/s00254-008-1678-1

Zabidi, H., Rahim, A., & Trisugiwo, M. (2019). Structural controls on groundwater inflow analysis of hardrock TBM. *Cogent Geoscience*, *5*(1), 1637556. https://doi.org/10.1080/23312041.2019.1637556

Acknowledgement:

One of the authors (Swarnim) acknowledges the research scholarship given by University of Allahabad. The authors are thankful to Central Ground Water Board (CGWB) India, Geological survey of India (GSI) for the data downloaded from their site.

Perturbations in the Rainfall Trends in India: New Insights from a Different Approach

Swagatika Chakra[1,2] and R. D. Deshpande[1]

[1] Physical Research Laboratory, Ahmedabad, India , [2]Indian Institute of Technology, Gandhinagar, India

E mail: swagatika@prl.res.in, desh@prl.res.in

SCIENTIFIC BACKGROUND

Most studies are based on all India rainfall data, which averages the rainfall pattern in different geographical region. Hence major regional patterns are missing and long-term trend for Indian rainfall is insignificant (Fig 1).

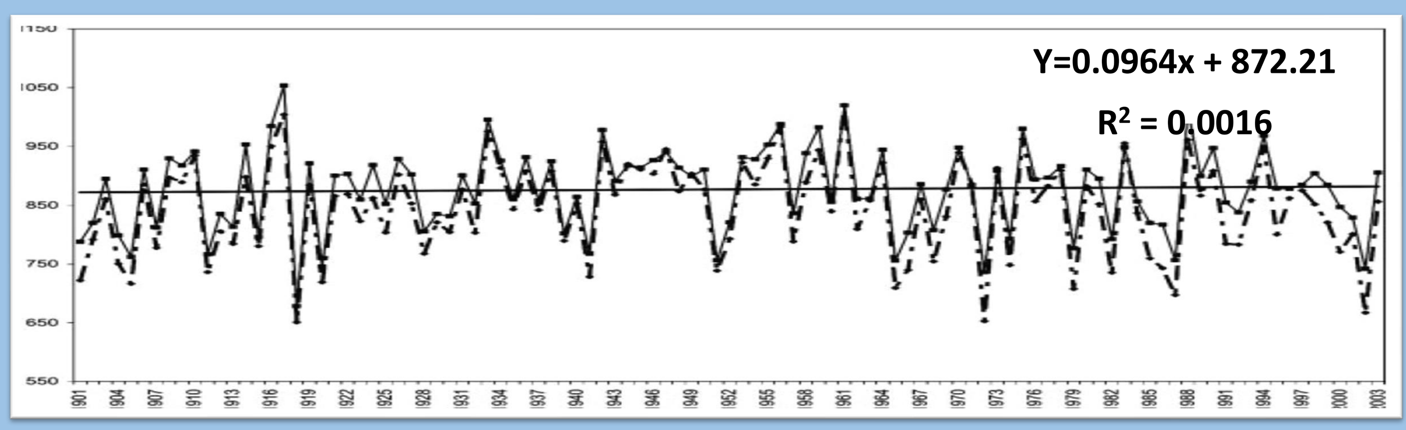

Fig 1: South-West Monsoon Rainfall of India (1901-2003) (P. Guhathakurtha and M. Rajeevan , 2007)

Long-term trend for smaller space domain (meteorological subdivision & district) rainfall is significant and varying across India(Fig 2) and (Fig 3).

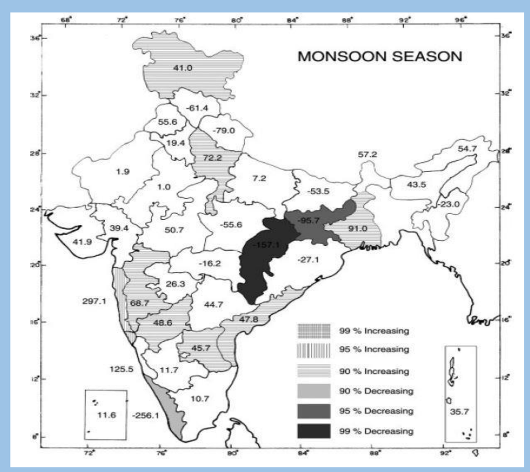

Fig 2: South-West Monsoon Rainfall Trend of Meteorological Subdivision (1901-2003) (P. Guhathakurtha and M. Rajeevan , 2007)

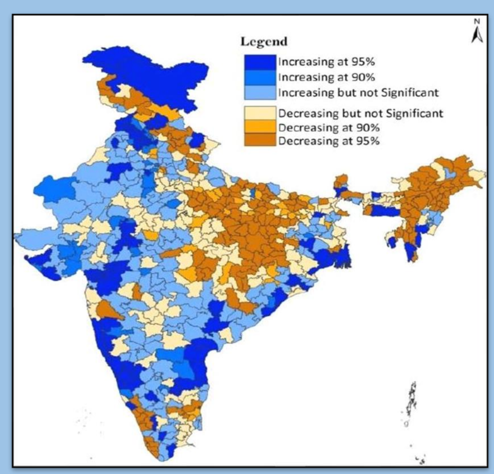

Fig 3: South-West Monsoon Rainfall Trend of Districts (1901-2013) (Diwakar et al., 2017)

Approach of linear regression is suitable for monotonic trend of rainfall. But rainfall is highly stochastic and irregular in nature. Many studies in rainfall have been done with this approach in larger spatial domain (Fig 2) and smaller spatial domain (Fig 2 & Fig 3). So important changes have been missing out (Fig 4).

Majority years in blue box and orange box time frame have rainfall above and below long-term avg. respectively. These important information (time frame) in rainfall are being missing out when trend analysis is performed.

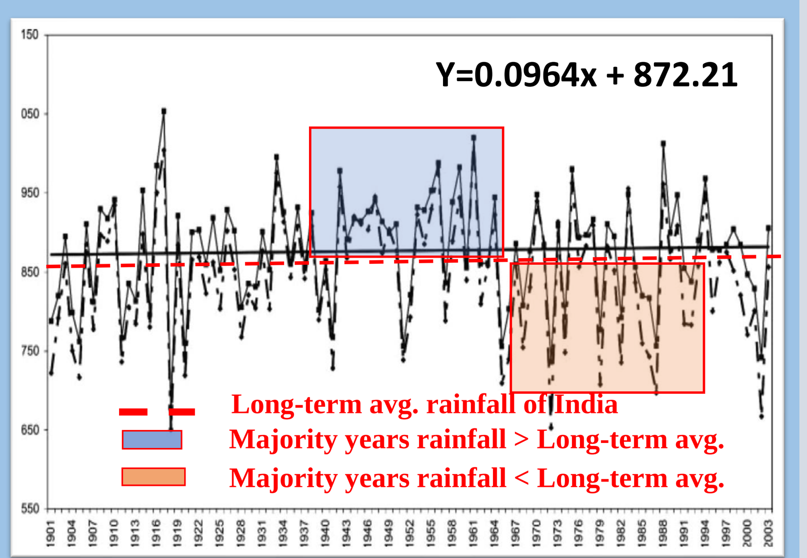

Fig 4: South-West Monsoon Rainfall of India (1901-2003) (P. Guhathakurtha and M. Rajeevan , 2007)

There are several coupled factors (Oceanic, Atmospheric, Terrestrial) which affect the regional rainfall differently. Due to averaging rainfall over large geographical area and performing monotonic trend analysis, the imprint of causal processes or linkages of rainfall with probable factors are being missed out. So the underlying causal processes are poorly understood

There are certain examples of discrepancy between proposed causal mechanism and their expected manifestation in rainfall (Fig 5, Fig 6, Fig 7).

Sea surface temperature trend is more as compare to landmass temperature as shown in Fig 5. As a result, land and sea thermal contrast, the major driver of Indian Monsoon is weakening giving rise to decreased rainfall trend over India. But rainfall trend over India is of both increasing and decreasing type and varied across space (Fig 3).

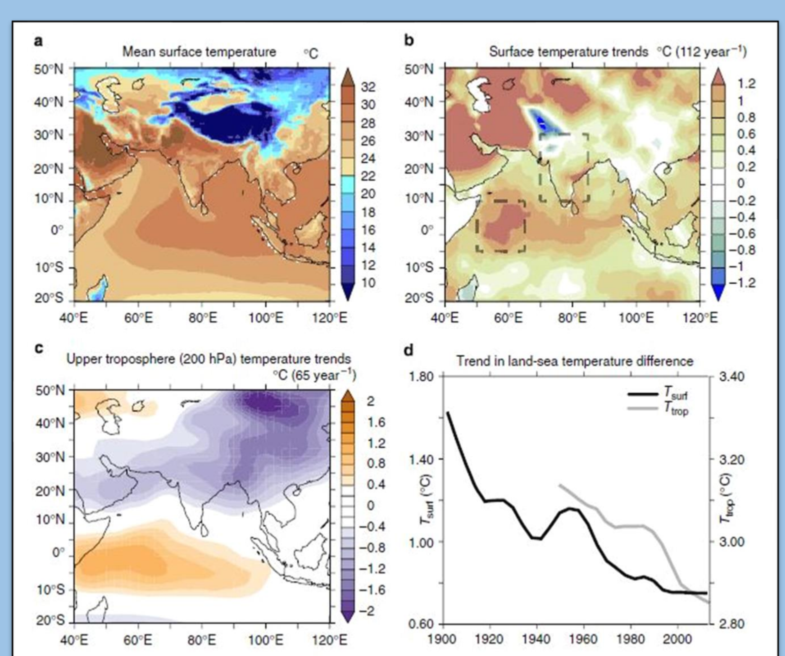

Fig 5: Land & Sea Thermal Contrast (Roxy et al., 2015)

Decrease in number of depression and cyclonic storms in Bay of Bengal (Fig 6) has been compared to decreased rainfall trend of Jharkhand & Chhattisgarh. If so, then Odisha & West Bengal should show same rainfall trend signature (Fig 2).

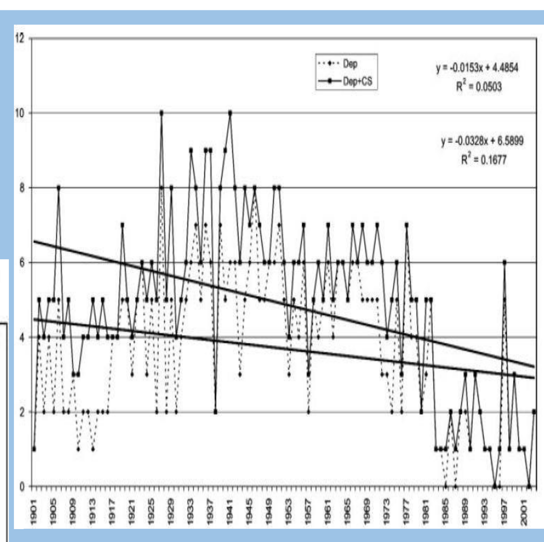

Fig 6: South-west Monsoon Depression & Cyclonic Storms (P. Guhathakurtha and M. Rajeevan , 2007)

Recent variation in Monsoon rainfall has been linked to variation in continental recycle rainfall amount due to land use land cover change (Fig 7).But the observed rainfall change is not matching with the simulated rainfall change particularly in coastal region of Maharashtra.

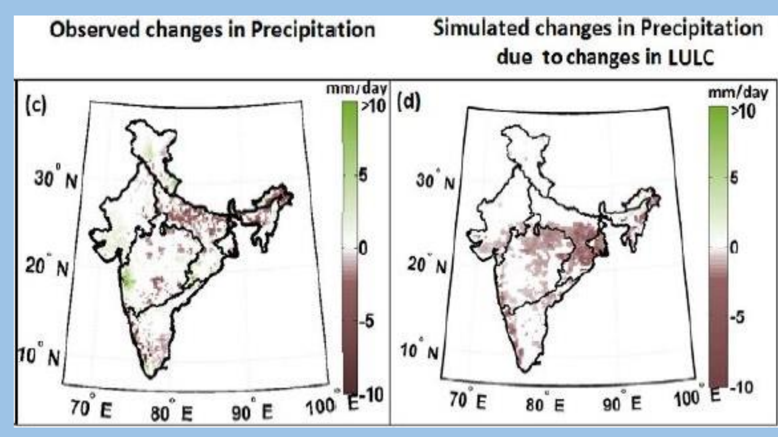

Fig 7: Land Use Land Cover Change (Supantha Paul and Subimal Ghosh, 2016)

OBJECTIVES

- Identification of prominent patterns in rainfall variability in different parts of India.
- Identification of geographical zones comprising more than one districts with similar patterns of rainfall variability.
- Identification of the time windows during which prominent change in rainfall trends are observed.
- Identification of possible factors controlling such spatially varied patterns.

DATASETS AND METHODOLOGY

- India Meteorological Department (IMD) gridded (0.25°×0.25°) daily rainfall datasets from 1901-2020 has been used in this study.
- Gridded data has been converted to district data by area weighted average method (Pai et al., 2013, Fig 8) instead of taking simple average of grid point rainfall value.
- Seasonal (Summer Monsoon: June-September) rainfall time series data has been prepared from daily rainfall data.
- Percentage departure of rainfall is calculated from climatological standard normal of 1961-1990.
- 31 years simple moving average is applied to the percentage departure time series. These final values are plotted against time (Fig 9).

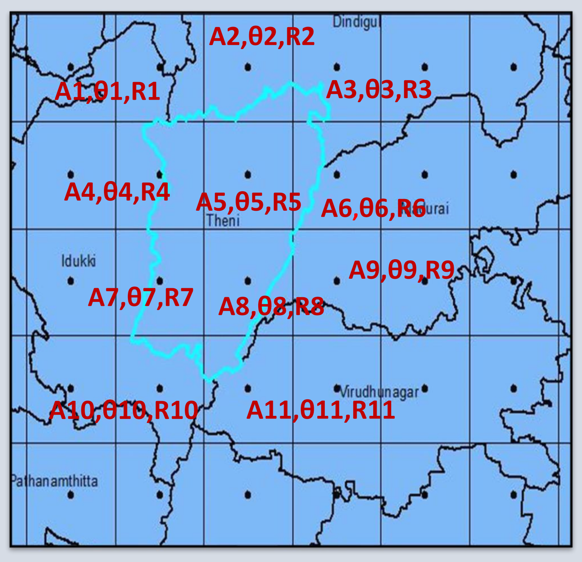

Fig 8: Area weighted Average Method

R(District) = $\sum$ Ai× cos(θi) × Ri
A=Fractional area, R=Rainfall
θ =Latitude

The rainfall patterns are identified based on following observations:

- Trends of progressive increase or decrease in 31 years moving average of percentage departure of summer monsoon rainfall with reference to climatological mean rainfall.
- The rate of increase/decrease in moving average of percentage departure (i.e. Total percentage departure/ Years).
- Year of point of inflections in rainfall departure trend.

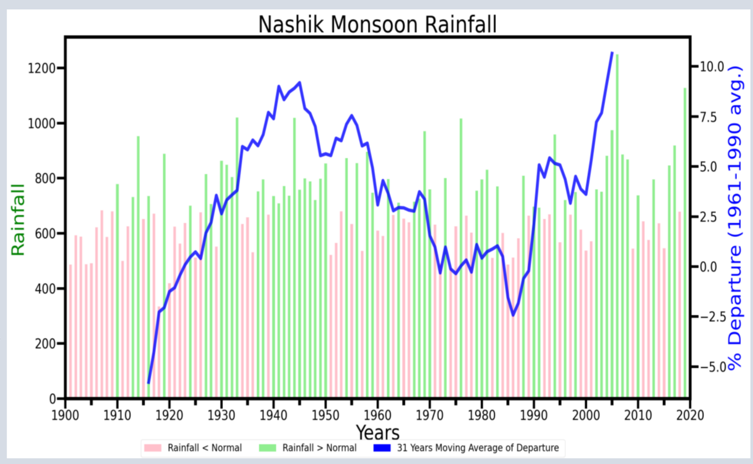

Fig 9: Rainfall pattern of Nashik District (Maharashtra)

Grouping of districts having similar rainfall pattern has been done based on above criteria and shown below (Fig 10).

PRELIMINARY RESULTS AND DISCUSSION

A comparison has been made between our geographical zoning and IMD homogeneous meteorological subdivisions (Fig 10).

Dissimilar rainfall pattern/ heterogeneity has been observed within Homogenous meteorological subdivisions(Fig 11).

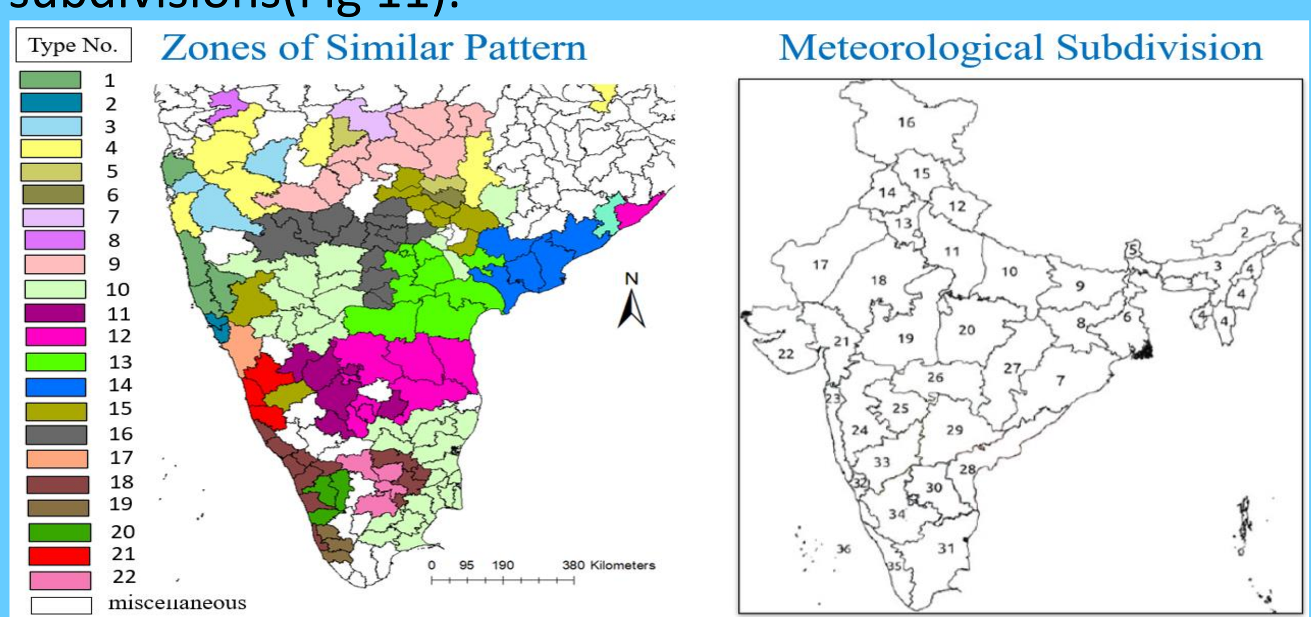

Fig 10: Zones of Similar rainfall pattern and its comparison with meteorological Subdivisions

Karnataka Western Coast & Ghats

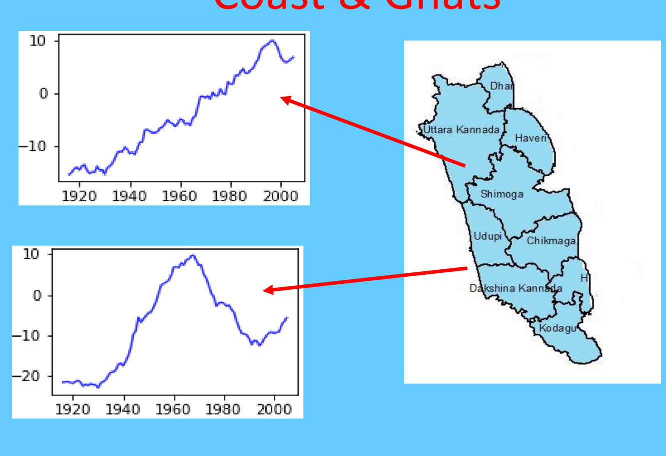

Fig 11: Heterogeneity within Homogeneous Meteorological Subdivision

REFERENCE

Guhathakurta, P., and M. Rajeevan. "Trends in the rainfall pattern over India." International Journal of Climatology: A Journal of the Royal Meteorological Society 28.11 (2008): 1453-1469

Kaur, Surinder, Sumant Kumar Diwakar, and Ashok Kumar Das. "Long term rainfall trend over meteorological sub divisions and districts of India." Mausam 68.3 (2017): 439-450.

Pai, D. S., et al. "Development of a new high spatial resolution (0.25× 0.25) long period (1901–2010) daily gridded rainfall data set over India and its comparison with existing data sets over the region." Mausam 65.1 (2014): 1-18.

Roxy, Mathew Koll, et al. "Drying of Indian subcontinent by rapid Indian Ocean warming and a weakening land-sea thermal gradient." Nature communications 6.1 (2015): 1-10.

Paul, Supantha, et al. "Weakening of Indian summer monsoon rainfall due to changes in land use land cover." Scientific reports 6.1 (2016): 1-10.

Long-term variation of the Sea Surface Temperature over 13 oceanic regions linked to Indian Summer Monsoon Rainfall

Ms. Riddhi M. Bhatt and Dr. Hiteshri K. Shastri
Department of Civil Engineering, CSPIT, CHARUSAT, Anand, Gujarat

Introduction

The prediction of Indian Summer Monsoon Rainfall (ISMR) has always been challenging due to its complexity and heterogenic nature. Traditionally predicated models were unable to identify the smaller irregularity and therefore the need of better predication model arises.

Objectives

The study aims to determine and evaluate presence of trend in SST(Sea Surface Temperature) of 13-oceanic regions linked with ISMR for time period (1901-2010; 110 years)

Methodology

Collection of data

- Monthly reconstructed global SST (ERSST) version 3b from National Oceanic and Atmospheric Administration (NOAA); National Centers for Environmental Information (NCEI)
- https://www1.ncdc.noaa.gov/pub/data/cmb/ersst/v3b/netcdf

Identification of zones

The 13 oceanic regions linked to ISMR are identified based on (Sahastrabuddhe & Ghosh, 2019)

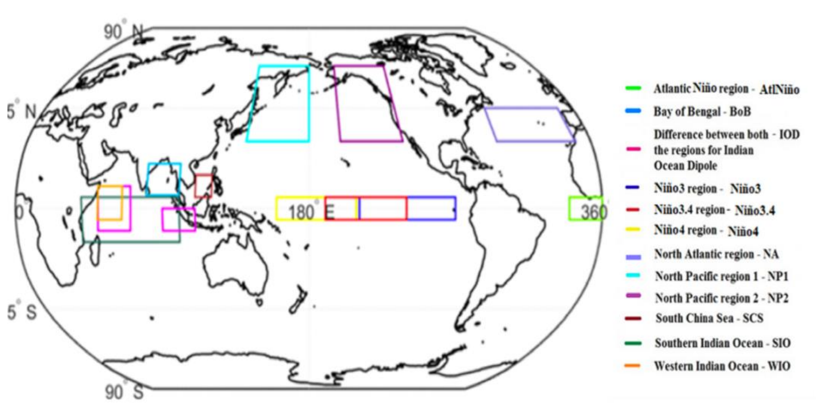

Data processing

Used Matlab application to process the data
Methods used :-
- Mann Kendall Rank Test
- Sen Slope estimator

Result

Sr no.	Name of sst region	Presence of trend	sen-slope value
1	Atlantic nino	1	0.268
2	Bay of Bengal	1	0.6244
3	Niño 3	1	0.1169
4	Niño 3.4	1	0.1717
5	Niño 4	1	0.3039
6	North Atlantic	1	0.1246
7	North Pacific	1	0.0999
8	North Pacific 2	1	0.1339
9	China sea	1	0.3639
10	Southern Indian ocean	1	0.4078
11	Western Indian ocean	1	0.3817
12	Zonal mode	1	0.2912
13	Indian ocean dipole	1	0.3846

- The results reveal a positive trend indicating warming for all oceanic regions except for North Pacific 2 which shows a negative trend.
- The Sen-slope values are recorded highest for North Atlantic region; while, lowest for North Pacific region.
- The three regions around Indian landmass namely Southern Indian Ocean, Western Indian Ocean and Bay of Bengal which shows statistically significant positive trend with estimated Sen-slope values nearly 0.0285, 0.0292 and 0.0243 respectively.

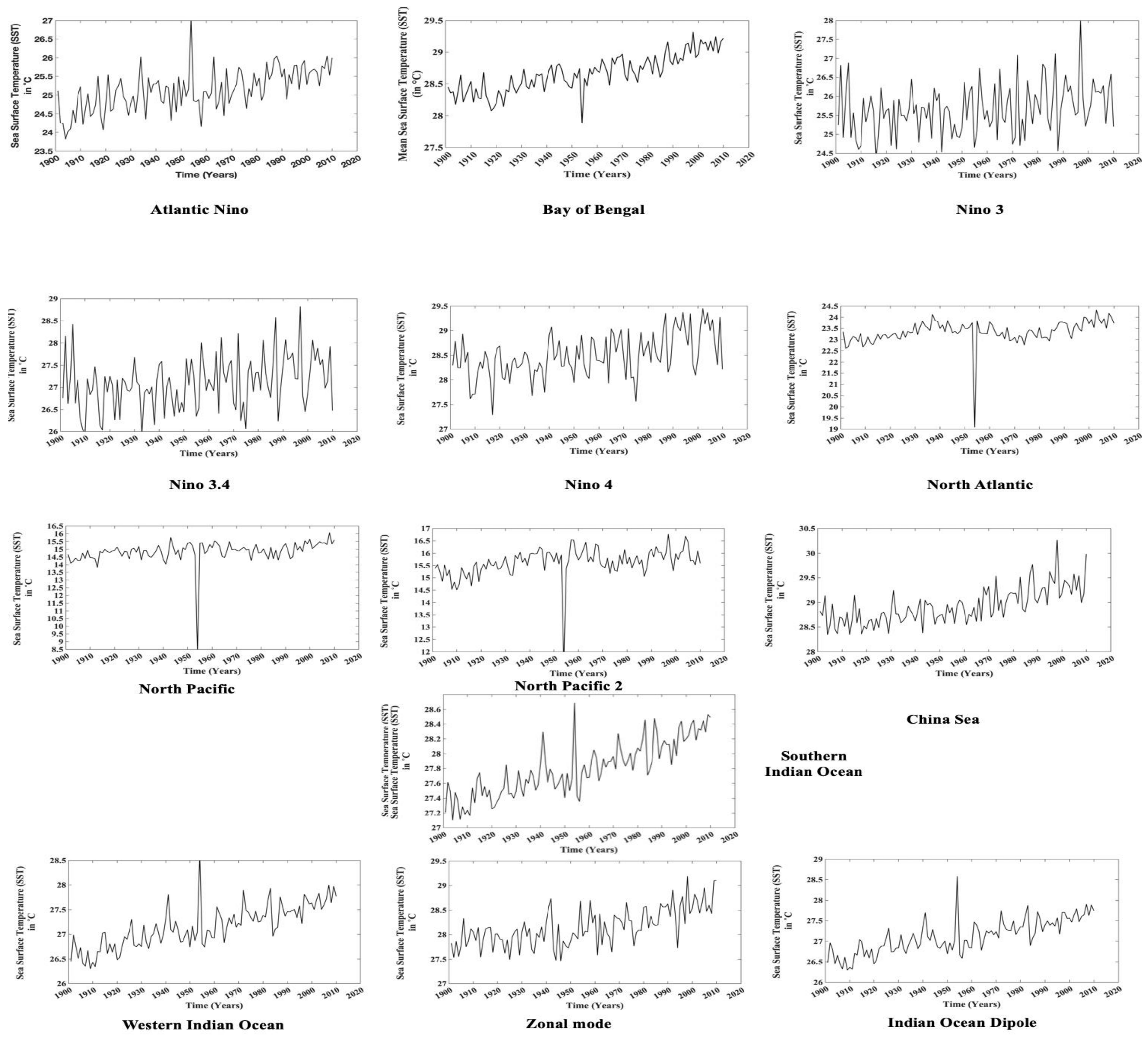

Observed Monthly SST over different oceanic region

References

- Socioeconomic impacts (Wang., 2015)
- Comprehensive Ocean Atmosphere Data Set (COADS) (Smith TM, 2008)
- Spatial patterns of rainfall anomalies (Sahastrabuddhe and Ghosh, 2019)

Estimation of Seasonal Base Flow Contribution to a Tropical River Using Stable Isotope Analysis

Himanshu Bhagat[1,3], Prosenjit Ghosh[1,2,3] and D. Nagesh Kumar[1,2,3,4]

Centre for Earth Science, Indian Institute of Science, Bangalore
Divecha Centre for Climate Change, Indian Institute of Science, Bangalore
Interdisciplinary Centre for Water Research, Indian Institute of Science, Bangalore
Department of Civil Engineering, Indian Institute of Science, Bangalore

FGRC 2021

Introduction

Sustainable Water flow in the Cauvery River relies on the predominantly availability of groundwater as baseflow during the Pre-Monsoon (PM) season and from surface runoff during the South-West Monsoon (SWM) season. Sustainable, efficient and equitable management of Cauvery riverwater and its distribution requires a thorough understanding of the contributing sources and hydrological processes influencing the availability of water resources.

Our Objectives

- Understanding the seasonal variations of δ^2H, $\delta^{18}O$ isotopes within the Cauvery River Basin .
- To discern and characterise the relative contributions of groundwater and surfacewater by using two-component end-member mixing analysis.
- Effect of large reservoirs on seasonal isotopic composition of Cauvery river water.

Sampling Locations

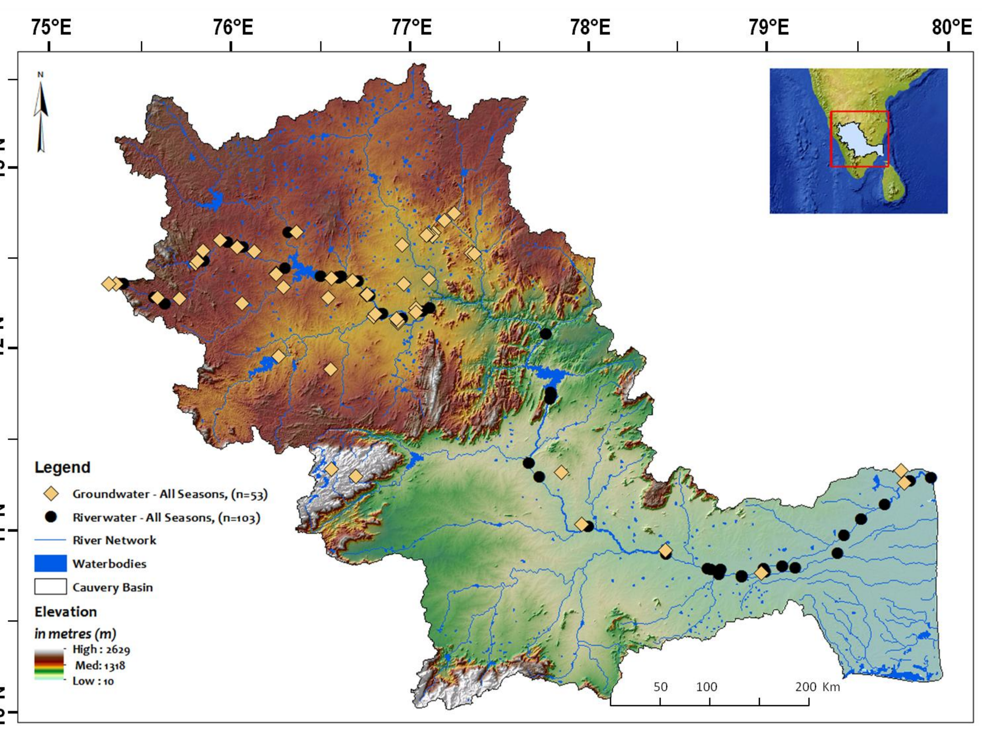

Fig 1: Digital Elevation Map (DEM) showing the sampling sites for River water (RW, n=103) and Groundwater (GW, n=54) within the Cauvery River Basin (CRB).

Research Methods

Stable Isotope Analysis of δD and $\delta^{18}O$ were accomplished through a Thermo Scientific Gas Bench II interface connected to a MAT 253 Isotope Ratio Mass-Spectrometer (IRMS) at CEaS, IISc. Two-component mixing model was used to quantify the relative contribution of the end-members i.e. base flow and surface runoff (rainfall).

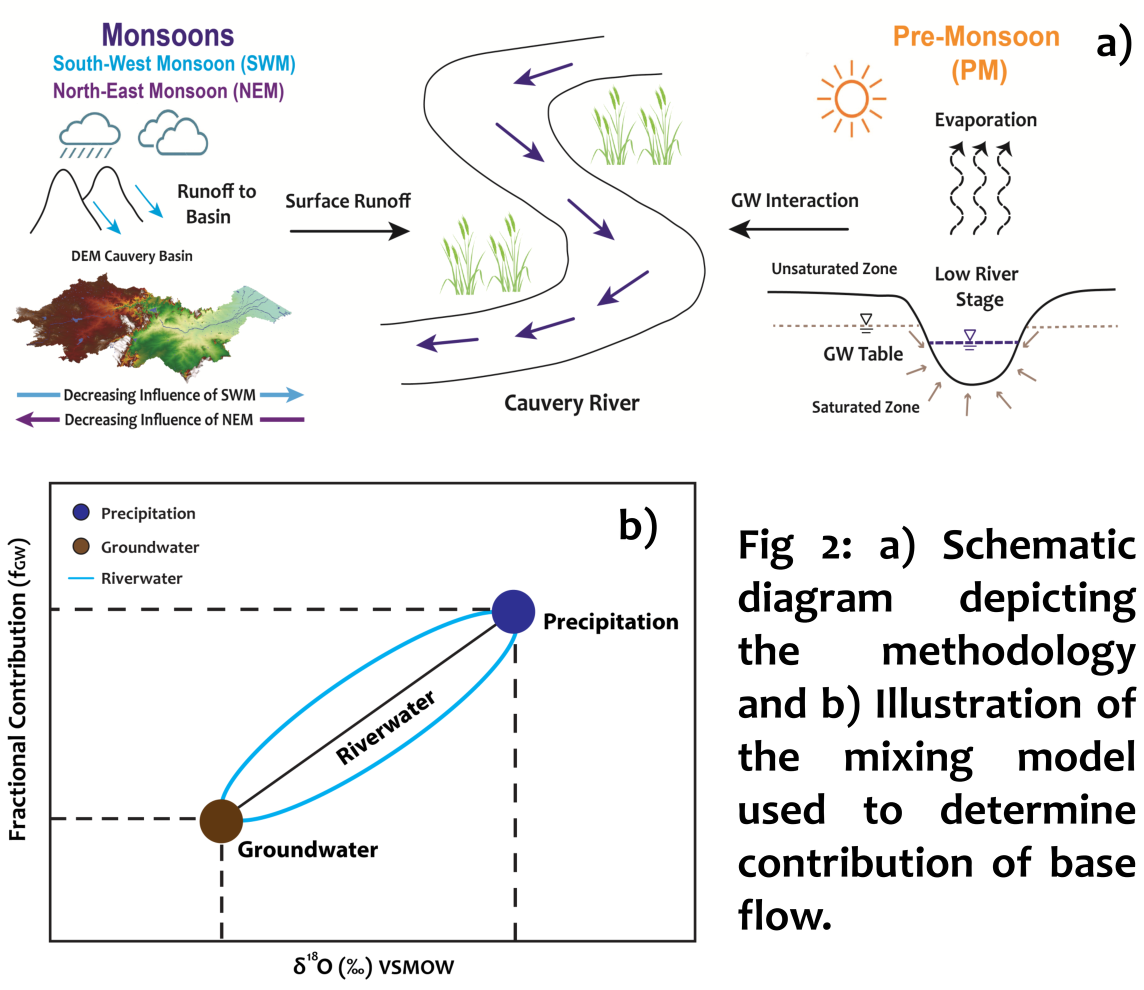

Fig 2: a) Schematic diagram depicting the methodology and b) Illustration of the mixing model used to determine contribution of base flow.

RESULTS

Bivariate plot of δ^2H - $\delta^{18}O$ systematics

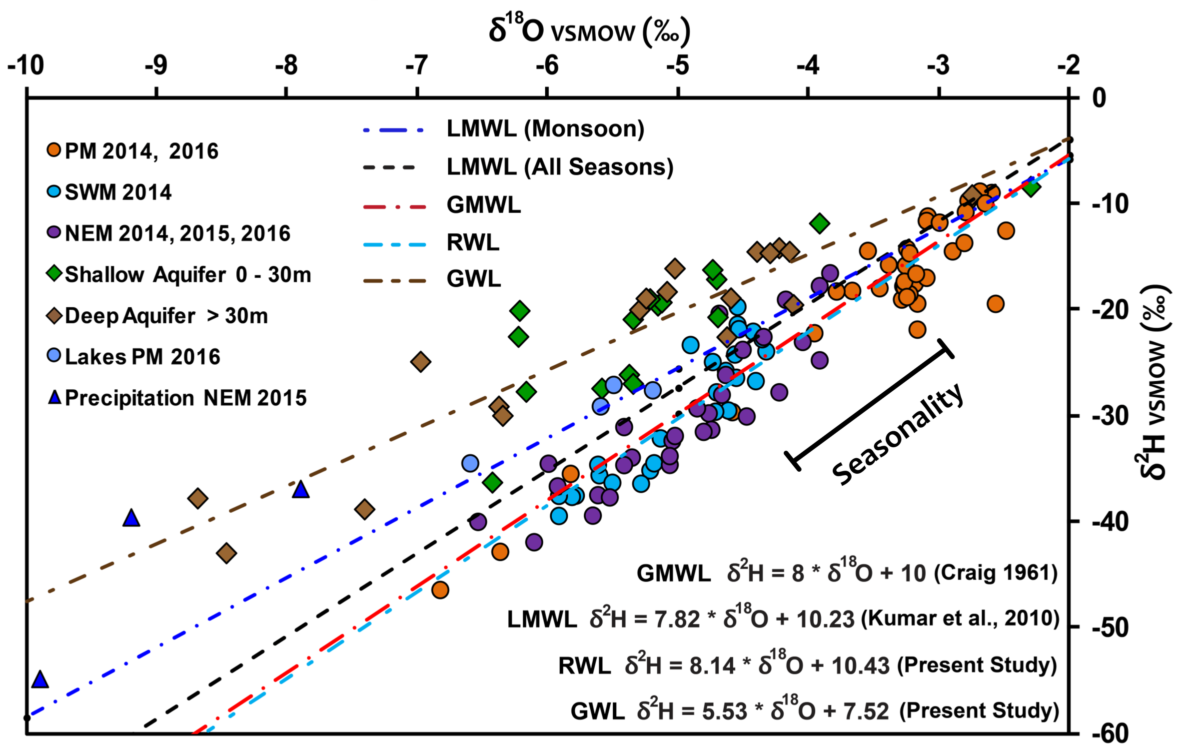

Fig 3: Stable isotopic composition (δ^2H, $\delta^{18}O$) of river water and groundwater across the Cauvery River Basin.

Reservoir Effect

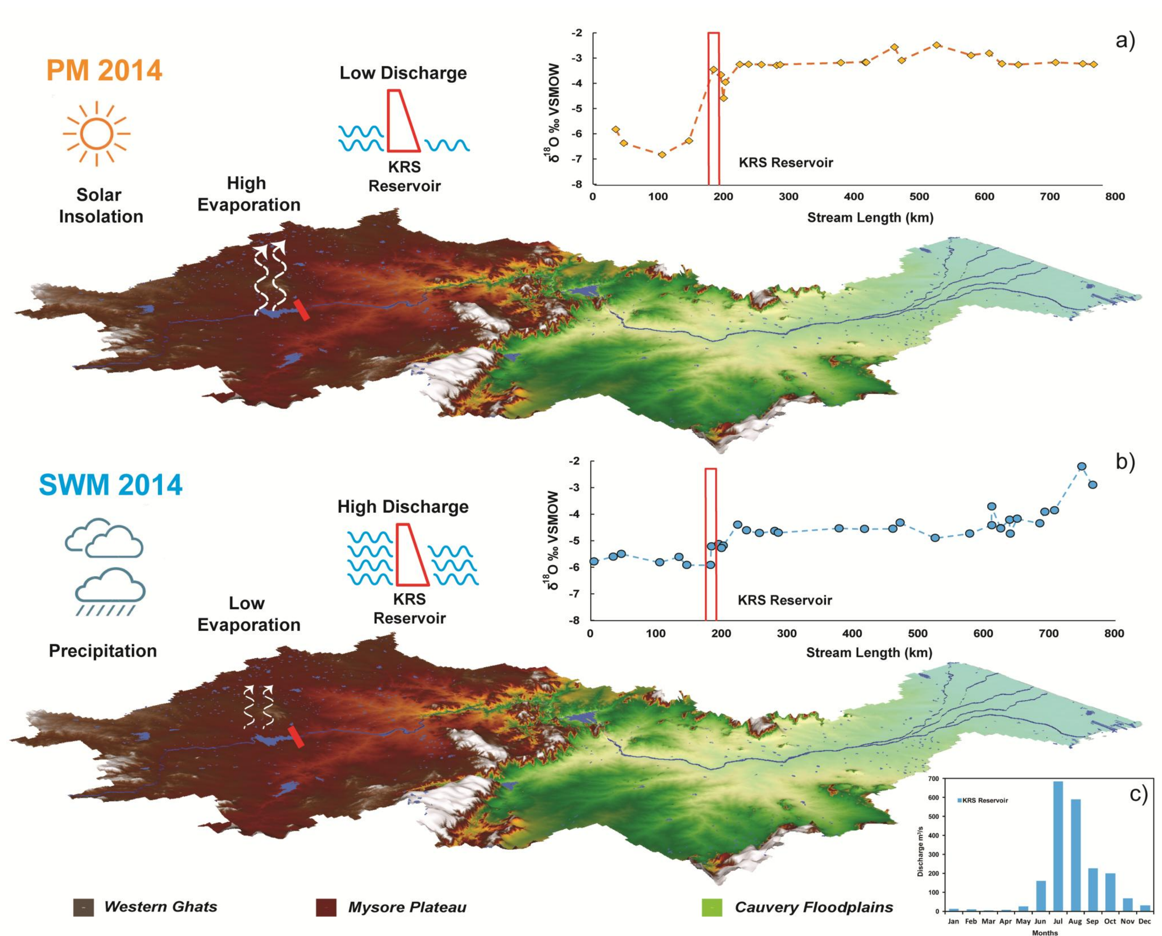

Fig 4: Modulation of seasonal $\delta^{18}O$ isotopic values of Cauvery River by the KRS reservoir.

Isoscapes of Riverwater & Groundwater

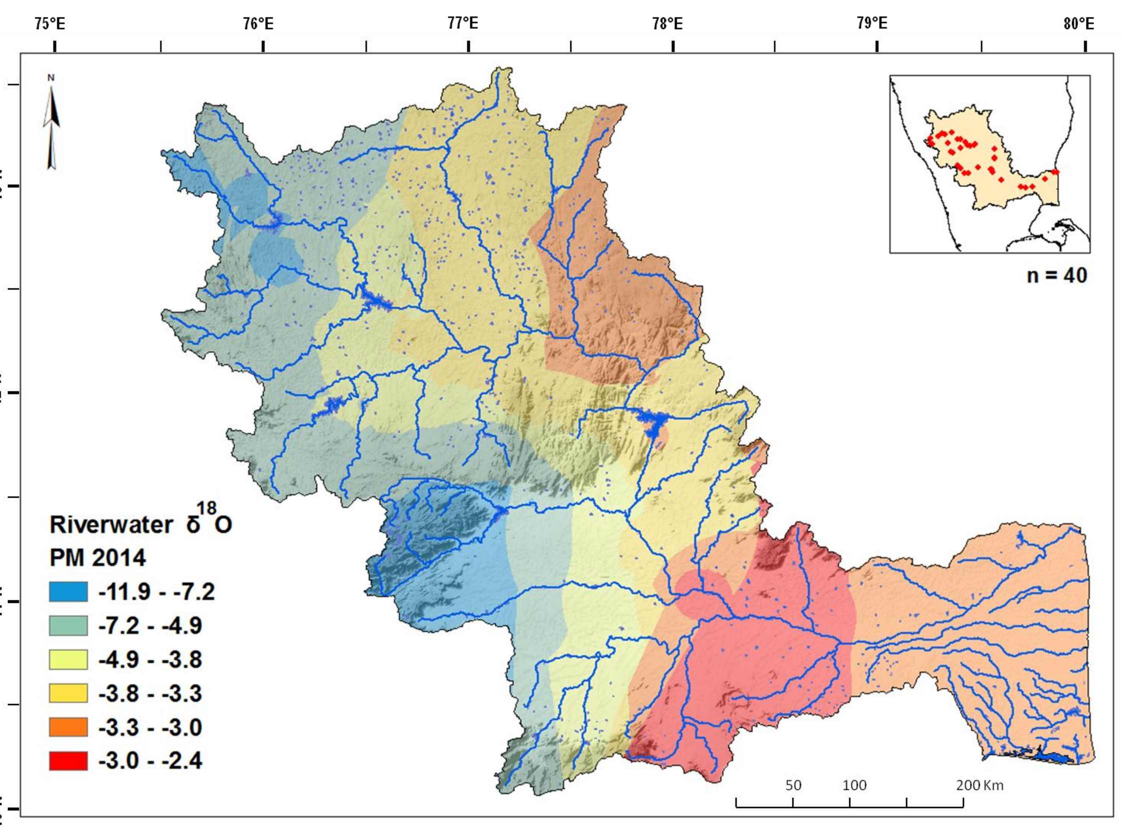

Fig 5: Isoscape depicting the spatial pattern of riverwater isotopic $\delta^{18}O$ composition during the Pre-Monsoon (PM) 2014 in Cauvery Basin.

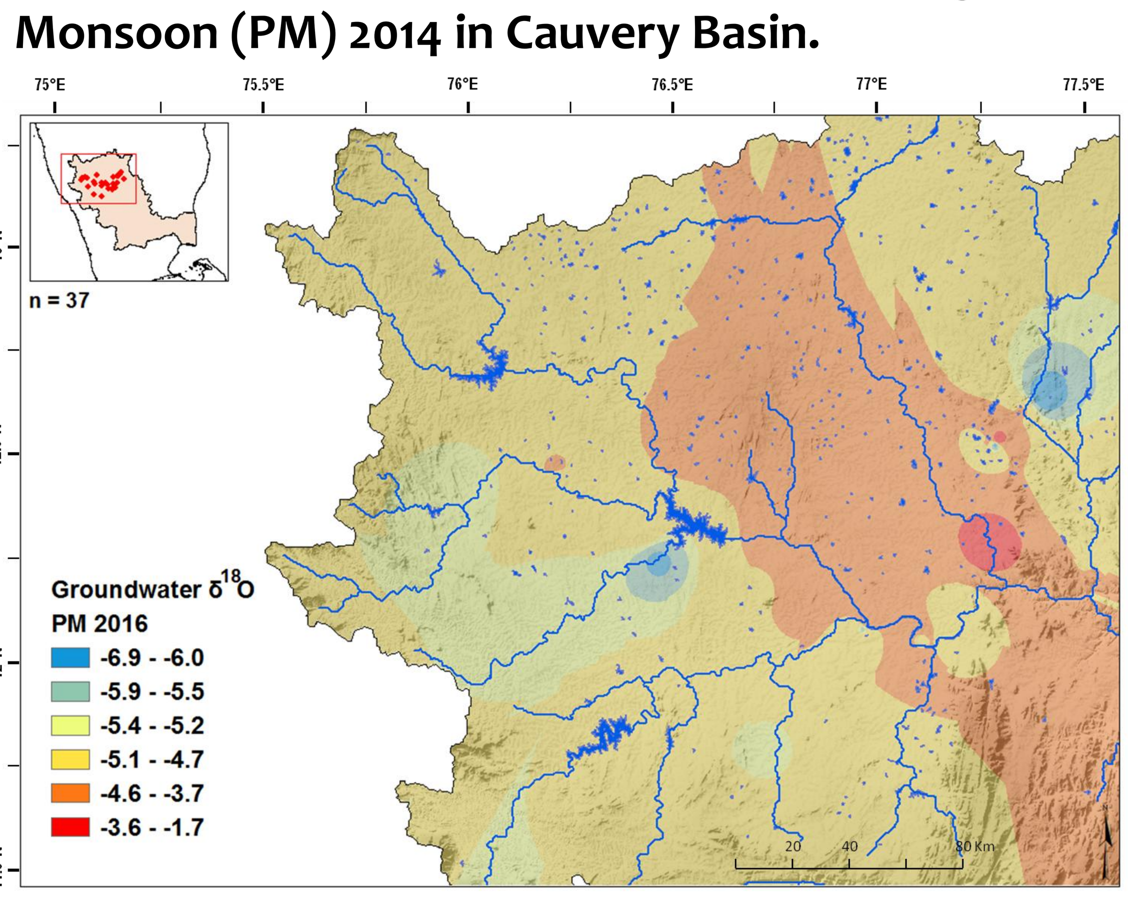

Fig 6: Isoscape depicting the spatial pattern of groundwater isotopic $\delta^{18}O$ composition during the Pre-Monsoon (PM) 2016 in upper Cauvery Basin.

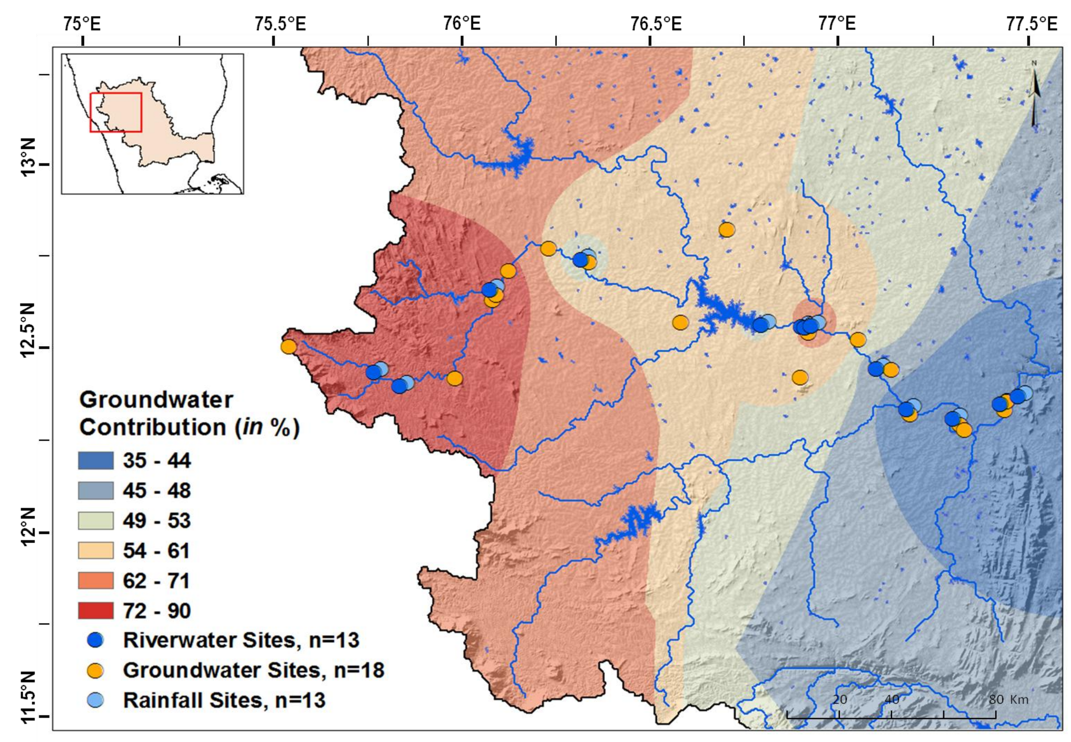

Fig 7: Spatial variation of groundwater contribution to the upper Cauvery river flow during Pre-Monsoon 2016.

Fractional Contribution & Conceptual Model

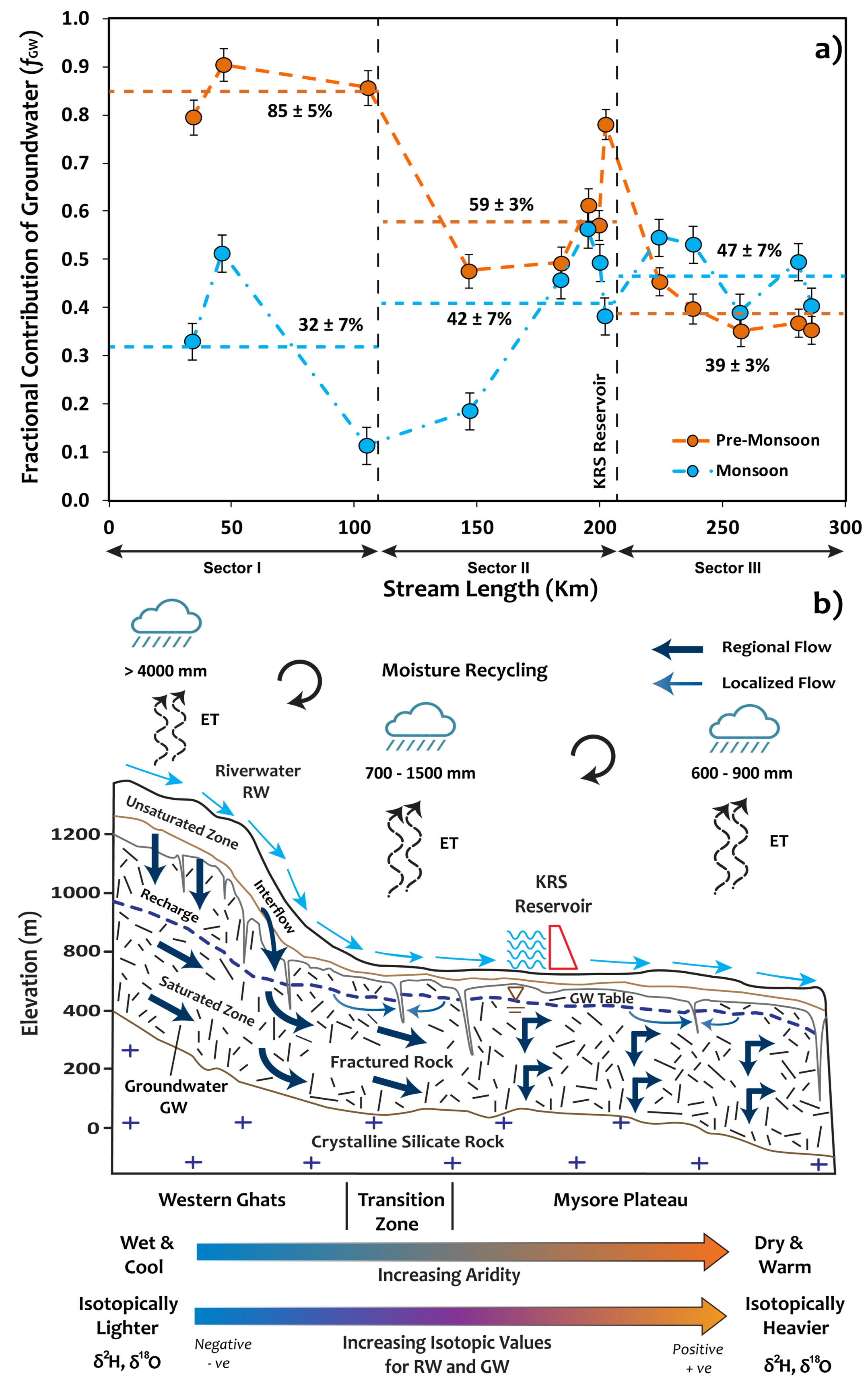

Fig 8: a) Baseflow contribution (%) estimated for the Cauvery main channel during PM and SWM seasons and b) Conceptual model showing the hydrological processes in groundwater system of the Cauvery River.

Conclusion

- Significant & distinct seasonal variability was observed in riverwater between seasons.
- Average Groundwater contribution to the Cauvery riverflow was estimated as 57% ± 4% and 42% ± 7% respectively during PM and SWM.
- Reservoir dynamics plays an important role in influencing isotopic composition of riverwater through homogenization and evaporative losses.

Follow our Work

Contact:
bhimanshu@iisc.ac.in

Influence of climate change on precipitation patterns in watersheds of Central Suvarnamukhi Basin, South Interior Karnataka, India

Decrease in Relative humidity trends shows reduced Rainfall

Decreasing Relative Humidity

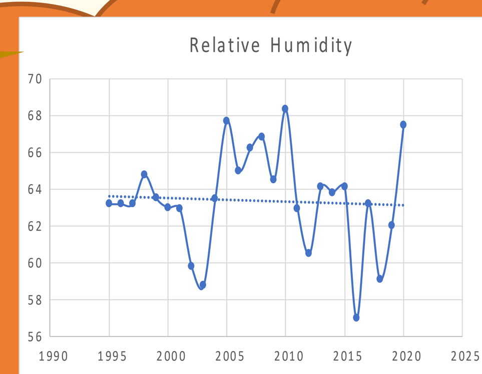

Decrease in Albedo shows increase in Temperature

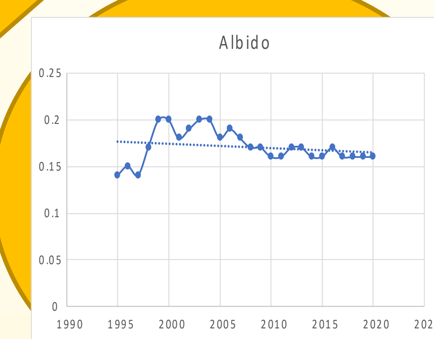

Decreasing Albedo

Increase in Land surface Pressure can cause clouds to fly away without precepitation

Increasing Surface Pressure

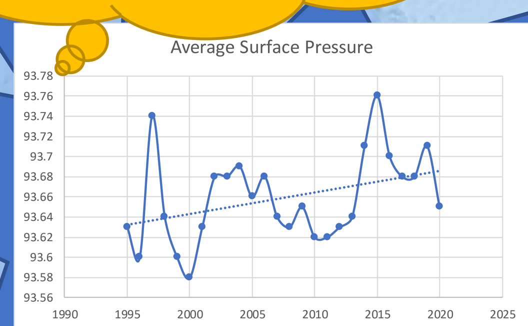

Increasing SST

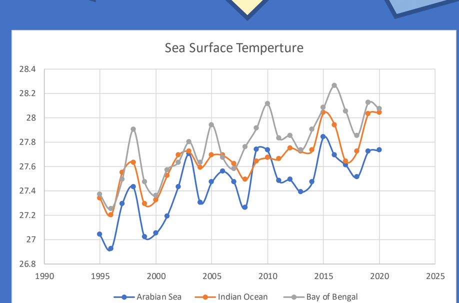

Sea surface temperature has been increasing causing PET increase that can affect rainfal

Decreasing Wind Speed

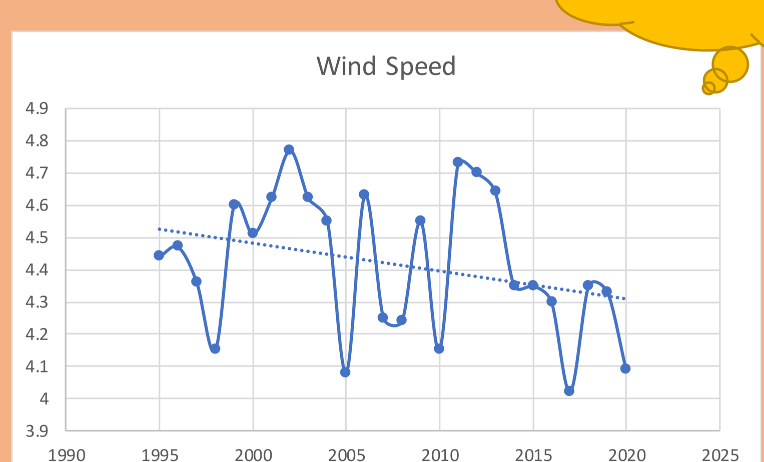

Decreasing Wind speeds can change the cloud movenment patterns and effect precipitation.

Return Period

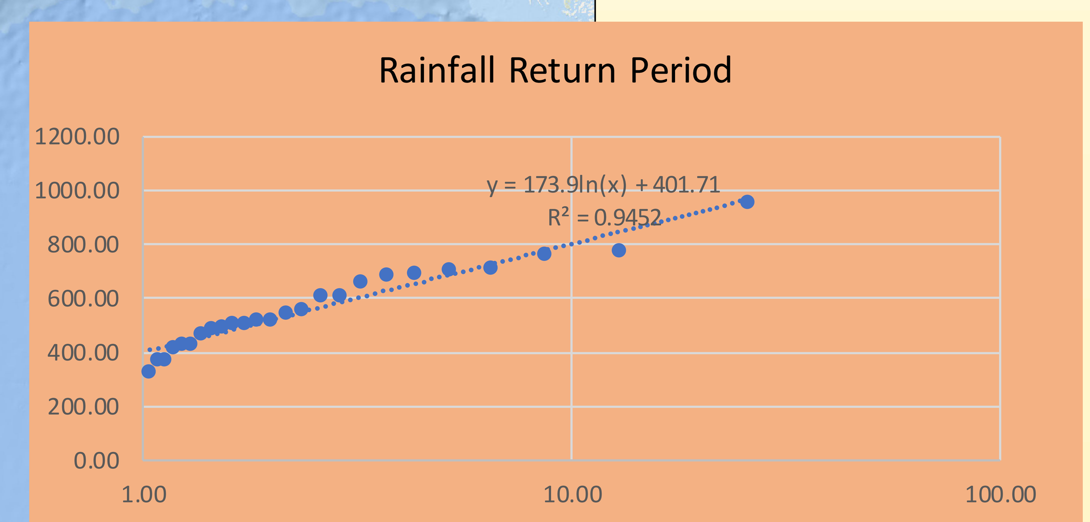

Drought Analysis

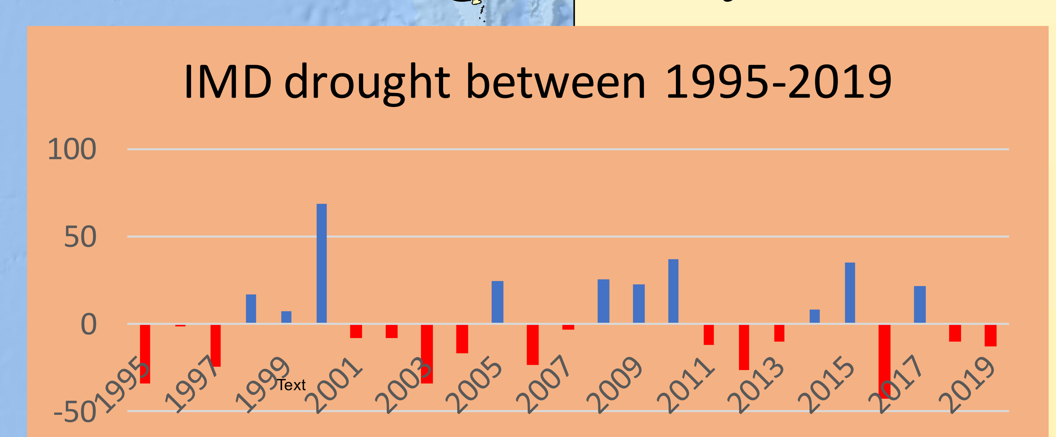

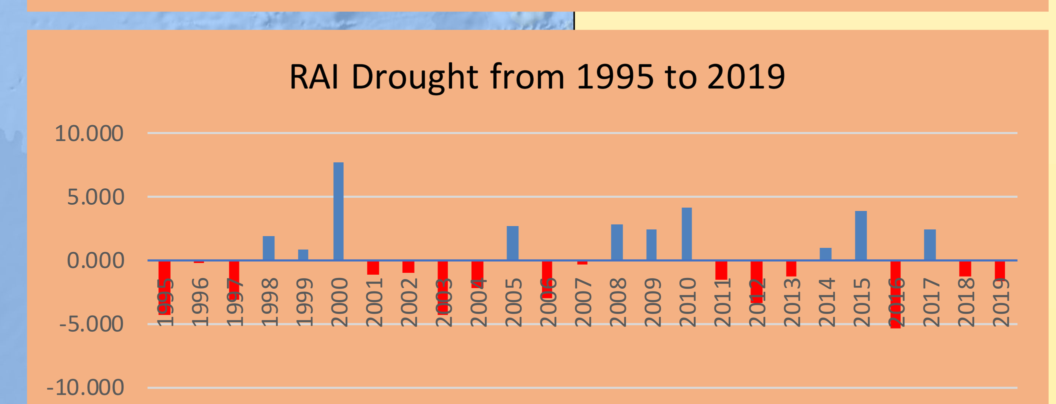

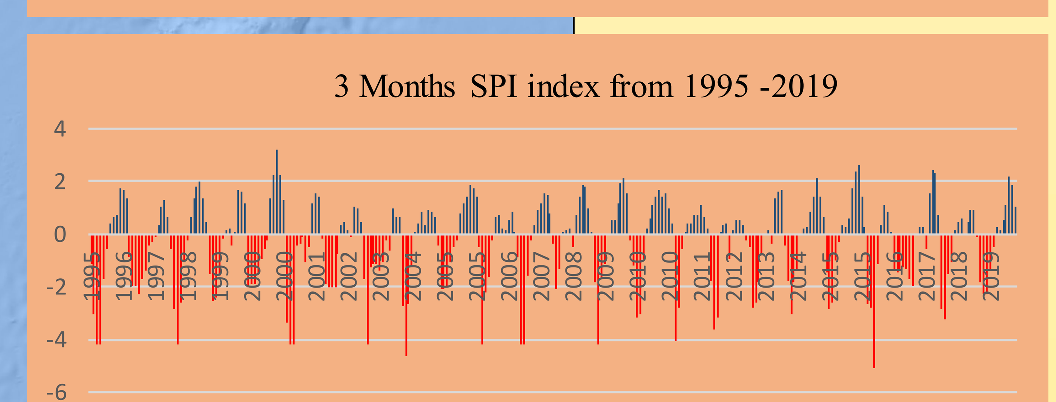

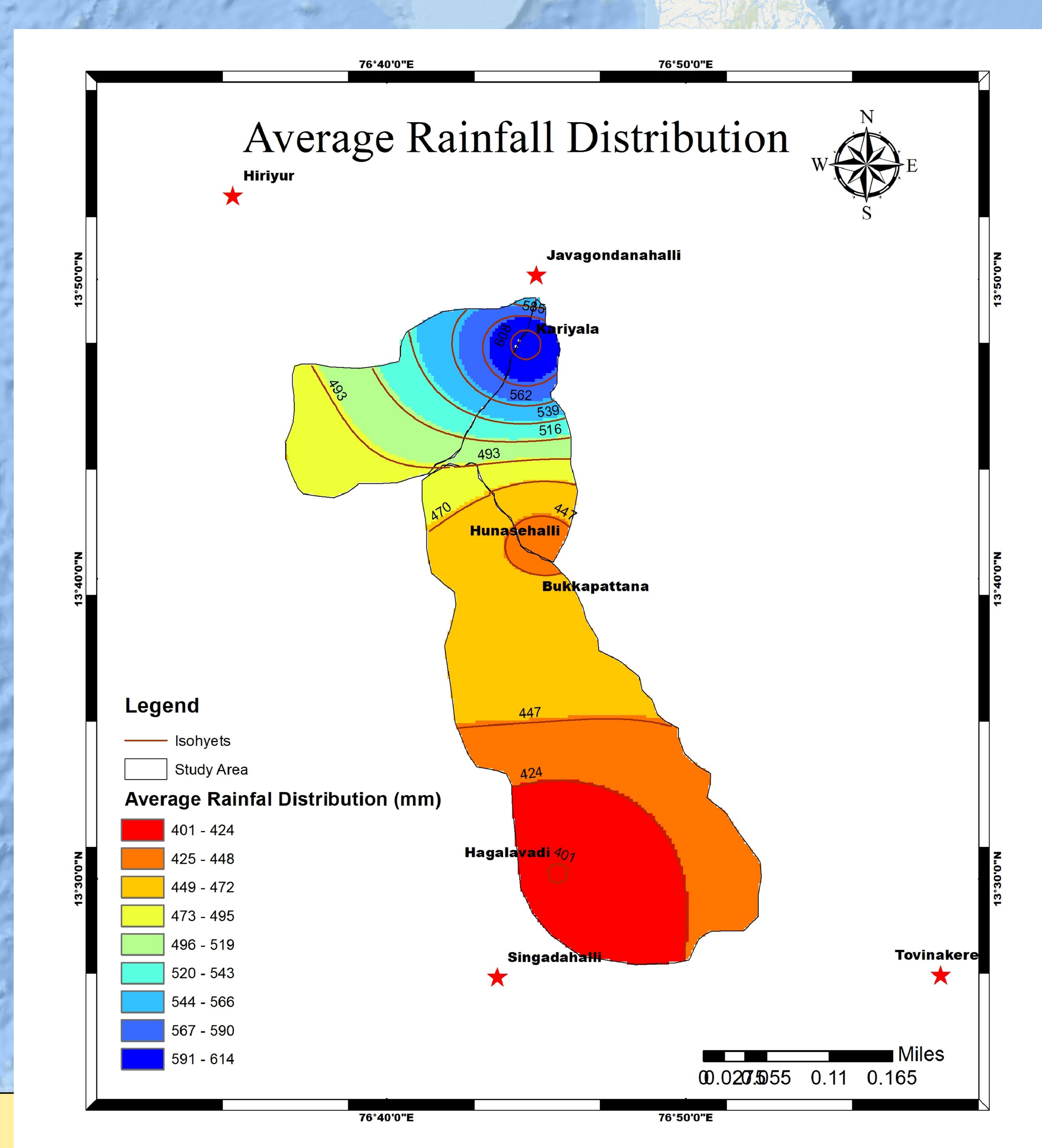

GIS and Field Photographs showing the effect of drought condition

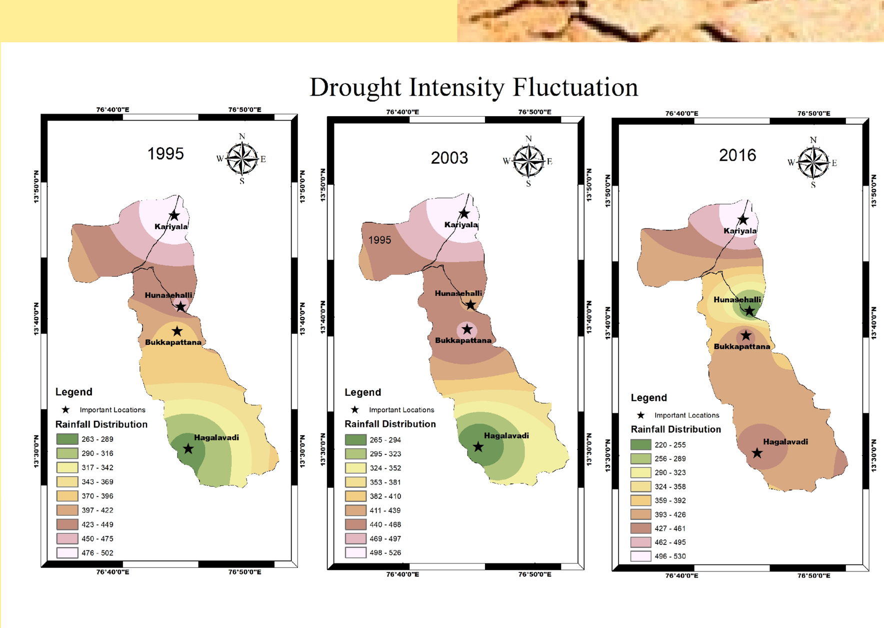

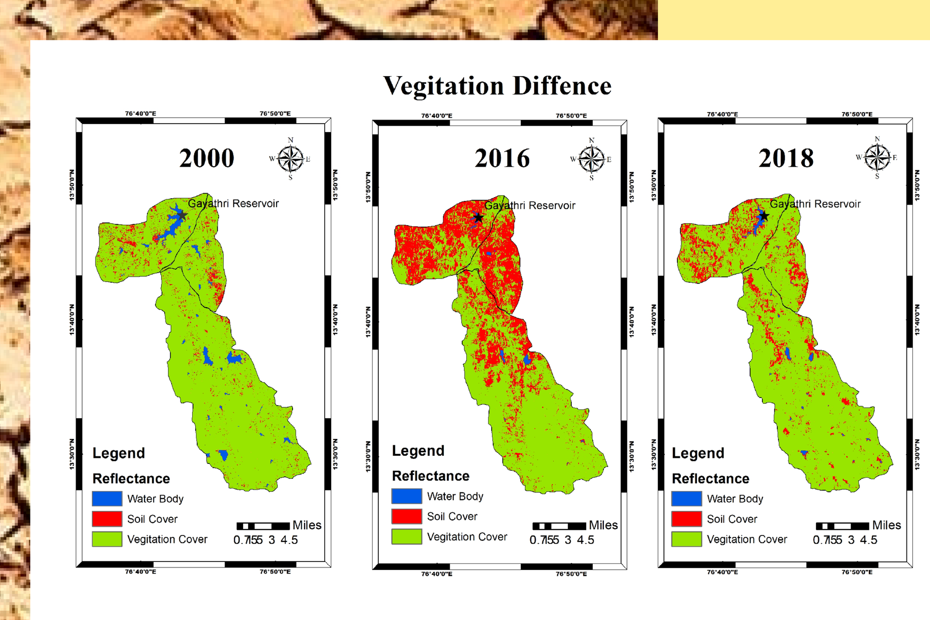

Tejas K, Radhika K N
Research Scholar, EWIT, Bangalore, Karnataka
Associate Professor, EWIT, Bangalore, Karnataka

Thermal state of Eocene-Oligocene tropical Indian Ocean based on carbonate clumped isotope thermometry of planktonic foraminifera from DSDP site 237

Thamizharasan,S.[1,2], Prosenjit Ghosh [1,2]

[1]Centre for Earth Sciences, Indian Institute of Science, Bangalore-560012

[2]Divecha Centre for Climate Change, Indian Institute of Science, Bangalore-560012

(Email Address: thamizharasa@iisc.ac.in; pghosh@iisc.ac.in)

A) Introduction:

- During Eocene and Oligocene, the Indian Ocean basin was well connected with the Pacific and Atlantic without any land boundary (1). It makes the sedimentary deposits in the Indian ocean the representative candidate recording the surface hydrography similar to the other global ocean.
- The physical state of the tropical Indian Ocean during Eocene Oligocene Transition (EOT) is poorly understood due to a lack of proxy data defining the surface temperature (SST).
- Here, we reconstructed the SST of tropical Indian Ocean using carbonate clumped isotope thermometry analysing planktonic foraminifera (*Dentoglobigerina galavisi*) from Middle Eocene to Early Miocene sedimentary section of DSDP site 237.
- Then, It is compared with the available tropical SST record derived from various proxies from the Atlantic and Pacific oceans. It includes TEX_{86} [2,3], Mg/Ca of foraminifera [4] and clumped isotope of foraminifera [5].

B) Objective:

- Fluctuation of Sea Surface Temperature over tropical Indian Ocean between Middle Eocene and Early Miocene.
- Relationship with other tropical oceans SST.

C) Sample Site:

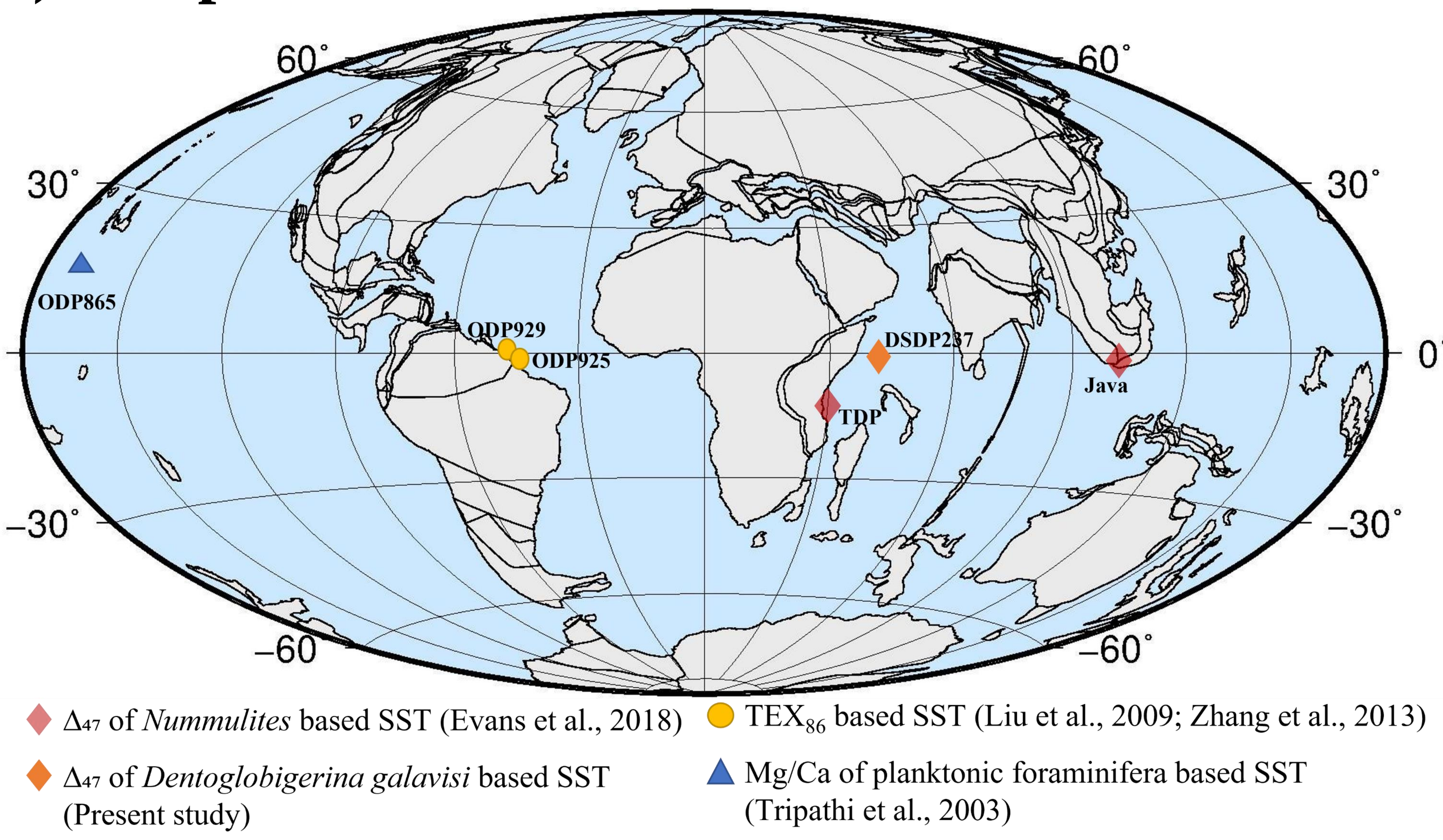

Fig. 1: Sample sites overlain on EOT paleogeography (created using www.odsn.de/odsn/services/paleomap/paleomap.html,).

D) Clumped isotope (Δ_{47}) analysis:

- Ultrasonically cleaned *D.galavisi* (250 to 350 μm size range) of around 8-10mg reacted with ~2ml of ~>104% orthophosphoric acid (density is ~1.92 g/cm^3) at 25(±0.1 °C) for a minimum 12 hrs following Break-seal method [6].
- The product CO_2 was extracted cryogenically and cleaned through Porapak-Q gas chromatography column (2m length, 1/8" diameter, 80-100 mesh range) held at ~25°C to remove any hydrocarbons and halocarbons responsible for isobaric interference using a constant helium flow at 12ml/min.
- The purified CO_2 was measured for Mass 44 to 49 using MAT253 IRMS associated dual inlet peripheral.
- The measurements were done at ~10000mV of mass 44.
- Standardization by OMC, MARJ1, ETH-1 & 3.
- The thermometry equation used to reconstruct temperature in the present study is adopted from the inorganic calcite experiment [7].

E) Tropical Sea Surface Temperature:

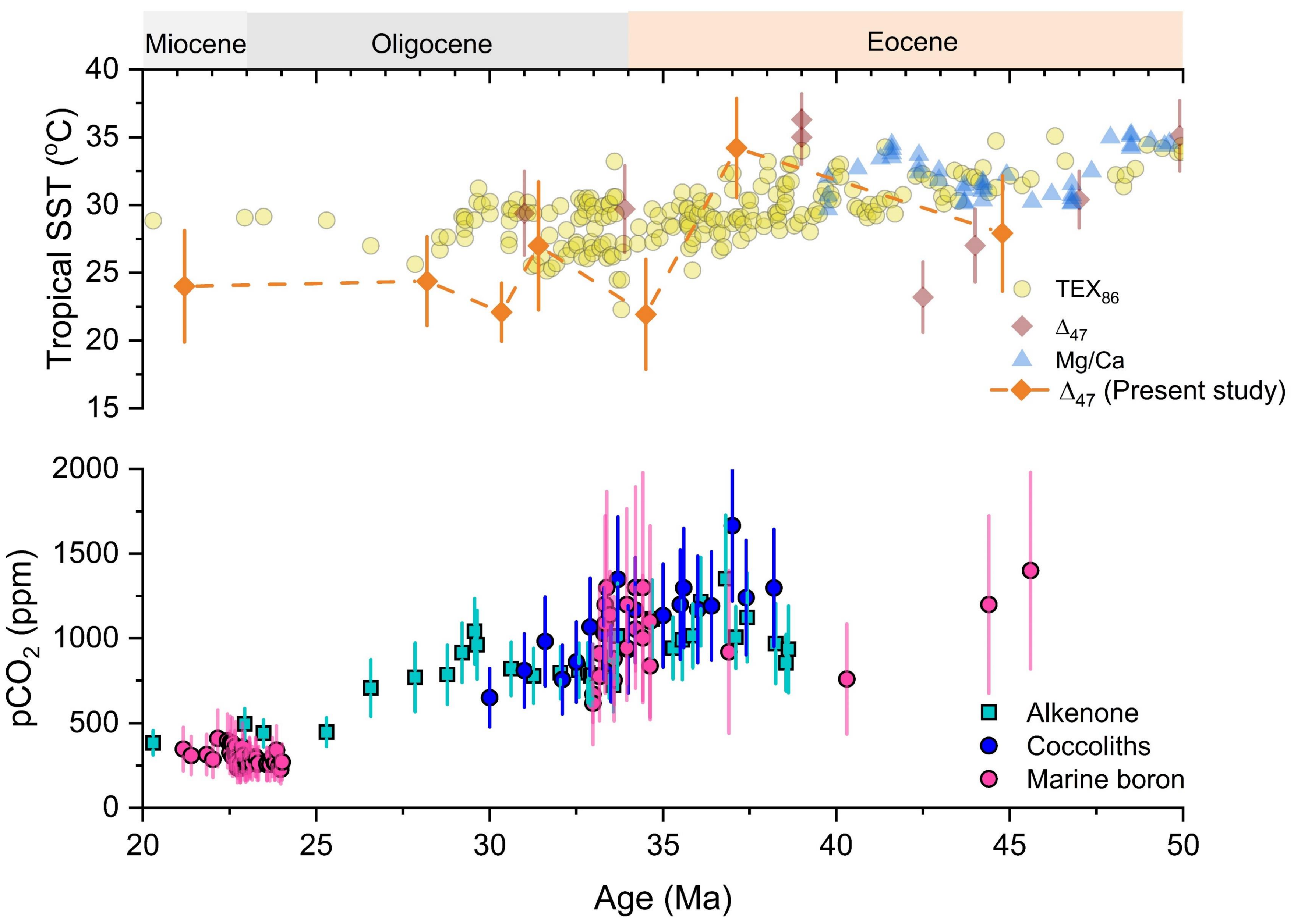

Fig. 2: **Eocene-Oligocene tropical Sea Surface Temperature and climate evolution.** a) Compilation of various proxy-based sea surface temperature from paleo-tropical location and present study data. b) proxy data CO2 estimates from alkenones, Coccoliths and Marine Boron.

- The SST reconstructed in the present study shows variation between 22±4°C and 34±3°C, and is consistent with the SST reconstruction record from Pacific and Atlantic Ocean.
- During Late Eocene, the SST was ~7°C warmer than modern median tropical SST (~27°C) which is associated with 1000-800 ppm of pCO_2. This shows the role of Green house emission on SST.
- However, during EOT the tropical Indian Ocean observed the drop of about 9°C which is synchronous with drop of pCO_2 from 1000-800 ppm to 700-600 ppm.

F) Conclusion:

- The tropical Indian Ocean SST strongly matches with the global tropical SST record during Eocene and Oligocene suggests ocean connectivity and near similar thermal state.
- The role of pCO_2 changing the climate is been seen in our study. It is a matter of great interest when we think of climate and pCO_2 relationship in global perspective

G) Reference:

1. Scotese, 2001. PALEOMAP Project. **2.** Liu et al., 2009. Science. Vol. 323, Pg No.: 1187–1190. **3.** O'Brien et al., 2020. PNAS, Vol. 117(41), pp.25302-25309. **4.** Tripati et al., 2003. Paleoceanography, Vol. 18(4). **5.** Evans et al., 2018. PNAS, 115(6), pp.1174-1179. **6.** Fosu et al., 2019. Rapid Communications in Mass Spectrometry, 33(2), pp.203-214. **7.** Zaarur et al., 2013. EPSL. Vol. 382. pp. 47-57.

PALEOMONSOONAL RECONSTRUCTION USING LAKE SEDIMENTS FROM COASTAL KARNATAKA, SOUTHERN INDIA: A MULTI-PROXY APPROACH

Yamuna Sali, A.S.[1], Powravi Sai[1], Warrier, A.K.[1], Sandeep, K.[2], Bharti Sharma[3], Shankar, R.[4]

[1]Manipal Academy of Higher Education, [2]Central University of Kerala, [3]Amity University, [4]Mangalore University

Introduction

- There is a dearth of high-resolution paleomonsoonal records from southwest coast of India.
- This study attempts to reconstruct the past changes in climate, in particular, the Indian Summer Monsoon (ISM) variability in coastal Karnataka, southern India.

Methodology

- Environmental Magnetism
- Sedimentology
- Loss on Ignition (LOI)

Results and Discussion

- Zone I (154-60 cm)-High values of concentration-dependent magnetic parameters (χ_{lf}, χ_{ARM} and SIRM)-High terrigenous input of iron minerals into the catchment → Increased rainfall.
- Zone II (60-35 cm)-Low values of concentration-dependent magnetic parameters, high values of sand and TOC.
- High values of S-ratio, χ_{fd}%, χ_{ARM}/ χ_{lf} and χ_{ARM}/SIRM-High concentration of SSD and SP-sized magnetite in the catchment soils → Stronger pedogenesis.

Study Area

Lake Ramasamudra

- Area: 0.15 sq. km.
- Average annual rainfall: ~4500 mm
- Length of the core: 154 cm; Sub-sampled at: 0.5 cm

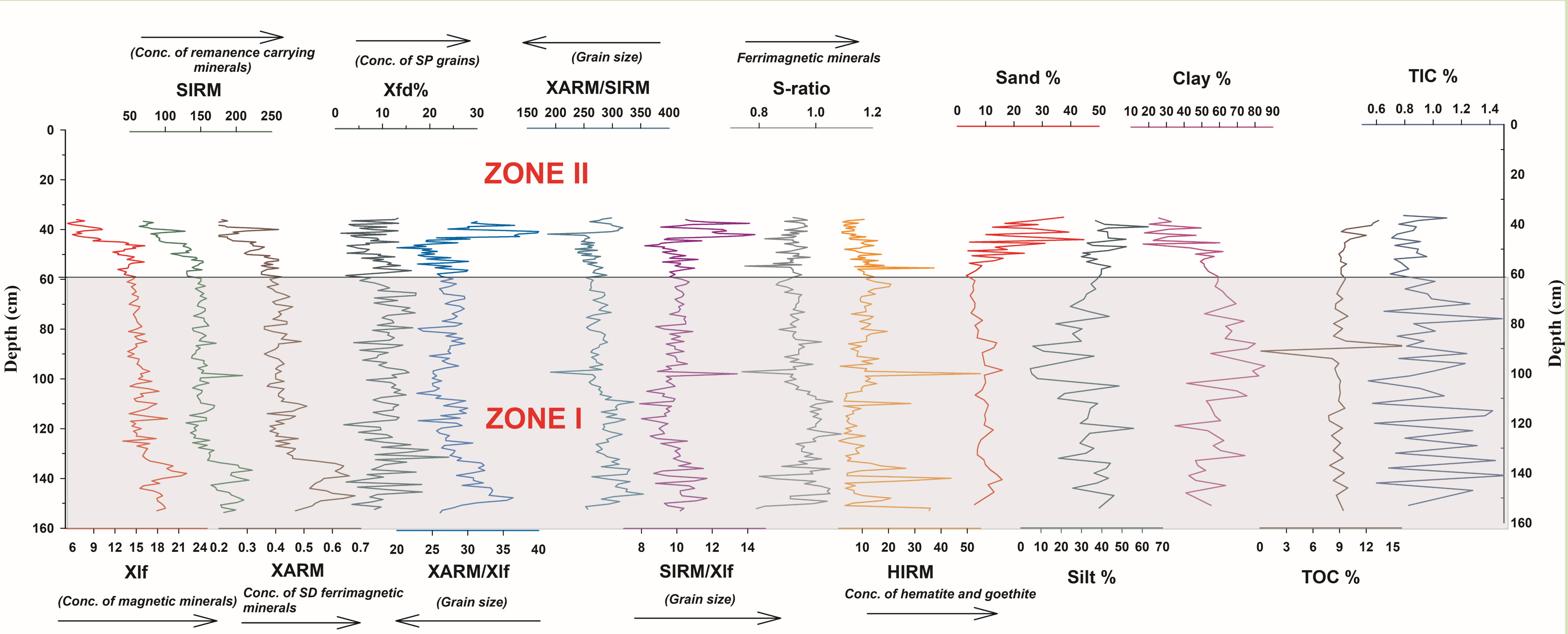

Conclusion

- The magnetic minerals present in the RSL sediments is mainly magnetite.
- The magnetic grains present in the sediments are mostly SSD and SP indicating stronger intensity of pedogenesis in the catchment.
- Zone I is characterized by a high terrigenous input of iron minerals and high lake-level, which might have resulted from a strong monsoon precipitation in the region.

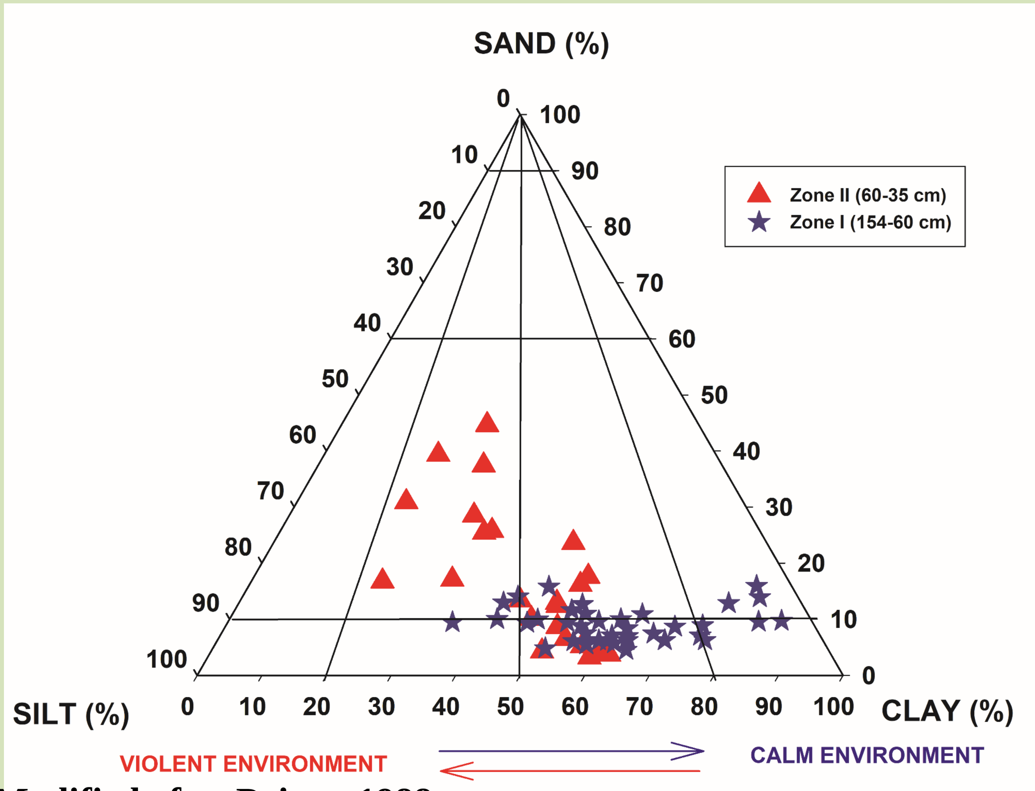

Modified after Pejrup 1988

Author profile

Yamuna Sali A S
CSIR JRF
Department of Civil Engineering
Manipal Institute of Technology
Manipal Academy of Higher Education
Email: yamuna.sali@learner.manipal.edu

References

Pejrup, M. (1988). The triangular diagram used for classification of estuarine sediments a new approach. Tide-influenced sedimentary environments and facies. Reidel Dordrecht, 289-300.

Acknowledgement

The author acknowledges CSIR-HRDG, New Delhi, for the Junior Research Fellowship awarded (File No.: 09/1165(0009)/2019-EMR-I).